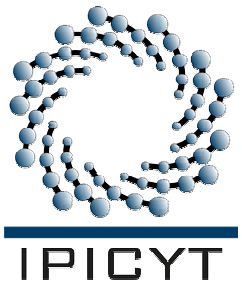

INSTITUTO POTOSINO DE INVESTIGACIÓN CIENTÍFICA Y TECNOLÓGICA, A.C.

POSGRADO EN CIENCIAS APLICADAS

Biosorption of Chromium (III) by agro-waste materials: characterization, sorption–desorption studies, mechanism, and adsorption kinetic experiments

Tesis que presenta

Refugio Bernardo García Reyes

Para obtener el grado de

Doctor en Ciencias Aplicadas

En la opción de

Ciencias Ambientales

Director de la Tesis:

Dr. José René Rangel Méndez

San Luis Potosí, S.L.P., Septiembre de 2009

IPICYT

La tesis "**Biosorption of Chromium (III) by agro-waste materials: characterization, sorption-desorption studies, mechanism, and adsorption kinetic experiments**" presentada para obtener el Grado de Doctor en Ciencias Aplicadas en la opción de Ciencias Ambientales fue elaborada por **Refugio Bernardo García Reyes** y aprobada el **11 de septiembre de 2009** por los suscritos, designados por el Colegio de Profesores de la División de Ciencias Ambientales del Instituto Potosino de Investigación Científica y Tecnológica, A.C.

Dr. José René Rangel Méndez
(Director de la tesis)

Dr. Felipe Alatriste Mondragón
(Asesor de la tesis)

Dra. Ma. Catalina Alfaro de la Torre
(Asesor de la tesis)

CRÉDITOS INSTITUCIONALES

Esta tesis fue elaborada en la División de Ciencias Ambiental del Instituto Potosino de Investigación Científica y Tecnológica, A.C., bajo la dirección del Dr. José René Rangel Méndez.

Durante la realización del trabajo el autor recibió una beca académica del Consejo Nacional de Ciencia y Tecnología (204219) y del Instituto Potosino de Investigación Científica y Tecnológica, A.C.

La investigación de esta tesis fue financiada parcialmente por el proyecto FMSLP-2008-C02-99664 del Fondo Mixto de Fomento a la Investigación Científica y Tecnológica, Consejo Nacional de Ciencia y Tecnología y Gobierno del Estado de San Luis Potosí, asignado al Dr. José René Rangel Méndez.

El autor de esta tesis recibió recursos financieros por parte de la División de Ciencias Ambientales del Instituto Potosino de Investigación Científica y Tecnológica, A.C. para la divulgación de los resultados parciales de esta investigación en un congreso internacional.

IPICYT

Instituto Potosino de Investigación Científica y Tecnológica, A.C.

Acta de Examen de Grado

El Secretario Académico del Instituto Potosino de Investigación Científica y Tecnológica, A.C., certifica que en el Acta 007 del Libro Primero de Actas de Exámenes de Grado del Programa de Doctorado en Ciencias Aplicadas en la opción de Ciencias Ambientales está asentado lo siguiente:

En la ciudad de San Luis Potosí a los 11 días del mes de septiembre del año 2009, se reunió a las 16:30 horas en las instalaciones del Instituto Potosino de Investigación Científica y Tecnológica, A.C., el Jurado integrado por:

Dr. Felipe Alatriste Mondragón	**Presidente**	**IPICYT**
Dra. Ma. Catalina Alfaro de la Torre	**Secretario**	**UASLP**
Dr. José René Rangel Méndez	**Sinodal**	**IPICYT**
Dr. Ramón Fernando García de la Cruz	**Sinodal externo**	**UASLP**

a fin de efectuar el examen, que para obtener el Grado de:

DOCTOR EN CIENCIAS APLICADAS
EN LA OPCIÓN DE CIENCIAS AMBIENTALES

sustentó el C.

Refugio Bernardo García Reyes

sobre la Tesis intitulada:

Biosorption of Chromium (III) by agro-waste materials: characterization, sorption–desorption studies, mechanism, and adsorption kinetic experiments

que se desarrolló bajo la dirección de

Dr. José René Rangel Méndez

El Jurado, después de deliberar, determinó

APROBARLO

Dándose por terminado el acto a las 19:15 horas, procediendo a la firma del Acta los integrantes del Jurado. Dando fe el Secretario Académico del Instituto.

A petición del interesado y para los fines que al mismo convengan, se extiende el presente documento en la ciudad de San Luis Potosí, S.L.P., México, a los 11 días del mes de septiembre de 2009.

Dr. Marcial Bonilla Marín
Secretario Académico

Mtra. Ivonne Lizette Cuevas Vélez
Jefa del Departamento de Asuntos Escolares

INSTITUTO POTOSINO DE INVESTIGACIÓN CIENTÍFICA Y TECNOLÓGICA, A.C.
IPICYT
SECRETARIA ACADEMICA

DEDICATORIAS

Dedico esta tesis a mi hijo y esposa porque son lo más importante en mi vida y me han permitido crecer junto con ellos pasando inolvidables momentos.

A mis hermanos: José Ángel, María Guadalupe, María de los Ángeles, Mónica, Aurora, Juan Manuel y Reina Isabel, porque de una u otra manera han contribuido para lograr esta meta.

A mi madre por todo el cariño, apoyo incondicional y por todos los sabios consejos que me ha dado.

A la memoria de mi padre José Refugio García Reza (Q.E.P.D.) que aunque no se encuentra físicamente a mi lado siempre permanecerá en un lugar muy importante en mi memoria prevaleciendo sus valiosas enseñanzas.

A mis compañeros y amigos que siempre estuvieron ahí cuando los necesitaba. A César, Luis, Paola, Nancy, José Luis, Guillermo, Dulce, Marisol, Javier, y todos aquellos que aunque no están nombrados aquí ayudaron a cumplir este sueño.

¡MUCHAS GRACIAS A TODOS USTEDES!

AGRADECIMIENTOS

Agradezco al Dr. José René Rangel Méndez la oportunidad de integrarme a su grupo de trabajo, por su disposición para escuchar y por su valiosa amistad.

A la Dra. Ma. Catalina Alfaro de la Torre (FCQ UASLP) por sus valiosos comentarios durante su participación como tutor de esta tesis, por sus interesantes clases y su disponibilidad para escuchar.

Al Dr. Felipe Alatriste Mondragón (IPICyT) por sus valiosas aportaciones durante su participación como tutor.

Por su efectivo apoyo técnico agradezco a los técnicos académicos del IPICyT M. en C. Dulce I. Partida Gutiérrez y M. en C. Rebeca Y. Pérez Rodríguez.

Al Dr. Ramón Fernando García de la Cruz por su participación como sinodal y por sus comentarios para mejorar la tesis.

Agradezco a Sydney Robertson-Jiménez (Peace Corps, EUA) sus acertados comentarios acerca de la redacción en inglés de esta tesis.

Finalmente, agradezco a la División de Ciencias Ambientales del Instituto Potosino de Investigación Científica y Tecnológica, A.C. por la infraestructura facilitada para realizar la investigación reportada en esta tesis.

TABLE OF CONTENTS

LIST OF TABLES

LIST OF FIGURES

SUPPORTING INFORMATION

ABSTRACT

Biosorption of Chromium (III) by agro-waste materials: characterization, sorption–desorption studies, mechanism, and adsorption kinetic experiments

Metal-containing effluents must be treated before discharge to avoid pollution of water sources and, consequently, health hazards associated to metal contamination. Some of the major toxic metal ions hazardous for humans, as well as other forms of life, are mercury, cadmium, lead, chromium, nickel, zinc and copper. These metals are of particular concern due to their toxicity, bio-accumulation, and persistence in nature. In particular, chromium is suspected of being carcinogenic and may affect the immune system of human beings. In addition, it has been recently reported that trivalent chromium (Cr (III)) affects human erythrocyte membranes in a higher extent in comparison with chromium (VI). Chromium effluents are generated from industries such as leather tannery, metal plating, textile, finishing, among others. Biosorption can be used to remove metals ions (e.g. Cr (III)) from aqueous solutions. Indeed, many low-cost biosorbents have been investigated for sequestering metals from water. Some examples of these materials include seaweed biomass, chitin and chitosan, microorganism biomass, lignocellulosic materials, etc. These biosorbents have a reasonable metal adsorption capacity and are widely available in many countries around the world. This thesis focused on the application of agro-waste materials such as sorghum straw (*Sorghum bicolor*), oats straw (*Avena monida*), and agave bagasse (*Agave salmiana*), as biosorbents of Cr (III) from aqueous solutions. These biosorbents were chemically and physically characterized by techniques such as infrared spectroscopy, acid–base titrations, sequential fiber extraction, surface area, pore volume, pore width distribution, and solid density. Sorption/desorption studies were conducted in batch systems and a sorption mechanism of Cr (III) was proposed. Also, adsorption kinetic studies of Cr (III) were performed by using a rotating basket reactor.

The agro-waste materials studied herein have a Cr (III) sorption capacity (5.3 to 22.4 mg/g at pH 4 and 25°C) similar to commercial ion exchangers. Quelating agents such as EDTA seem to be a promising alternative to regenerate chromium-loaded agro-waste materials (8 to 100%) without apparent loss of the biosorbents, in contrast to either acid or alkaline eluting-agents which produce a weight loss (1% to 43%). This loss may be attributed to the hydrolysis of the biopolymer components. The sorption mechanism of Cr (III) is coupled with the release of calcium or hydrogen ions. Nevertheless, complexation of metals also takes place on oxygen-containing groups (i.e. carboxyl and hydroxyl). Based on our results we proposed that carboxyl groups on agro-waste materials are the main binding-sites on Cr (III) removal. However, hydroxyl groups are capable of complexing metal cations as well. Among all structural polymers of agro-waste materials involved in metal adsorption, hemicelluloses and lignin are the major contributors to the removal of Cr (III) from aqueous solutions. In addition, cellulose apparently does not participate to the removal of metal cations. These later findings also support

the idea of adsorption of metal cations on carboxyl groups. The adsorption kinetics of Cr (III) on agro-waste biosorbents were predicted by using empirical or diffusion kinetic models. However, the film diffusion model seems to be the most appropriate based on the low deviation (0.5–5.8%) between the experimental and the predicted data. The physical properties (low porosity (0.004–0.007), low surface area (0.6–1.2 m^2 g^{-1}) and low pore volume (0.003–0.004 cm^{-3} g^{-1})) of the selected agro-waste materials support the idea that intraparticle diffusion may be neglected and that the adsorption of Cr (III) is mainly limited by the film resistance surrounding the adsorbent particle. Furthermore, the external mass transfer coefficient estimated with the film diffusion model has a physical meaning that helps to explain the diffusion of solutes across the film resistance in agro-waste biosorbents.
Finally, biosorption of heavy metals by using agro-waste materials is a promising way of treating wastewater of several industries such as leather tannery, finishing, metal plating, mining, textile, organic chemicals, among others. In addition, these biosorbents may be available at an accessible cost and have a comparable or higher sorption capacity than commercial adsorbents even at low metal concentrations.

Keywords: Functional groups, equilibrium constants, ion exchange, sequential fiber extraction, biopolymers, film diffusion, intraparticle diffusion.

RESUMEN

Biosorption of Chromium (III) by agro-waste materials: characterization, sorption–desorption studies, mechanism, and adsorption kinetic experiments

Los efluentes que contienen metales deben ser tratados antes de descargarlos a cuerpos receptores para evitar la contaminación de fuentes de agua y, por consiguiente, el riesgo a la salud humana asociado a la contaminación por metales. Algunos de los metales más tóxicos y peligrosos para los humanos, así como también otras formas de vida, son mercurio, cadmio, plomo, cromo, níquel, zinc y cobre. Estos metales son de interés particular debido a su toxicidad, tendencia a bioacumularse, y persistencia en la naturaleza. En particular, el cromo es cancerígeno y puede afectar el sistema inmune de los seres humanos. Además, recientemente se reportó que el cromo trivalente (Cr (III)) afecta la membrana de los eritrocitos de los seres humanos en mayor proporción que el cromo (VI). Los efluentes de cromo son generados de industrias tales como tenerías, recubrimientos metálicos, textil, acabados, entre otras. La adsorción puede ser utilizada para remover iones metálicos (e.g. Cr (III)) de soluciones acuosas. De hecho, muchos biosorbentes de bajo costo han sido investigados para remover metales del agua. Algunos ejemplos de estos materiales incluyen biomasa de algas marinas, quitina y quitosano, biomasa de microorganismos, materiales lignocelulósicos, etc. Estos biosorbentes tienen una capacidad de adsorción de metales razonable y están disponibles ampliamente en muchos países alrededor del mundo. Esta tesis se enfocó en la aplicación de desechos agrícolas tales como paja de sorgo (*Sorghum bicolor*), paja de avena (*Avena monida*), y bagazo de agave (*Agave salmiana*), como biosorbentes de Cr (III) de soluciones acuosas. Estos biosorbentes se caracterizaron química y físicamente por medio de técnicas tales como espectroscopia de infrarrojo, titulaciones ácido–base, extracción secuencial de fibras, área específica, volumen de poro, distribución de tamaño de poro, y densidad. Se realizaron estudios de adsorción/desorción en sistemas en lote y se propuso un mecanismo de adsorción de Cr (III). También se desarrollaron estudios de cinética de adsorción en un reactor de canastilla rotatoria.

Los desechos agrícolas estudiados en esta investigación tienen una capacidad de adsorción de Cr (III) (5.3 to 22.4 mg/g at pH 4 and 25°C) similar a la de intercambiadores iónicos comerciales. Los agentes quelantes (tales como EDTA) parecen ser una alternativa prometedora para regenerar los desechos agrícolas saturados con cromo (8 to 100%) sin aparente pérdida de los biosorbentes en contraste con los agentes eluentes ácidos o alcalinos los cuales producen una pérdida de peso (1% to 43%). Esta pérdida puede ser atribuida a la hidrólisis de los componentes de los biopolímeros. El mecanismo de adsorción de Cr (III) está asociado a la liberación de iones calcio o hidrógeno. Sin embargo, la acomplejación de los metales también se lleva a cabo en grupos funcionales que contienen oxígeno (i.e. carboxilo e hidroxilo). Basados en nuestros resultados proponemos que los grupos carboxilo en los desechos agrícolas son principales

sitios de enlace en la eliminación de Cr (III). Sin embargo, los grupos hidroxilo son también capaces de acomplejar cationes metálicos. De todos los componentes estructurales de los desechos agrícolas involucrados en la adsorción de metales, la hemicelulosa y la lignina contribuyen en mayor proporción en la eliminación de Cr (III) de soluciones acuosas. Además, al parecer la celulosa no participa en la eliminación de cationes metálicos. Estos últimos resultados soportan la idea de adsorción de cationes metálicos en los grupos carboxilo. La cinética de adsorción de Cr (III) en desechos agrícolas se predijo por modelos cinéticos empíricos y difusionales. Sin embargo, el modelo de difusión en la película parece ser el más apropiado basado en la pequeña desviación (0.5–5.8%) entre los resultados experimentales y predichos. Las propiedades físicas de los desechos agrícolas (baja porosidad (0.004–0.007), baja área específica (0.6–1.2 $m^2 g^{-1}$) y volumen de poro (0.003–0.004 $cm^{-3} g^{-1}$)), soportan la idea de que la difusión intraparticular puede ser despreciada y que la adsorción de Cr (III) está limitada principalmente por la resistencia de la película alrededor de la partícula del adsorbente. Además, el coeficiente de transferencia de masa externo estimado con el modelo de difusión en la película tiene un significado físico que ayuda a explicar la difusión de solutos a través de la resistencia en la película alrededor de los desechos agrícolas.

Finalmente, la biosorción de metales pesados por desechos agrícolas es una forma prometedora de tratar aguas residuales de varias industrias tales como tenerías, acabados, recubrimientos metálicos, minería, textil, y compuestos químicos orgánicos, entre otras. Además, estos biosorbentes pueden estar disponibles a un costo accesible y tienen una capacidad de adsorción comparable o mayor que la de adsorbentes comerciales, incluso a bajas concentraciones de metales.

Palabras clave: Grupos funcionales, constantes de equilibrio, intercambio iónico, extracción secuencial de fibras, biopolímeros, difusión en la película, difusión intraparticular.

Chapter 1

1.1 INTRODUCTION

Water is an essential resource for human living and enables industrial activities. According to the Fourth World Water Forum, to produce food for one person seventy times more water is required than for domestic use. This fact helps to understand the importance of keeping water supplies clean and safe from pollution, for example free of heavy metals.

1.1.1 Water contamination with metals

The major toxic metal ions hazardous for humans, as well as other forms of life, are mercury, cadmium, lead, chromium, nickel, zinc, copper, etc. These metals are of particular concern due to their toxicity, bio-accumulation tendency, and persistence in nature [1-6]. For example chromium is suspected of being carcinogenic and may affect the immune system of human beings (see Table 1.1) [3, 7-18]. In addition chromium (III) has been recently reported to affect human erythrocyte membranes to a higher extent than chromium (VI) [16]. Also, exposure to Cr (VI) causes nausea, diarrhea, liver and kidney damage, dermatitis, internal hemorrhage, and respiratory problems.

Several organizations around the world, namely World Health Organization (WHO), U.S. Environmental Protection Agency (EPA), Secretaría de Medio Ambiente y Recursos Naturales, México (SEMARNAT), and Secretaría de Salud, México (SSA) among others have set the maximum allowed concentrations for the discharge of toxic metals in the aquatic systems and also for drinking water. These limits and the possible health hazards associated to various heavy metals are given in Table 1.1.

Diverse industries discharge metal-containing wastewater; for example chromium effluents are generated from industries such as leather tannery, metal plating, textile, finishing, among others [9-14, 18-21]. Further details of heavy metals in various major industries are shown in Table 1.2. Although control technologies

have been applied to many industrial and municipal sources of metals, it was reported in 1988 that the global discharges of chromium to the environment were 142000, 30000, and 896000 metric tons/year to water, air, and soil, respectively [22].

1.1.2 Removal of metals from aqueous solutions by adsorption processes

Metal-containing effluents must be treated before discharge to avoid pollution of water sources and, consequently, health hazards associated to metal contamination. A number of treatments can be applied for metal removal from aqueous solutions, for instance chemical precipitation, coagulation–flocculation, chemical/oxidation reduction, membrane–based methods, etc. Nevertheless, the high cost of chemicals and membranes make these conventional treatments less viable. In addition, the sludge production is the major shortcoming in the removal of metals by either chemical precipitation or coagulation–sedimentation systems. Moreover the recommended discharge concentration (RDC) of metals is not always achieved by chemical precipitation or coagulation–sedimentation systems because metals are present at higher concentrations than those indicated in the RDC. In these cases, another separation operation, such as adsorption, can be applied to accomplish the RDC of metals.

Adsorption is a mass transfer operation in which substances present in a fluid (liquid or gas) are accumulated on a solid phase and thus removed from the fluid. The constituent that undergoes adsorption is referred to as the adsorbate, whereas the solid onto which the constituent is adsorbed is referred to as the adsorbent [23]. In the adsorption process, the driving force is the concentration gradient and the adsorbates are transported to the adsorbent by diffusion until the equilibrium is reached (i.e. in batch equilibrium studies, at least three successive measurements in three days are similar).

Table 1.1. Permissible limits (mg/L) and health effects of various toxic heavy metals [24].

Metal	SEMARNAT		SSA	WHO[d]	EPA[e]	Health hazard
	NOM-001-SEMARNAT-1996[a]	NOM-002-SEMARNAT-1994[b]	NOM-127-SSA-1994[c]			
Mercury	0.005–0.020	0.01	0.001	0.001	0.002	Corrosive to skin, eyes and muscle membrane, dermatitis, anorexia, kidney damage and severe muscle pain.
Cadmium	0.05–0.10	0.50	0.005	0.003	0.005	Carcinogenic, causes lung fibrosis, dyspnea and weight loss.
Lead	0.20–5.00	1.00	0.025	0.01	0.005	Suspected carcinogen, loss of appetite, anemia, muscle and joint pains, diminishing IQ, cause sterility, kidney problems and high blood pressure.
Chromium	0.50–1.00	0.50	0.05	0.05	0.10	Suspected human carcinogen, producing lung tumors, allergic dermatitis, and affects immune system activity.
Nickel	2.00	4.00	–	–	–	Causes chronic bronchitis, reduced lung function, lung cancer and nasal sinus.
Zinc	10.00	6.00	–	–	–	Causes short-term illness called “metal fume fever” and restlessness.
Copper	4.00	10.00	5.00	–	1.30	Long-term exposure causes irritation of nose, mouth, eyes, headache, stomachache, dizziness, and diarrhea.

[a]Norma Oficial Mexicana NOM-001-SEMARNAT-1996, que establece los límites máximos permisibles de contaminantes en las descargas de aguas residuales en aguas y bienes nacionales [25].

[b]Norma Oficial Mexicana NOM-001-SEMARNAT-1996, que establece los límites máximos permisibles de contaminantes en las descargas de aguas residuales a los sistemas de alcantarillado urbano o municipal [26].

[c]Norma Oficial Mexicana NOM-127-SSA1-1994, "Salud ambiental, agua para uso y consumo humano-límites permisibles de calidad y tratamientos a que debe someterse el agua para su potabilización" [27].

[d]WHO Guidelines for drinking-water quality [28].

[e]U.S EPA 40 CFR Parts 141, 142 and 143, National Primary Drinking Water Regulations [29].

Adsorption can be classified as physical adsorption or chemical adsorption, depending on the nature of forces between adsorbate and adsorbent. Physical adsorption involves only relatively weak forces, whereas in chemical adsorption a chemical bond is formed. Table 1.3 shows the differences between these two kinds of adsorption [23]. Physical adsorption is a rapid process caused by a nonspecific binding mechanism such as van der Waals forces (i.e. electrostatic interaction), and is the most common mechanism by which adsorbates are removed in water treatment.

Table 1.2. Heavy metals in various major industries [30].

Industry source	Mercury	Cadmium	Lead	Chromium	Nickel	Zinc	Copper
Automobile		X	X	X	X	X	
Petroleum refining			X	X	X	X	X
Pulp and paper	X		X	X	X	X	X
Textile				X			
Steel		X	X	X	X	X	
Organic chemicals	X	X	X	X		X	
Inorganic chemicals	X	X	X	X		X	
Fertilizers	X	X	X	X	X	X	X
Leather tanning and finishing				X			
Steel power plants				X		X	
Mining	X	X	X				X
Acid mine drainage						X	X
Metal plating		X		X		X	X
Glass							
Coal and gasoline			X				

To select the adsorbent that has the highest adsorbate sorption capacity, equilibrium adsorption experiments are required. Two different batch techniques can be chosen. In the first one, the adsorbent mass is fixed and the initial adsorbate concentration is varied in every batch experiment. In the second technique, the initial adsorbate concentration is fixed and the quantity of adsorbent added to each batch experiment is varied. Regardless of the technique selected, the mass of adsorbent as well as the initial and final adsorbate concentrations must be recorded to determine the adsorption capacity of the material. The amount of

solute adsorbed per unit mass of adsorbent is obtained by using the mass balance expression:

$$Q_e = \frac{V(C_o - C_e)}{m} \quad (1)$$

where Q_e is the solute adsorption capacity (mg/g), C_o and C_e are the initial and equilibrium concentrations (mg/L), m the dry mass of adsorbent (g) and V is the volume of solution (L).

Table 1.3. Differences between the two kinds of adsorption [23].

Parameter	Physical adsorption	Chemical adsorption
Forces of adsorption	Weak intermolecular forces where interactions between adsorbate and adsorbent surface are due to Columbic, van der Waals or dipole forces. No electron transfer or dipole forces.	Chemical bonding between adsorbate and adsorbent surface via electron transfer.
Energy of adsorption	Less than 10 kcal/mol.	Varying between 20-100 kcal/mol.
Nature of adsorbed phase	Both monolayer and multilayer adsorption may occur on the surface of the adsorbent. No dissociation of adsorbed species.	Only monolayer exists. Adsorbed species may dissociate.
Specificity	Non-specific in terms of site for adsorption. Molecules or ions are free to cover the entire surface.	Highly specific. Molecules or ions are attached at specific sites.
Reversibility	Rapid and fully reversible.	May be slow and irreversible.
Temperature	Significant at relatively low temperature.	Possible over a wide range of temperature. Often occurs at high temperatures.

It is important to mention that the conditions (at least solution pH and temperature) at equilibrium must be specified in order to compare the sorption capacity of different adsorbents for certain adsorbates.

Once the solute adsorption capacity is obtained, different isotherm models could be used to adjust the experimental data. The most commonly used models include Freundlich and Langmuir isotherms.

The Langmuir adsorption isotherm describes the surface as homogeneous assuming that all the adsorption sites have equal adsorbate affinity, that adsorption at one site does not affect adsorption at an adjacent site, and that adsorption allows accumulation only up to a monolayer. The Langmuir isotherm can be represented by the following expression:

$$Q_e = \frac{Q_{max}\, b\, C_e}{1 + b\, C_e} \tag{2}$$

where C_e is the equilibrium concentration of the adsorbate in solution (mg/L), Q_e is the equilibrium loading of adsorbate on adsorbent (mg/g), Q_{max} is the maximum adsorption capacity (mg/g), and b is the relative energy of adsorption (L/mg).

The Freundlich adsorption isotherm describes the equilibrium on heterogeneous surfaces and does not assume monolayer capacity. The Freundlich isotherm is represented as:

$$Q_e = k\, C_e^{\,1/n} \tag{3}$$

where Q_e is the amount adsorbed (mg/g), C_e the equilibrium concentration of the adsorbate (mg/L), and k and n are the Freundlich constants related to the adsorption capacity and adsorption intensity, respectively.

A great variety of adsorbent materials may be used for water treatment and the most important ones are discussed in the subsequent section.

1.1.3 Adsorbent materials

Adsorbents commonly used in the removal of pollutants from water include activated carbon (the adsorbent generally preferred worldwide), zeolites, and polymeric resins. Also, in the last decades, biosorbents have been extensively investigated to be used in water treatment. Details of the main characteristics of these adsorbents are discussed in the following sections.

1.1.3.1 Activated carbon

Activated carbon (AC) is a crude form of graphite with a random or amorphous structure, which is highly porous, exhibiting a broad range of pore sizes, from visible cracks, crevices and slits of molecular dimensions [31]. Natural or synthetic precursors have been used to manufacture AC. Natural carbonaceous precursors consist of wood, coal, lignite, peat, coconut shells, rice hulls, bone char, sawdust, etc., whereas synthetic precursors employ fabrics made from several polymeric materials such as nylon, rayon, cellulose, phenolic resins, polyacrylonitrile, etc.

The manufacture of AC starts with the pyrolytic carbonization of the raw material. In this step, the volatile components are released and graphite is formed. Parallel or subsequent to carbonization, activation is required to develop a highly porous structure. Physical or chemical activation are the two options for activating carbons.

Physical or thermal activation involves carbonization at 500–600°C to eliminate the bulk of the volatile matter followed by partial gasification usually conducted between 800°C and 1000°C in the presence of an oxidizing gas (e.g. steam, carbon dioxide, air or mixtures of these) to develop the porosity and surface area. The activation mechanism consists of two stages; firstly the disorganized carbon on the surface is burned off, and in the second stage the carbon of the aromatic sheets starts burning, producing active sites, wider pores and thus new porosity [32].

Chemical activation involves the incorporation of inorganic additives, metallic chlorides such as zinc chloride or phosphoric acid into the precursor before the carbonization [33], generally at temperatures (400–600°C) lower than physical activation.

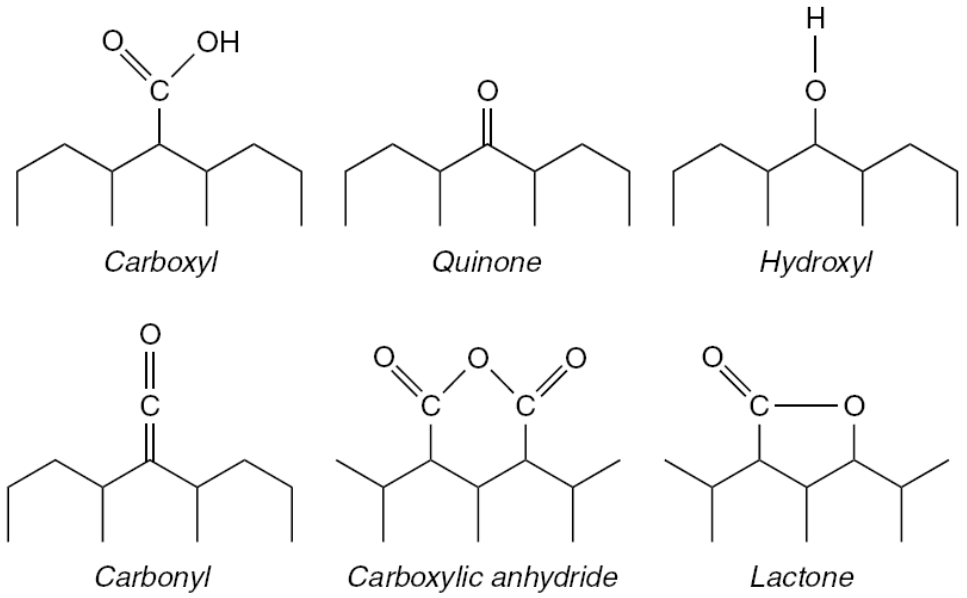

Figure 1.1. Acidic groups chemisorbed at the edges of graphene layers in activated carbon [34].

The AC surface chemistry depends on the starting material, the activation method, the activation conditions and temperatures employed, among others. Surface groups on AC are classified as acidic and basic functional groups. Oxygen-containing groups chemisorbed on the edges of graphene layers (see Figure 1.1), give acidic properties to AC and allow cation exchange properties [34]. It has been reported that an increase in carboxylic groups, by chemical modification of AC with nitric acid or air at high temperature, enhance the metal cations adsorption capacity [32].

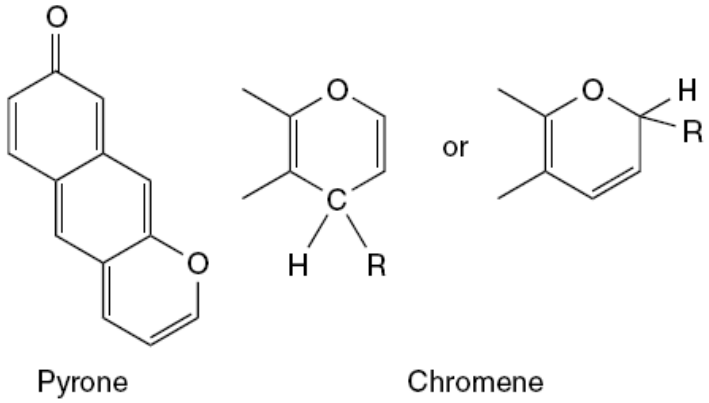

Figure 1.2. Possible basic groups on activated carbons [34].

Basic functional groups on AC can be associated to a chromene type structure [35] or more likely to γ-pyrone-like structures [36, 37] (see Figure 1.2). Basic groups can be used as adsorption sites of anionic species.

1.1.3.2 Zeolites

Zeolites are crystalline, hydrated aluminosilicates of alkali and alkaline earth cations (i.e. sodium, potassium, and calcium) and are represented by the chemical composition [34]:

$$M_{x/n}[(AlO_2)_x(SiO_2)_y] \cdot zH_2O \quad (4)$$

where x and y are integers with y/x equal to or greater than 1, n is the valence of cation M, and z is the number of water molecules in each unit cell. The primary structural units of zeolites are the tetrahedra of silicon and aluminum, SiO_4 and AlO_4. These units are assembled into secondary polyhedral building units such as cubes, hexagonal prisms, octahedra, and truncated octahedra. The silicon and aluminum atoms, located at the corners of the polyhedra, are joined by shared oxygen. The final zeolite structure consists of assemblages of the secondary units in a regular three-dimensional crystalline framework. The tetrahedral can be arranged in numerous ways, resulting in the possibility of some 800 crystalline structures, less than 200 of which have been found in natural deposits or synthesized in laboratories around the world [38].

Zeolites have received increasing attention for pollution control. There are more than 30 natural zeolites known. Only seven (mordenite, clinoptilolite, chabazite, erionite, ferrierite, phillipsite, and analcime) occur in sufficient quantity and purity to be considered exploitable. A review of natural zeolite utilization in metal effluent treatment applications has been published [39]. The removal of metal cations from water by zeolites is due to ion exchange mechanism. Alkali or alkali earth cations (such as Na, K, Ca, Mg, etc.) are exchanged by contaminant metals. Nevertheless the major shortcoming in using zeolites as adsorbents is that these materials can be dissolved by relatively acid or basic solutions.

1.1.3.3 Polymeric resins

Most commercial macroreticular polymers are based on synthetic polymers (Figure 1.3) such as styrene crosslinked by divinylbenzene (M1), phenol-formaldehyde (M2) and acrylic ester (M3). Cross-linking provides high surface area as well as the rigidity and mechanical strength. These polymeric matrices can be functionalized with a variety of functional groups which give cation or anion exchange properties to the resins. For example, polystyrene can be sulfonated with sulfuric acid resulting in a $-SO_3-H^+$ group attached to the benzene ring, and the proton can be easily exchanged with other cations. Likewise, attaching ammonium or amine groups results in anion exchange resins. Several matrices and ion exchange functional groups are shown in Figure 1.3.

Ion-exchange resins have been used for water treatment. Ionized pollutants are exchanged with ions that neutralize the charge of functional groups in the polymeric resins. For example, chromium (III) ions are exchanged with protons in strong acid sulfonate or weak acid carboxyl resins (see Figure 1.3 C1), whereas arsenate anions exchange with chloride anions in strong-base anion-exchange resins (see Figure 1.3 A1 and A2). In contrast, organic pollutants could be adsorbed by means of π–π interactions with aromatic rings of the polymeric resins.

Among the ion exchange resins, those based on weak bases and weak acids exhibit higher ion-exchange capacities than those based on strong bases and strong acids [34, 40]. However, regeneration of strong-acid or strong-base resins is easier than for the weak-acid or weak-base resins. This could be due to the formation of covalent coordinated bonds between the contaminants and the chelating resins functionalities (e.g. weak base secondary amine groups).

19

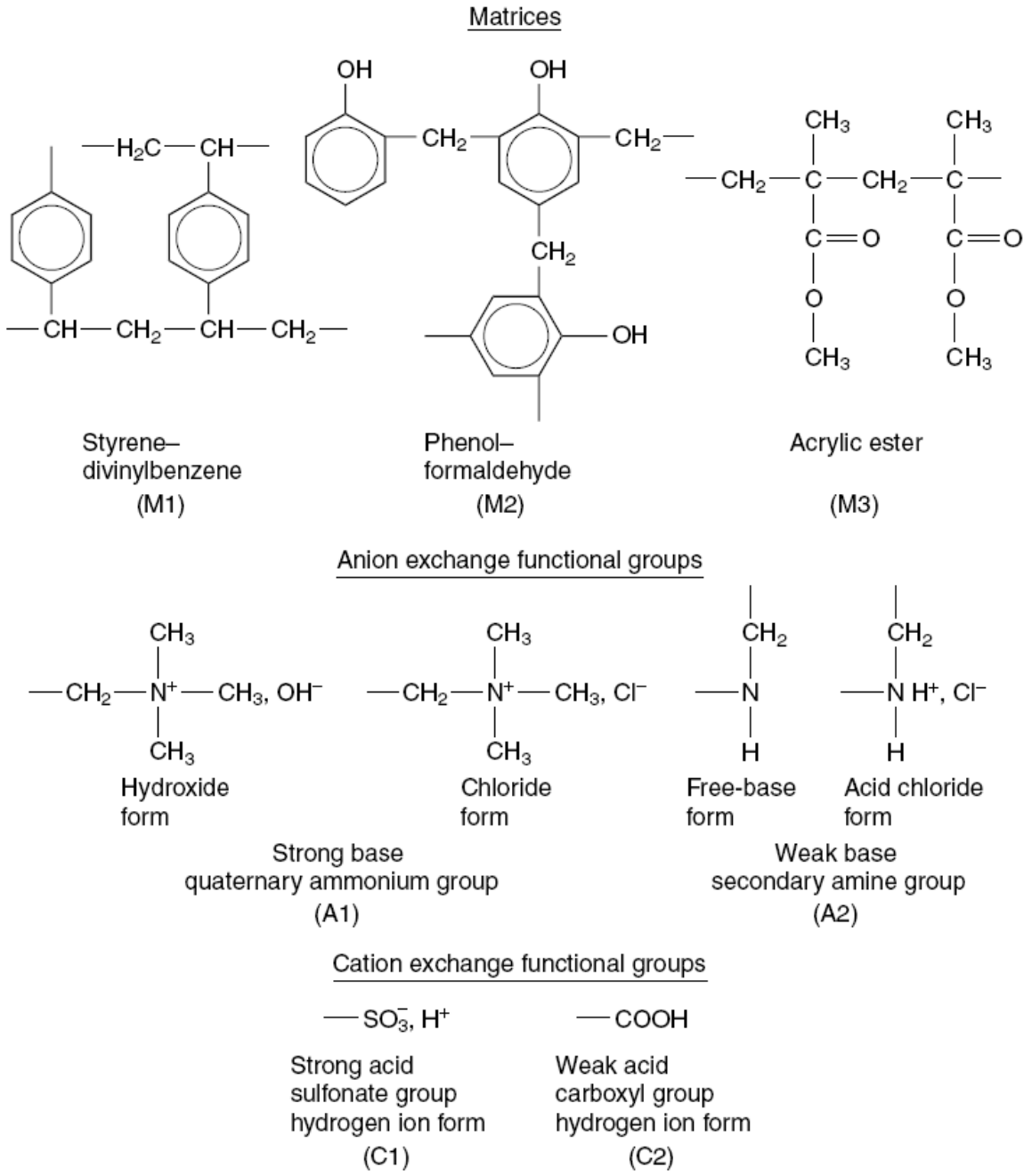

Figure 1.3. Polymeric resin matrices and ion exchange functional groups [34].

1.1.3.4 Biosorbents

Biosorption can be defined as the removal of substances (organic or inorganic) from aqueous solution by biological materials such as living or dead biomass [1]. In this thesis, the term biosorption will be used to describe any system where an

adsorbate (i.e. ions and/or molecules) interacts with a biosorbent resulting in an accumulation at the solute-biosorbent interface, and a consequent reduction in the adsorbate concentration in solution.

In recent years, many low-cost biosorbents have been investigated to remove pollutants from aqueous solutions, for example: seaweed biomass, chitin and chitosan, living or dead microorganism biomass, lignocellulosic materials, etc. The main characteristics of these biosorbents are discussed in the following section.

1.1.3.4.1 Seaweed biomass

Among all biosorbents, brown seaweed biomass seems to be the most effective and promising substrate to remove metal cations from aqueous solutions. Nevertheless, the low availability of seaweed biomass limits their use at an industrial scale.

The cell wall of algae is composed of at least two different layers. The innermost layer consists of a microfibrillar skeleton that imparts rigidity to the wall. This layer is made up of a cellulose polymer (β 1→4 linked unbranched glucan) in brown algae, whereas in green and red algae it is composed of cellulose, xylan (principally a β(1→4)-linked D-xylose) and mannan (a β(1→4)-linked D-mannose). The outer layer is an amorphous embedding matrix that contributes to the strength of the cell wall of brown algae in addition to imparting flexibility. The main components of this embedding matrix are predominately alginic acid or alginate and a sulfated polysaccharide (fucoidan). These two components occur in the matrix and also within the inner cell wall [41].

Alginic acid or alginate, the salt of alginic acid, is the common name given to a family of linear polysaccharides containing 1,4-linked β-D-mannuronic (M) and α-L guluronic (G) acid residues arranged in a non-regular, blockwise order along the chain. Fucoidan is a branched polysaccharide sulfate ester with 1-fucose-4-sulfate building blocks as the major component: these are predominantly α(1→2)-linked. Figure 1.4 shows the chemical structure of alginate and fucoidan biopolymers.

The adsorption of metals in brown seaweed biomass has mainly been attributed to the carboxyl groups of alginate biopolymer and to a lesser extent to the sulfonic

groups contained in fucoidan polymer (see Figure 1.4) [43]. The maximum metal adsorption capacity is obtained at pH values around 5 because at this condition most of the carboxyl groups are ionized and sulfonic groups are fully dissociated. In addition, the importance of carboxyl groups in metal adsorption has been assessed by means of FTIR analyses [18] and, indirectly, by chemical modification of these groups [43].

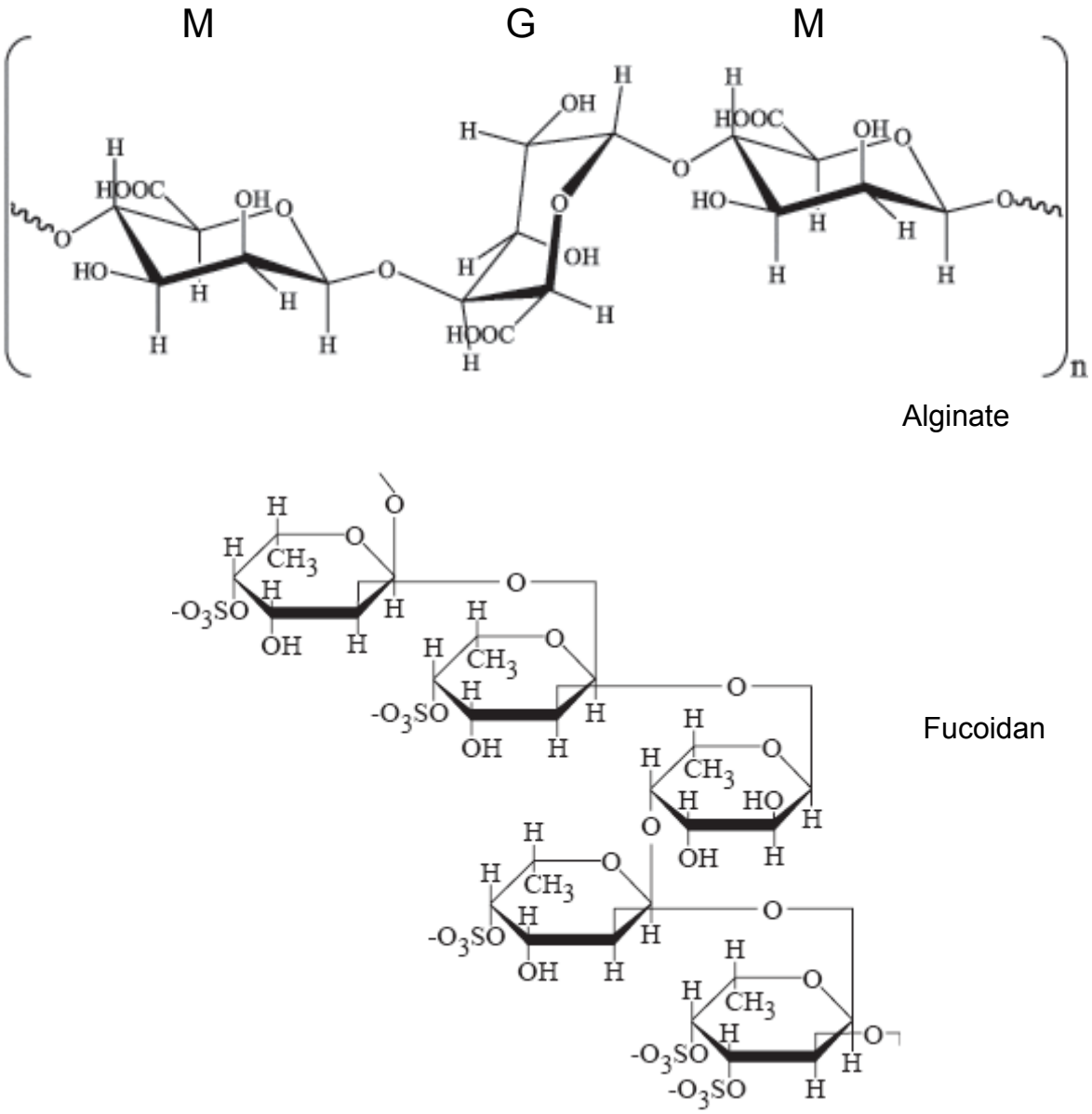

Figure 1.4. Structure of alginate acid and fucoidan polymers [42].

1.1.3.4.2 Chitin and chitosan

Chitinous biomass is the second most abundant biopolymer around the world. Chitin can be obtained from fungi, insects, lobster, shrimp and krill, although the most preferred commercial source is the exoskeletons of crab. These wastes are obtained from seafood industrial processing. In crab shells, chitin is associated to proteins, inorganic materials (e.g. $CaCO_3$), pigments and lipids. In order to obtain chitin from crab shells, it is required to dissolve the inorganic materials by acid solutions, to extract proteins by alkali solutions, and to remove pigments with solvents such as alcohol or acetone. Chitosan, a derivative of chitin, can be obtained under strongly basic conditions aided by heating.

Chitin is a natural homopolysaccharide consisting of (1, 4) 2-acetamide-2-deoxy-D-glucose units (acetyl glucosamine). Chitosan (glucosamine) is the deacetylated form of chitin. Figure 1.5 shows the repeating units of these two biopolymers.

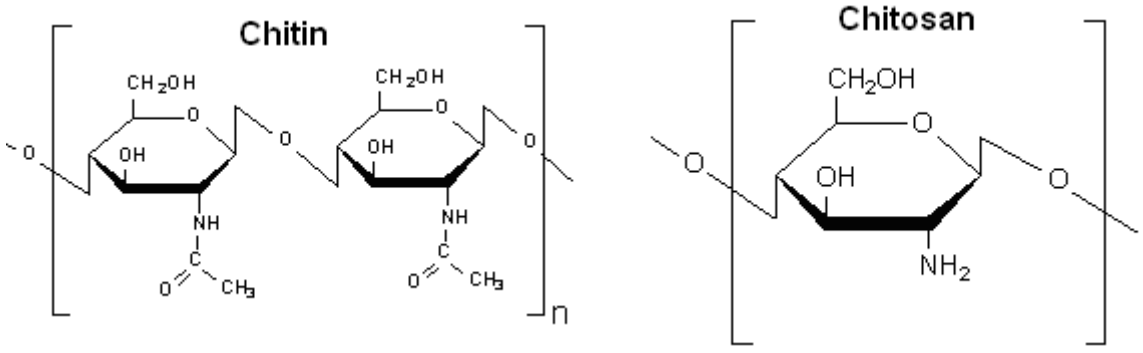

Figure 1.5. Repeating units of chitin and chitosan biopolymers.

The acid dissociation constant (pK_a) of chitosan is 6.5 and <3.5 for chitin. Protonated amine/amide groups of chitinous biosorbents are the binding sites to remove anions from aqueous solutions such as arsenate [44], fluoride [45, 46], chromate [47], etc. To enhance the adsorption of anions, the solution pH must be below the pK_a values of the binding sites (i.e. amine/amide). In contrast, if metal cations are going to be removed, the solution pH should be above the pK_a of the binding sites since an electrons pair is available to form complexes with metals such as lead, cadmium, zinc, copper, etc. In summary, amine and/or amide

functional groups of chitinous biomass play an important role in adsorption of pollutants from aqueous solutions. Nevertheless, the major shortcoming of using chitin/chitosan biosorbents is that can be dissolved in acidic solutions; consequently, regeneration with acids is not adequate because of the biosorbent loss.

1.1.3.4.3 Microorganism biomass

Bacterial and fungal biomasses can be inexpensive and are available from the wastes of some industries. These biosorbents are effective in removing contaminants from aqueous solutions. However, the raw materials may contain residual chemicals that affect the metal adsorption performance and a variable biosorbents quality may be obtained due to the process where these are collected [41]. Moreover, it is sometimes required to immobilize microorganism biomass before these can be used in reactors, which increases the cost of these biosorbents.

Adsorption of cations and anions may be due to the nitrogenated and phosphated biomolecules contained in the cell wall of fungi and bacteria [41]. Nitrogenated biomolecules include chitosan, chitin, and peptidoglycan, whereas phosphated biomolecules include teichoic acid, lipopolysaccharides, and phospholipids. Carboxyl and phosphate groups are the major contributors to the removal of cations from aqueous solutions since these functional groups are negatively charged at an appropriate pH. On the contrary, protonated amine groups create a positive charge in the microorganism biomass, allowing the removal of anions from aqueous solutions at certain conditions. Nitrogen-containing groups can also form complexes with metal cations because of the free electron pairs of these groups.

1.1.3.4.4 Lignocellulosic materials

The removal of pollutants by lignocellulosic materials has been widely investigated in the past decades. These biosorbents have a reasonable adsorption capacity and are widely available in many countries around the world. The functional groups (e.g. carbonyl, phenolic, amide, amine, sulfate, etc.) present in agricultural waste

biomass have affinity for heavy metal ions, forming metal complexes or chelates. The mechanism of biosorption process includes complexation, electrostatic interaction as well as ion exchange.

This thesis focuses on the application of agro-waste materials sorghum straw (*Sorghum bicolor*), oats straw (*Avena monida*), and agave bagasse (*Agave salmiana*), locally available in Mexico as biosorbents of chromium (III) from aqueous solution including their chemical and physical characterization, sorption/desorption studies, sorption mechanism and adsorption kinetic experiments.

In the following sections, an extensive review of the removal of metals from water by using biosorbents materials is presented. The topics discussed next include the components and functional groups of lignocellulosic materials, adsorption/desorption studies in both batch and continuous operation, and kinetic experiments.

1.2 GENERAL REVIEW

The selection of a proper adsorbent to remove certain contaminants is a complex problem. For example, if adsorption is chosen for removing metals from water, various details should be known such as the solute chemistry and physical–chemical properties of the adsorbent material [34]. Indeed, the chemical composition of biosorbents is a key factor to understand the possible functional groups able to sequester metals from aqueous solutions.

1.2.1 Components of lignocellulosic materials

The plant cell wall is a dynamic compartment that changes throughout its life. The new primary cell wall (Figure 1.6) is born in the cell plate during cell division and rapidly increases in surface area during cell expansion, in some cases by more than a hundred-fold. The middle lamella forms the interface between the primary walls of neighboring cells; it is a polysaccharides–rich matrix. Middle lamella maintains primary cell walls together. In older cells, middle lamella is sometimes degraded and an air space forms. Finally, multilayered secondary cell walls (Figure

1.6 S1, S2, S3) are developed within the primary wall when plants have achieved their final size and shape, building complex structures uniquely suited to the function of the cell [48].

The plant cell wall is a highly-organized composite of many different polysaccharides, proteins, and aromatic substances [49]. Some structural molecules act as fibers, others as a cross-linked matrix, analogous to the glass-fibers and plastic matrix in fiberglass. The molecular composition and arrangements of the wall polymers differ among species, tissues of a single species, individual cells, and even among regions of the wall around a single protoplasm.

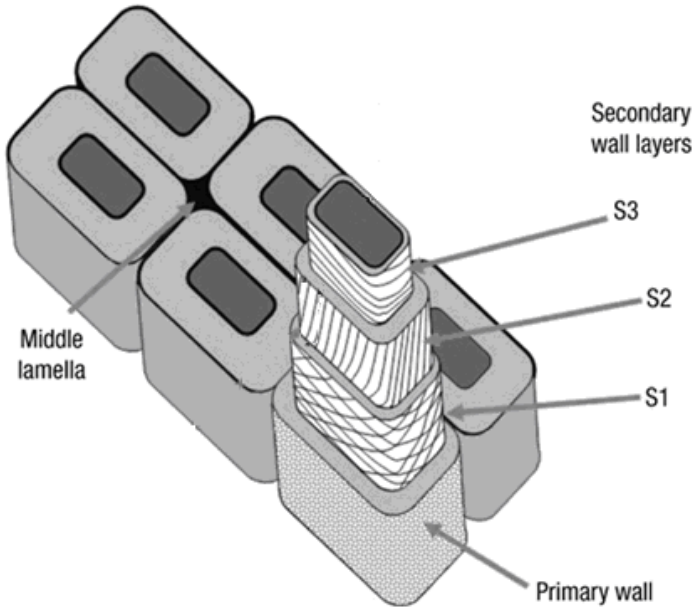

Figure 1.6. Schematic representation of the plant cell wall [49].

Most plant tissues are mainly made of such structural carbohydrates as cellulose, hemicelluloses, pectin, lignin, proteins, suberines, cutines, mineral salts and waxes [48-50]. Structural and functional properties of the cell wall mainly depend on the chemical composition and the physical and chemical interactions among all the structural and amorphous constituents [51]. Cell wall components are linked together by covalent bonds, ionic bonds, hydrogen bonding and hydrophobic interactions. These interactions are essential to join neighbor cells, to resist

chemical and/or enzymatic attacks, and to give a net surface charge to the lignocellulosic matrix. Figure 1.7 shows a schematic model of the primary plant cell wall, showing major structural polymers and their likely arrangement in the wall. These chemical constituents are the most abundant natural compounds available on earth. In addition, they are the most important renewable natural resource, and will be used intensively both as a source of energy and as raw materials for industrial processes [48].

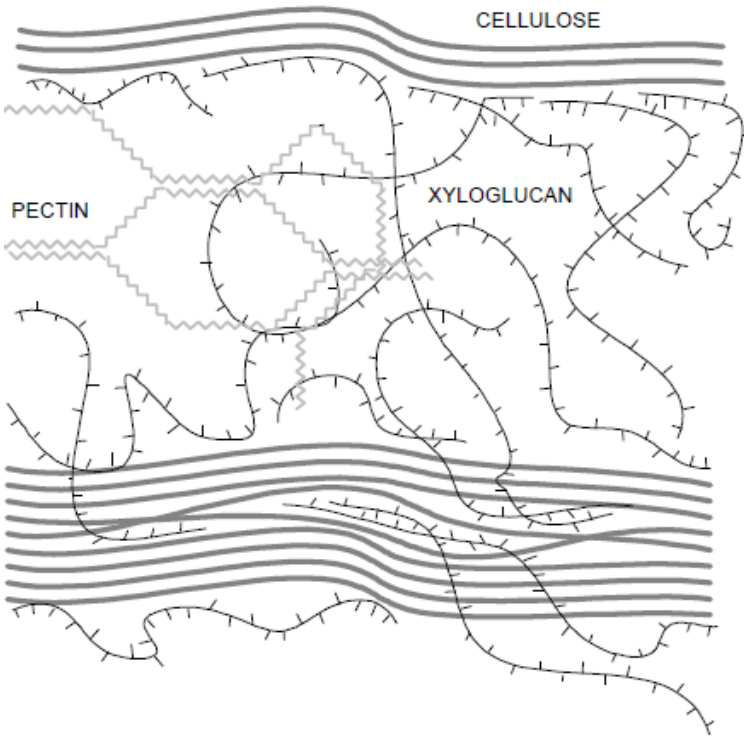

Figure 1.7 Schematic model of the primary plant cell wall, showing major structural biopolymers and their likely arrangement in the wall [52].

1.2.1.2 Cellulose

Cellulose is the most abundant plant polysaccharide in the world. This biopolymer is naturally found as arrays of microfibers, with variable length (0.2–2 μm) and diameters (5–30 nm). Also smaller fibers (length of 0.2–2 μm, and diameters of 3–5 nm) named elemental fibers can be observed which are arrayed in parallel positions to form microfibers [50]. By means of X-ray diffraction analyses, it has

been demonstrated that each microfiber is composed of 40–70 linear chains ordered in parallel position. Every biopolymer chain is a cellulose molecule constituted of a number (500–5000) of glucose residues linearly polymerized by means of β-(1-4) glycosidic bonds. Besides this linkage, biopolymer chains are linked together by hydrogen bridges (Figure 1.8).

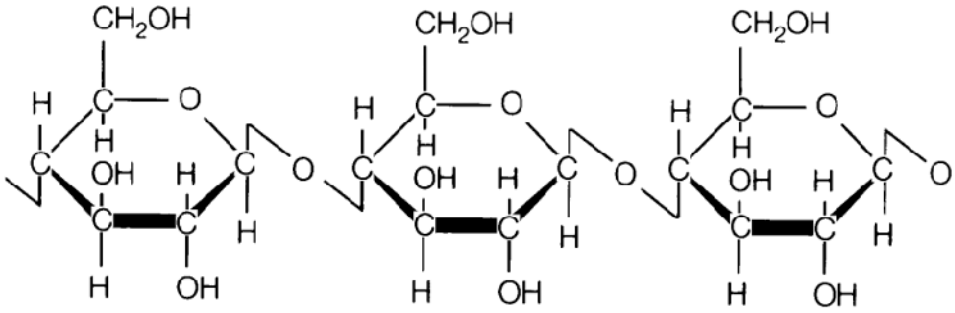

Figure 1.8. Chemical structure of the building blocks of cellulose biopolymer.

1.2.1.3 Hemicelluloses

Hemicelluloses can be any of several heteropolymers (matrix polysaccharides) present in almost all plant cell walls along with cellulose. While cellulose is crystalline, strong, and resistant to hydrolysis, hemicellulose has a random, amorphous structure with little strength. It is easily hydrolyzed by dilute acid or base as well as some enzymes. Hemicelluloses are a complex heteropolymers of glucose, mannose, xylose, galactose, rhamnose, arabinose, among others [50]. Hemicelluloses also contain most of the D-pentose sugars, and occasionally small amounts of L-sugars as well. Xylose is the sugar monomer always present in the largest amount, but mannuronic acid and galacturonic acid also tend to be present. These components contain carboxyl groups which could be used as adsorption sites of positively-charged species (i.e. metal cations). Because xyloglucans are longer (50–500 nm) than the spacing between cellulose microfibrils (20–40 nm), these have the potential to link microfibrils together (see Figure 1.7) [52].

1.2.1.4 Pectin

Pectin is a complex mixture of polysaccharides found in the middle lamella of the cell wall (see Figure 1.6 and Figure 1.7), gradually decreasing as one passes through the primary wall toward the plasma membrane [53]. The structure of pectin is very difficult to determine because this can change during isolation of plants, storage, and processing of plant material [54]. In addition, impurities can accompany the main components. At present, pectin is thought to consist mainly of D-galacturonic acid units [55], joined in chains by means of α-(1-4) glycosidic linkage. These uronic acids have carboxyl groups (possible sorption sites for metal cations), some of which are naturally present as methyl esters depending on the degree of esterification. In addition to the galacturonic segments, neutral sugars are also present. Rhamnose is a minor component of the pectin backbone and introduces a kink into the straight chain and other neutral sugars such as arabinose, galactose and xylose [54]. Hydrogen bonding, a long neutral or acid polysaccharides, as well as calcium bridges in carboxyl moieties link adjacent pectin chains.

1.2.1.5 Lignin

Lignins are complex racemic aromatic heteropolymers derived mainly from three hydroxycinnamyl alcohol monomers differing in their degree of methoxylation, p–coumaryl, coniferyl, and sinapyl alcohols [49, 50]. These monolignols produce, respectively, p-hydroxyphenyl, guaiacyl, and syringyl phenylpropanoid units when incorporated into the lignin polymer [56]. Lignin deposition is one of the final stages of xylem cell differentiation and takes place mainly during secondary thickening of the cell wall [49]. Generally, secondary cell walls consist of three layers: the outer (S1), middle (S2), and inner (S3) (see Figure 1.6). Lignin deposition proceeds in different phases, each preceded by the deposition of carbohydrates, and starts at the cell corners in the region of the middle lamella and the primary wall when S1 formation has initiated. When the formation of the polysaccharide matrix of the S2 layer is completed, lignification proceeds through the secondary wall. The bulk of lignin is deposited after cellulose and hemicelluloses have been deposited in the

S3 layer. Generally, lignin concentration is higher in the middle lamella and cell corners than in the S2 secondary wall [49]. However, because it occupies a larger portion of the wall, the secondary wall has the highest lignin content. The amount and composition of lignins vary among taxa, cell types, and individual cell wall layers and are influenced by developmental and environmental conditions [49, 50]. Lignin is crucial for the structural integrity of the cell wall as well as stiffness and strength of the stem. In addition, lignin waterproofs the cell wall, enabling transport of water and solutes through the vascular system, and plays a role in protecting plants against pathogens [50].

1.2.2 Techniques used to identify and quantify functional groups

To identify functional groups on lignocellulosic materials various techniques have been used, for example: Fourier transform infrared (FTIR) spectroscopy to identify surface functional groups [4, 19, 20, 57-60], X-ray absorption spectroscopy (XAS, XANES, EXAFS, XPS) to determine the electronic configuration of metal species adsorbed as well as possible sorption sites [4, 61-65], acid-base titrations to quantify functional groups and their equilibrium constants [18, 20, 58, 66], and chemical modifications to indirectly corroborate if carboxyl-binding sites are responsible for metal adsorption [43, 62, 65], among others.

The use and the principal characteristics of these techniques as well as the findings by using these strategies are discussed in detail in the following sections.

1.2.2.1 Fourier transform infrared (FTIR) spectroscopy

FTIR spectroscopy is of great interest because it could be used in conjunction with other techniques to determine the molecule structure. Infrared radiation is absorbed and converted by an organic molecule into energy of molecular vibration [16]. The frequency or wavelength of absorption depends on the relative masses of atoms, the force constants of the bonds, and the geometry of atoms. In the spectrum, each wavenumber can be related to a particular vibration of a functional group.

Functional groups identified on lignocellulosic materials by Fourier transform infrared analyses [4, 19, 20, 57-60] include hydroxyl, carbonyl, carboxyl, nitrogen-containing groups (i.e. amine, amide), etc. The characteristic absorbance peaks of these groups correspond to those reported in literature [67, 68]. Moreover these groups are associated to the components (cellulose, pectin, hemicelluloses, lignin, and glycoprotein) of the lignocellulosic materials [48-50].

1.2.2.2 X-ray absorption spectroscopy (XAS)

X-ray absorption spectroscopy (XAS) is useful to speciate and quantify the form of metals in structurally and chemically complex heterogeneous matrices such as soils, sediments, and various wastes [64]. This technique provides information on the coordination environment of the absorbing element, for instance the nearest neighboring atoms and the ligands involved in the binding of metals [63-65].

Results from XAS revealed that metal cations are preferentially bound to oxygen-containing groups. For example, in soils contaminated with alkyl-tetravalent lead compounds, lead was found to be divalent and complexed to salicylate and catechol-type functional groups of humic substances [64] and near a smelter, lead was found to be divalent and coordinated to O and OH ligands. In other studies, it was reported that aqueous Cr (VI) is reduced to Cr (III) on rice husk [63], saltbush biomass [65], and seaweed biomass [61] through a reduction and adsorption combine mechanisms on carboxyl and hydroxyl groups.

1.2.2.3 X-ray photoelectron spectroscopy (XPS)

XPS is a quantitative spectroscopic technique that measures the elemental composition, empirical formula, chemical state and electronic state of the elements that exist within a material.

Krishnani *et al.* [4] used XPS to determine the speciation of Cr, Cd, and Hg loaded on treated rice husk. The XPS spectrum of chromium-treated biomatrix revealed an extensive reduction of Cr (VI) sorbed onto biomatrix to its trivalent form. Likewise XPS spectra indicated that the Cr (VI) bound to brown seaweed biomass was completely reduced to Cr (III) under various tested conditions [61].

1.2.2.4 Acid-base titrations

Functional groups of adsorbents are dissociated or protonated in function of the solution pH. Potentiometric titrations are used to determine the quantity and equilibrium constants of the functional groups. Potentiometric titrations of seaweed biomass revealed that biomass contains at least four types of functional groups: sulfate, carboxyl, hydroxyl and other functional groups (i.e. phosphoryl, amine, and imidazole group) having pK_a values around 7.2 [18, 43]. These functional groups, except sulfate groups, were also found in heterogeneous organic matter, dead fungi and bacteria [69] and lignocellulosic materials (further details are given in Chapter 2 of this thesis) [20] by potentiometric titrations.

1.2.2.5 Chemical modifications

There is another way to indirectly confirm if carboxyl groups on lignocellulosic adsorbents are the binding sites of metals. Some of the most important results are given herein. Partial esterification of carboxyl groups on seaweed biomass [43], alfalfa shoot biomass [62], and saltbush biomass [65] decreased the metal adsorption capacity. In contrast, oxidation with HNO_3 and chemical modification with citric acid of corncob increased considerably the metal adsorption capacity [66]. These findings evidently demonstrate that carboxyl groups play a major role in metal cations adsorption. In the case of seaweed biomass, sulphates also contribute to a lesser extent, to heavy metal binding by electrostatic interaction, particularly at low pH [43].

1.2.3 Biosorption of heavy metals on lignocellulosic materials

Several researchers have used lignocellulosic materials as biosorbents to remove heavy metals from aqueous solutions [2-5, 9, 15, 17, 19, 20, 60, 62, 66, 71-74]. The advantages for using these types of biosorbents are their low-cost, availability, and competitive metal adsorption capacity. Moreover, lignocellulosic materials, by-products of various industries or agricultural residues, are produced in large quantities as wastes, creating environmental problems if these are burned or disposed of inappropriately. However the major disadvantages of lignocellulosic

adsorbents of metals are their degradability and that their use in sorption columns is limited since the characteristics of the particles introduce hydrodynamic limitations and column fouling [75].

As previously mentioned, adsorption processes depend on the physical-chemical properties of the adsorbent and also of the experimental conditions, for instance the solution pH that affects the ionization of surface functional groups on the adsorbent and the speciation of solutes in aqueous solutions. However, due to the heterogeneity of the lignocellulosic biosorbents, it is necessary to conduct equilibrium, kinetic and flow-through column experiments in order to select an appropriate adsorbent as well as the optimal conditions of operation. These topics are going to be discussed in the following sections.

1.2.3.1 Equilibrium adsorption studies

The adsorption of metals at equilibrium has been extensively explored. For example, Krishnani *et al.* [4] reported that the maximum uptake of divalent metals (Pb, Cd, Co, Zn, Hg, Cu, Mn, Ni) on alkali-treated rice husk at 32°C took place at pH 5.5–6.0. Maximum adsorption capacities ranged from 5.5 to 58.1 mg/g which increased in the order: Ni<Zn<Mn<Co<Cu<Cd<Hg<Pb. At pH 2, lower adsorption capacities (1–13 mg/g) were achieved in comparison with the optimal pH value (pH 5.5–6.0). At pH 6.0, Dang *et al.* [76] determined Q_{max} of Cd (14.61 mg/g) and Cu (11.44 mg/g) on acid- and alkali-washed wheat straw (*Triticum aestivum*) biomass, which are similar to the reported values by Krishnani *et al.* [4] (16.7 mg/g for Cd and 10.9 mg/g for Cu). Riaz *et al.* [59] studied the adsorption of Pb on water-washed *Gossypium hirsutum* (Cotton) waste biomass, they found that the adsorption capacity increases as pH rise from 3 to 5 achieving Q_{max} at pH 5 (196.07 mg/g). Parab *et al.* [72] used water-washed coir pith to adsorb Co (II) and Ni (II); the optimum pH values for maximum metal-ion adsorption were determined as 4.3 for cobalt (7.22 mg/g), and 5.3 for nickel (11.40 mg/g). In another study, Reddad *et al.* [5] used water-washed sugar-beet pulp for sequestering various divalent metal ions (Pb, Cu, Zn, Cd, and Ni) from aqueous solutions. The maximum sorption capacities, at initial pH of 5.5 and 20°C, predicted by the Langmuir model

varied from 11.86 to 73.76 mg/g (higher than the base-treated rice husks) in the next order: Ni<Zn<Cu<Cd<Pb. It is important to note that lead ions have a high affinity towards adsorption groups of lignocellulosic adsorbents.

The removal of metals by using chemically modified biosorbents has been also tried; for example, Leyva-Ramos *et al.* [66] demonstrated that the maximum adsorption capacity of cadmium, at pH 6 and 25°C, was increased 10.8 to 3.8 times (Q_{max} of natural corncob equal to 5.09 mg/g) when the corncob was modified with citric acid and oxidized with nitric acid, respectively. Tiemann *et al.* [62] studied the adsorption of Ni (II) on acid-washed, esterified with acidic methanol and hydrolyzed with 0.1 N NaOH alfalfa biomass at pH 5.0. The Ni (II) adsorption capacity of acid-washed biomass was 12.3 mg/g, whereas the esterification of the biomass caused a reduction of 91% of the binding of Ni (II), and the hydrolysis of the biomass increased 29% the adsorption capacity of Ni, compared to the results of non-treated biomass. In general, chemically modified plant wastes (with citric acid, base-hydrolysis or both) exhibit higher adsorption capacities than unmodified biosorbents [58, 62, 66, 73, 77]. Various review articles are available in the literature [14, 24, 58, 78, 79] that collect metal adsorption results from many investigations.

Finally, although the adsorption capacity of metals of lignocellulosic materials is lower than or similar to commercial ions exchangers (i.e. polymeric resins) the main advantages of using these biosorbents are the low-cost and availability of these materials.

1.2.3.2 Effect of pH on metal adsorption by biosorbents

Most research studies reported in the literature have evaluated the influence of pH on the adsorption capacity. These results have demonstrated that the removal of metal ions is highly dependent on pH [5, 18, 20, 66, 72]. This can be explained since the solution pH affects both the surface charge of the adsorbent (i.e. the degree of ionization of surface functional groups) and the speciation of metals in solutions.

As an example, to evaluate the properties of carboxyl groups on biomass (R-COOH) in function of the solution pH, their reaction with a proton and their equilibrium constant (K_a) can be defined as follows:

$$R\text{-}COOH \leftrightarrow R\text{-}COO^- + H^+ \qquad K_a = \frac{[R-COO^-][H^+]}{[R-COOH]} \tag{5}$$

The total concentration ($[R\text{-}COOH]_T$) of the functional group is equal to the sum of the protonated [R-COOH] and ionized [$R\text{-}COO^-$] configurations. After some arrangements, the concentration of the ionized group can be expressed as a function of the total concentration of the sites and of the proton concentration:

$$[R-COO^-] = \frac{[R-COOH]}{1+[H^+]/K_a} \tag{6}$$

The concentration of protonated groups [R-COOH] is calculated as the difference between the total concentration ($[R\text{-}COOH]_T$) and ionized [$R\text{-}COO^-$] groups. Figure 1.9 shows the effect of pH on the ionization of carboxyl groups that have pK_a values of 4.0 and density of 0.5 mmol/g.

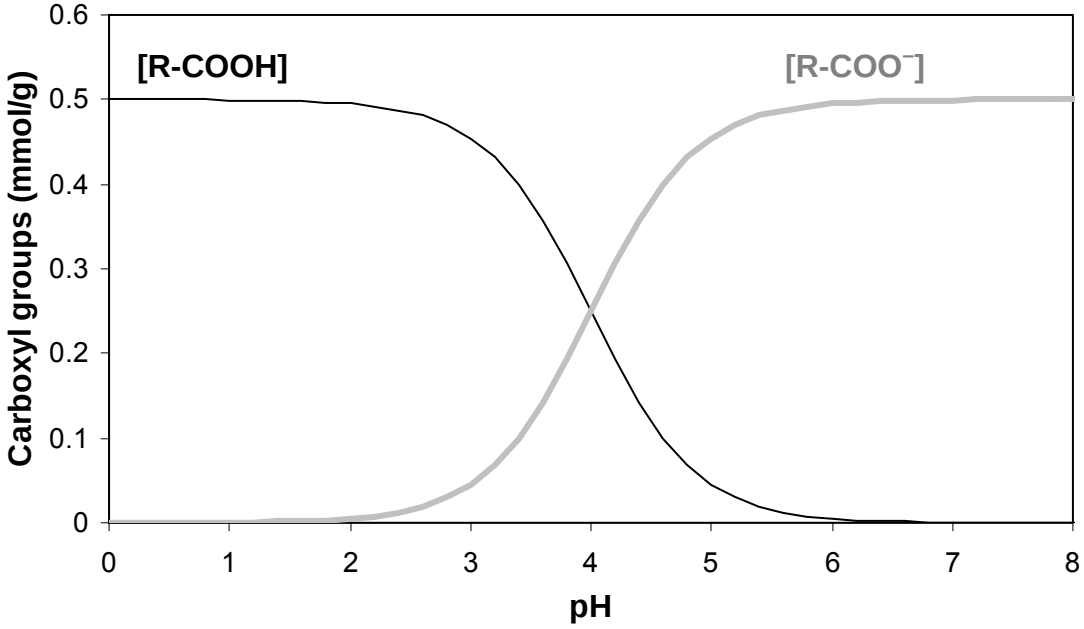

Figure 1.9 Effect of pH on the ionization of carboxyl groups ($[R\text{-}COOH]_T$=0.5 mmol/g and pK_a 4.0). Black line represents the protonated carboxyl groups [R-COOH] and gray line represents the ionized carboxyl groups [$R\text{-}COO^-$].

At pH=pK_a, the number of ionized and protonated groups is the same. As pH increases (pH>pK_a), the quantity of ionized groups increase, for example: at pH 6, 99% of the total carboxyl groups are ionized and metal adsorption will achieve the highest capacity (see Figure 1.9). In contrast, as pH decreases (pH<pK_a) the quantity of protonated groups increases, for instance: at pH 2, 99% of the total carboxyl groups are protonated, consequently the adsorption of metal cations is less (see Figure 1.9).

Furthermore, above the point of zero charge (pH_{pzc}), the adsorbent surface charge is predominantly negative and therefore could adsorb positively-charged species (metal cations or H^+). When increasing the solution pH, the metal adsorption capacity increases because more ionized groups (e.g. carboxyl) are available to adsorb metals.

Table 1.4. Equilibrium reactions of the solubility of $Cr(OH)_3$.

Reaction	log K (I = 0)	log K (I = 0.01)
$Cr(OH)_{3\,(s)} \leftrightarrow Cr^{3+} + 3OH^-$	-30.0	-29.4
$Cr^{3+} + OH^- \leftrightarrow CrOH^{2+}$	10.0	9.8
$Cr^{3+} + 2OH^- \leftrightarrow Cr(OH)_2^+$	18.3	17.9
$Cr^{3+} + 3OH^- \leftrightarrow Cr(OH)_3^+$	24.0	23.7
$Cr^{3+} + 4OH^- \leftrightarrow Cr(OH)_4^-$	28.6	28.1
$3Cr^{3+} + 4OH^- \leftrightarrow Cr_3(OH)_4^{5+}$	47.8	47.5
$H^+ + OH^- \leftrightarrow H_2O$	14.0	13.9

Equilibrium constants (25°C) were taken from Baes and Messmer [80].

Regarding metal species in aqueous solutions, the solution pH determines the dissolution and precipitation of metal species. The extent of dissolution or precipitation reaction for systems that attain equilibrium can be estimated by considering the equilibrium and solubility constants. For example, Stumm and Morgan [81] estimated the solubility of Cr (III) hydroxide as a function of pH. These authors considered the reactions given in Table 1.4, associated to their equilibrium

constants, in calculating the metal species in solution. It was concluded that the solubility of Cr (III) hydroxide is markedly affected on the acid side (pH<6) by the polynuclear species $Cr_3(OH)_4^{5+}$. In addition, various softwares such as VMINTEQ and PHREEQ [82, 83] are available free of charge on the web that can be used to compute speciation diagrams of metals in aqueous solutions. Further details about the Cr (III) species present in aqueous solutions are shown on Figure 2.3 in Chapter 2.

1.2.3.3 Adsorption kinetics of metals on various biosorbents

Besides equilibrium adsorption data of solutes, adsorption kinetics is also required to select an adsorbent and to design an adsorber. Although its known that mass transfer is limited by diffusion of solutes into porous adsorbents, most adsorption studies have reported that adsorption kinetics follows pseudo-first order model [84] or pseudo-second order model [85]. However these models only predict the overall adsorption rate and do not help to understand physically the mass transfer in adsorption processes. On the contrary, diffusion models [66, 86, 87] consider various resistances along the solute movement to the adsorbent particle. Such resistances are film diffusion and intraparticle diffusion (pore-volume diffusion and/or surface diffusion). Film diffusion resistance is related to the layer surrounding the adsorbent particle and intraparticle diffusion is associated with the transport of solutes into the pores of the adsorbent. Figure 4.1 in Chapter 4 shows a schematic representation of these resistances in adsorption processes.

This section will address the process of diffusion and its influence on the overall adsorption rate. Empirical and diffusion models developed to predict the adsorption kinetics of metals are briefly described in the following sections. More details are given in Chapter 4.

1.2.3.3.1 Empirical models

The overall rate of adsorption of various heavy metals has been predicted by using empirical models. This rate can be considered to follow pseudo-first order [84] or

pseudo-second order [85] reactions based on the quantity of solute adsorbed by the adsorbent.

The adsorption kinetics of dyes on orange peel wastes [88], organic compounds on chitin [89] and metal ions on sheep manure waste [90] was predicted with the pseudo-first order reaction model. Nevertheless, the pseudo-second order rate equation was most commonly used to describe the adsorption rate of metals on various biosorbents such as sphagnum moss peat [85], water-washed sugar-beet pulp [5], wheat straw [76], and coir pith [72].

1.2.3.3.2 Diffusion models

Only some research studies have reported the use of diffusion models in predicting the adsorption kinetics of metals on lignocellulosic materials and activated carbons. These models explain the mass transfer of solutes from solutions to the solid adsorbents.

The adsorption kinetics of cadmium, copper, and dyes on peat, lignite and activated chars was investigated [93] and the film diffusion models [91, 92] were successfully applied to predict the adsorption rate in batch reactors. At high sorbent doses, intraparticle diffusion can be neglected and the external resistance is the rate-controlling step. However, when lower masses of adsorbent are involved, the influence of intraparticle diffusion becomes apparent. These behaviors are quite different when dyes are adsorbed on peat and lignite: a single resistance model cannot predict well the adsorption process and intraparticle diffusion becomes important. Research studies have confirmed the importance of intraparticle diffusion in controlling the adsorption rate of Cd (II) and Zn (II) on activated carbons [66] and the adsorption of pentachlorophenol on activated carbon fibers [87].

Although empirical models are commonly used to predict metal adsorption kinetics, it is believed that diffusion models help to understand the mass transfer phenomena as occurs on adsorption of solutes in porous and non–porous materials. Readers are referred to Chapter 4 where more details are given

regarding the use of diffusion models in predicting and explaining the adsorption of Cr (III) on agro-waste materials.

1.2.3.4 Desorption of metals previously adsorbed by biosorbents

A small number of biosorption studies have reported desorption of metals from lignocellulosic materials. Sawalha *et al.* [60] conducted batch desorption experiments of Cd (II) bound to saltbush biomass. About 85% of the bound Cd was recovered using only 0.1 mM concentration of either HCl or sodium citrate. Diniz and Volesky [94] studied the desorption of La, Eu, and Yb from seaweed biomass (*Sargassum polycystum)* by using various eluting agents including nitric and hydrochloric acids, calcium nitrate and chloride salts, EDTA, oxalic acid and diglycolic acid at several concentrations. For all metals, desorption of individual metals with 0.3 M HCl varied from 95% to 100%. Similar desorption percentages were obtained by using HNO_3. Lower desorption percentages were attained by the other eluting agents. They also found that the use of either acid, HCl or HNO_3, resulted in a weight loss between 27–30%. A slightly lower weight loss, compared to the other results, was observed when 0.1 M HCl was used; consequently the authors recommended 0.2 M HCl for metal desorption to decrease the biomass loss. Leyva-Ramos *et al.* [66] conducted desorption batch experiments of Cd (II)-loaded corncob. It was found that Cd (II) desorbs almost completely from the corncob when the pH of the solution was reduced to 2.

All given results showed strong evidence that mineral acids are preferred as eluting agents in metal recovery from biosorbents. Nevertheless it is important to note that strong acid conditions highly affect some components of the biosorbents matrix, which can significantly reduce their adsorption capacity.

1.2.3.5 Adsorption mechanisms of metals on various biosorbents

The biosorption mechanism of metals is not easily elucidated since biosorbents have a complex structure. The building blocks of this complex structure have several binding sites which in turn can participate in different adsorption

mechanisms. Figure 1.10 shows the most probable adsorption mechanisms of metals and these are briefly analyzed in the following sections.

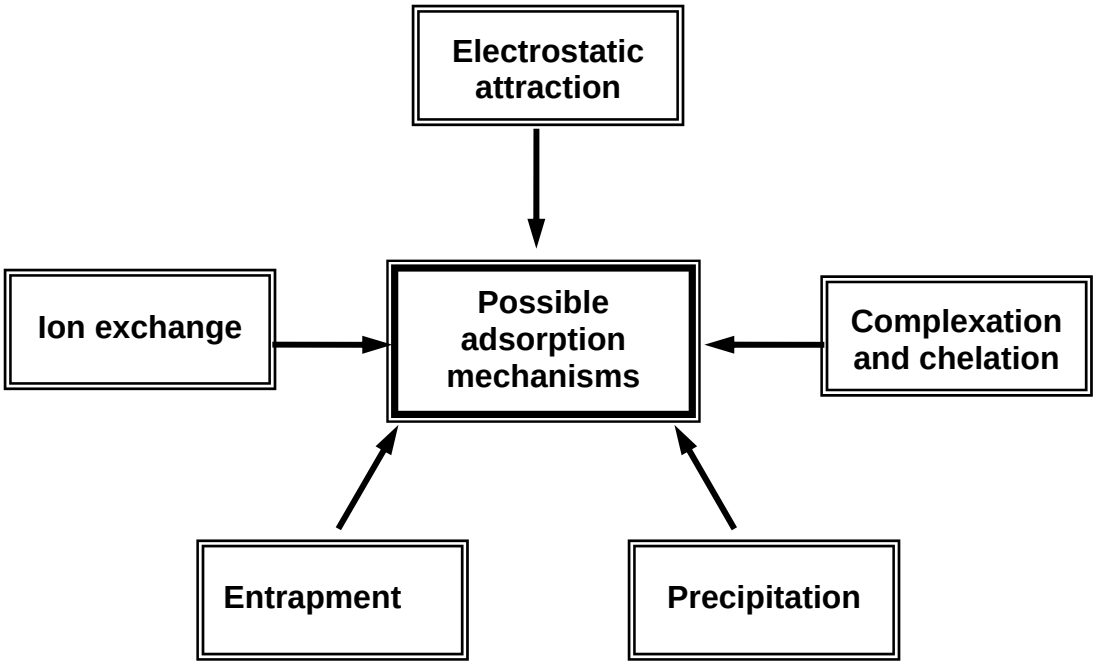

Figure 1.10 Most probable adsorption mechanisms of metals on adsorbents.

1.2.3.5.1 Electrostatic attraction

As previously mentioned, the solution pH affects the surface charge of biosorbents (i.e. the degree of ionization of surface functional groups). Ionized or protonated functional groups can interact with positively or negatively-charge adsorbate species to be adsorbed. For example, metals cations (M^{n+}) can be adsorbed by electrostatic attraction with any ionized carboxyl [4, 13, 17-20, 43, 60-62, 66, 74, 94], sulfonate [43] or phosphate groups as:

$$n[\equiv R\text{–}COO^{-}] + M^{n+} \leftrightarrow [\equiv R\text{–}COO]_n\text{–}M \quad (7)$$

$$[\equiv R\text{–}OPO_3^{2-}] + M^{n+} \leftrightarrow [\equiv R\text{–}OPO_3]\text{–}M^{n-2} \quad (8)$$

$$n[\equiv R\text{–}SO_3^{-}] + M^{n+} \leftrightarrow [\equiv R\text{–}SO_3]_n\text{–}M \quad (9)$$

In the same way, electrostatic attraction of protonated amine groups with anionic species (A^{-}) has been already reported as follows:

$$n[\equiv R\text{-}NH_2^{+}] + A^{n-} \leftrightarrow [\equiv R\text{-}NH_2]_n\text{–}A \quad (10)$$

1.2.3.5.2 Complexation or chelation

Ligands of the biomass (e.g. carboxyl, nitrogen-containing groups) can form complexes (or coordination compounds) or chelates with metal species. The electron pairs of ligands (donor atoms) are shared with metals (acceptor atoms) to form a coordinated bond. Metal chelates are metal complexes where there is an organic compound bound to the metal by two or more donor atoms. The adsorption mechanism of metal cations (M^{n+}) on carboxyl and nitrogen-containing [95] sites could be:

$$n[\equiv R\text{–}COOH] + M^{n+} \leftrightarrow [\equiv R\text{–}COO]_n\text{–}M + nH^{+} \quad (11)$$

$$n[\equiv R\text{-}NH_2] + M^{n+} \leftrightarrow [\equiv R\text{-}NH_2]_n\text{–}M \quad (12)$$

1.2.3.5.3 Ion exchange

It has also been reported that metal cations are exchanged with calcium or magnesium ions on lignocellulosic and seaweed biosorbents [4, 5, 20]. Calcium and magnesium ions are linked to carboxyl moieties associated to hemicelluloses and pectin biopolymers in lignocellulosic materials and alginates in seaweed biomass. Metal cations have a higher affinity for carboxyl groups than calcium and magnesium; consequently these ions are exchanged as follows:

$$[\equiv R\text{-}COO]_2\text{–}Ca + M^{2+} \leftrightarrow [\equiv R\text{-}COO]_2\text{–}M + Ca^{2+} \quad (13)$$

$$[\equiv R\text{-}COO]_2\text{–}Mg + M^{2+} \leftrightarrow [\equiv R\text{-}COO]_2\text{–}M + Mg^{2+} \quad (14)$$

1.2.3.5.4 Precipitation

Microprecipitation may occur if the solution pH is not controlled. Depending on the solubility of metal cations which is highly dependent on the solution pH and available ligands, these metal species can be in solution or precipitated. Shashirekha *et al.* [96] did not set the solution pH and may be the reason for obtaining Cr (III) sorption capacity as high as 125 mg/g which is approximately 5 times higher than other similar adsorbent (28 mg/g) [97]. The precipitation of metals cations (M^{n+}) as metal hydroxides ($M(OH)_{n\,(s)}$) can be represented as:

$$M^{n+} + nOH^{-} \leftrightarrow M(OH)_{n\,(s)} \quad (15)$$

1.2.3.5.5 Entrapment

The removal of metal species can also be by entrapment in the polysaccharides complex network. There are some free spaces in the biosorbents structure that accumulate pollutants as a result of the concentration gradient (diffusion through the pore-volume biosorbents). Nevertheless, the contribution of this mechanism to the removal of metals seems to be minor due the low pore volume of biosorbents.

In summary, understanding the adsorption mechanism of metals allows modeling of the adsorption process. These models can be applied to predict the influence of certain parameters such as ionic strength and pH [18, 98] on the metal adsorption capacity. Furthermore, the eluting agent can be chosen based on the adsorption mechanism. For instance, metals adsorbed on acidic functional groups can be recovered by lowering the solution pH; acidic groups protonate and metals are released to the solution [20].

1.2.3.6 Continuous flow-through adsorption experiments

A packed-bed flow-through column is the configuration commonly preferred in continuous adsorption processes. The performance of packed-bed adsorbers is analyzed using the breakthrough curves and the elution curves. Both curves are a function of the column flow parameters, sorption equilibrium and mass transport factors [99].

In this thesis, the adsorption process of Cr (III) on continuous operation was not explored; however it is important to mention some studies reported in literature. Several heavy metals were removed by using packed-bed columns with rice husks biomass (Pb, Cd, Al, Cu, and Zn) [74], silica-immobilized sorghum biomass [71] and *Agave lechuguilla* biomass (Cr (III)) [100], rice husk biomass (Pb, Hg, Cd, Ni, Co, Mn, and Zn) [4], and seaweed biomass (Cu) [99]. Regeneration of metal-loaded biosorbents was conducted with mineral acids (HCl) [71] or a mixture of $CaCl_2$ and HCl [99]. The adsorption capacity as well as the desorption of metals decreased every sorption–desorption cycle suggesting biomass hydrolysis and mass loss [71, 99]. Nevertheless, a continuous biosorption operation seems to be feasible.

Finally, it is important to mention that more continuous operations (i.e. adsorption and desorption cycles) are required by using either raw or immobilized biomass in order to demonstrate the effectiveness of this promising technology.

1.3 BACKGROUND

1.3.1 Removal of Cr (III) by biosorbents in aqueous solutions

For removing Cr (III) from aqueous solutions, a number of adsorbents have been tested. For example polymeric resins [11, 12, 101], activated carbon [95, 102, 103], seaweed biomass [10, 18, 21, 104], microorganism biomass [96, 97], raw and chemically modified lignocellulosic materials [9, 15, 19, 20, 60, 62, 65, 71, 72, 100, 105], etc.

Regardless of the adsorbent selected for the removal of Cr (III), to preserve Cr (III) species in aqueous solution instead of being precipitated as $Cr(OH)_3$, adsorption experiments of Cr (III) must be conducted at pH values lower than 4.6 based on the speciation diagram (see Figure 2.3 in Chapter 2) [18, 20].

It has been demonstrated that adsorption of Cr (III) on lignocellulosic materials is highly influenced by the solution pH; the adsorption capacity of Cr (III) increases with increasing solution pH [20, 57, 65, 71, 72, 106]. This can be explained since lignocellulosic materials contain carboxyl functional groups, previously identified by FTIR analyses [19, 20, 57, 60], which are able to be ionized or protonated in function of pH (see Figure 1.9). As pH increases (at $pH>pK_a$) more than 50% of the carboxyl groups are being ionized; therefore more metal cations are able to be adsorbed on it increasing the metal sorption capacity. To the contrary, as pH decreases ($pH<pK_a$), more carboxyl groups are protonated and metal sorption capacity decreases because H^+ ions compete for the same sorption sites.

Moreover the role of carboxyl groups on the adsorption of Cr (III) on lignocellulosic materials has been demonstrated direct or indirectly. Direct analysis of metal-loaded lignocellulosic materials by X-ray absorption spectroscopy suggested that Cr (III) binding mostly occurs through coordination with oxygen ligands [62, 63, 65]. Similar results have been reported by using seaweed biomass [61]. Indirectly, the importance of carboxyl groups on the lignocellulosic materials for binding metal

cations has been assessed because the esterification of carboxyl groups decreased the Cr (III) sorption capacity [60, 62, 65]. In addition, the adsorption of Cr (III) on agro-waste materials was coupled to the release of calcium ions or protons to the solution [20]. Ibañez and Umetsu [13] also reported an ion exchange mechanism between Cr (III) and H^+ ions when protonated dried alginate beads were used as adsorbents. Furthermore it has been reported that hemicelluloses and lignin (which have carboxyl groups) of agro-waste materials are the main contributors to the removal of Cr (III) from aqueous solutions [19]. These results clearly suggest that carboxyl groups on lignocellulosic adsorbents are the binding sites of Cr (III) ions (further details are given in Chapter 2 and 3).

Lignocellulosic materials used to remove Cr (III) and their maximum adsorption capacity include: water-washed alfalfa biomass (10.7 mg/g at pH 5.0) [62], acid-washed sorghum straw biomass (10 mg/g at pH 4.5–5.0) [71], acid-washed saltbush biomass (16.3, 22.7, 27.0 mg/g for steams, leaves and flowers, respectively, at pH 5.0) [65], water-washed coir pith (11.56 mg/g at pH 3.3) [72], acid-washed agave lechuguilla biomass (11.3 mg/g at pH 4.0) [15], and acid-washed plant biomass (28 mg/g at pH 5.0) [57] (further details are given in Table 2.2 in Chapter 2).

Tiemann *et al.* [62] reported that esterification of alfalfa biomass caused a reduction of 100% of the binding of Cr (III), whereas hydrolysis of the biomass increased 111% in comparison to non-modified acid-washed biomass (10.7 mg/g). In contrast, Sawalha *et al.* [65] reported dissimilar results; the maximum average sorption capacity of Cr (III) on native, esterified and hydrolyzed biomass was 22.0, 6.0 and 25.0 mg/g, respectively. In this case, Cr (III) adsorption capacity decreased 72% due to esterification of the biomass, while increased 13% by basic hydrolysis. Nevertheless, these results confirmed that carboxyl groups play an important role on the adsorption of Cr (III) on lignocellulosic materials.

In order to make a biosorption process more attractive, desorption of metal-loaded biosorbents are needed. Cano-Rodriguez *et al.* [71] conducted sorption–desorption cycles of Cr (III) in a flow-through column packed with immobilized sorghum straw. Desorption of the Cr (III)-loaded biomass, by using 0.1 N HCl, achieved 82% and

decreased 6% in each consecutive cycle reducing the life time use of the column. Sawalha *et al.* [60] also conducted batch desorption of Cr (III)-loaded saltbush biomass. Concentrations of 0.1 M, 0.5 M, and 1.0 M HCl desorbed more than 72–74% of the Cr (III); however, the Cr recovery did not exceed 40% when using sodium citrate. Garcia-Reyes *et al.* [20] tested several eluents (HNO_3, NaOH and EDTA) at various concentrations and temperatures to desorb Cr (III) from agro-waste materials. Readers are referred to Chapter 2 for further information.

Parab *et al.* [72] reported that the adsorption rate of Cr (III) on coir pith can be predicted by a pseudo-second order model. At C_o=50 mg/L, the initial sorption rate of Cr (III) was 0.029 mmol/(g min). Oliveira *et al.* [106] obtained lower initial sorption rate of Cr (III) on water-washed rice bran (0.001 mmol/(g min)) at pH 5.0 and C_o=5 mg/L. Besides these two reported studies, to the best of our knowledge, adsorption kinetics of Cr (III) on lignocellulosic materials are not reported in literature. Furthermore diffusion models have not been explored to predict the adsorption rate of Cr (III) on agro-waste materials. Comparison of the empirical models (i.e. pseudo–first and pseudo–second order equations) and diffusion models are discussed in Chapter 4.

1.4 MOTIVATION OF THIS RESEARCH

Lignocellulosic materials are generated in considerable amounts in agricultural countries throughout the world. These residues or by-products include rice husks, sugar-cane bagasse, rice straw, sorghum straw, oats straw, peanut hull, etc. In Mexico, sorghum (*Sorghum bicolor*) and oat (*Avena sativa*) are produced to obtain grains; however the residues (straw) are used for livestock or disposed of in the same place where these are produced. Besides these residues, agave bagasse (*Agave salmiana*) is a lignocellulosic waste generated in the industry of *mezcal* that produces ecological problems because it is burned or disposed of inappropriately. These lignocellulosic materials have the advantage of being readily available and could provide value-added products that otherwise would be considered as waste. For instance, the intensive use of lignocellulosic materials as adsorbents in removing heavy metals from aqueous solutions has been reported.

Taking the advantage that agro-waste biosorbents such as sorghum straw, oats straw, and agave bagasse are accessible in Mexico, and on the other hand that chromium (III) is a contaminant that has recently been reported to affect human erythrocyte membrane in a higher extent compared with Cr (VI), this research studied in detail the adsorption capacity performance of this biosorbents to remove Cr (III) from aqueous solutions, the sorption–desorption mechanism, and the contribution of the structural components (hemicelluloses, cellulose and lignin) of agro-waste materials to the removal of Cr (III).

1.5 GENERAL OBJECTIVE

The purposes of this research are to propose a sorption mechanism of Cr (III) on agro-waste materials (sorghum straw, oats straw, and agave bagasse), to determine the contribution of the major components (hemicelluloses, cellulose, and lignin) to the removal of Cr (III), and to assess the effect of external mass transfer and intraparticle diffusion on the overall rate of adsorption of Cr (III).

1.6 SPECIFIC OBJECTIVES

a) To chemically and physically characterize agro-waste materials by acid-base titrations, FTIR analyses, sequential extraction methods, surface area, pore volume, pore width distribution, and solid density.
b) To conduct batch adsorption experiments to determine the effect of pH and temperature on the chromium (III) sorption capacity.
c) To perform batch desorption studies of partially saturated biosorbents with HNO_3, NaOH, and EDTA at different concentrations and temperatures.
d) To determine the quantity of Cr (III) adsorbed and the quantity of other ions (such as calcium, magnesium and hydrogen) released when agro-waste materials are used as adsorbents.
e) To quantify the agro-waste materials main components (hemicelluloses, cellulose, and lignin) by sequential extraction methods.

f) To identify the functional groups of agro-waste materials, their fractions (residues remaining after sequential extraction methods), and commercial standards (pectin, cellulose, and lignin) by ATR-FTIR analyses.
g) To determine the Cr (III) sorption capacity of agro-waste materials, their fractions and commercial standards by carrying out batch experiments at selected pH and temperature.
h) To conduct adsorption kinetic experiments of chromium (III) on agro-waste materials at different initial concentrations and several stirring speeds.
i) To estimate the parameters of the empirical and diffusion kinetic models.
j) To predict the adsorption kinetics of Cr (III) on agro-waste materials by means of empirical and diffusion models.

1.7 HYPOTHESIS

The adsorption mechanism of chromium (III) on agro-waste materials will be based on ion exchange with calcium and also on complexation with oxygen-containing sites of the biosorbents constituents. Complexation of chromium on agro-waste materials will prevent the desorption of this contaminant when regenerating the exhaust biosorbents with acid eluents, fact that will be improved when using metal-complexing agents such as EDTA.

1.8 STRUCTURE OF THE THESIS

First of all, a review of the components present in lignocellulosic materials and biosorption studies of metals is presented in this chapter. The following chapters are distributed as follows:

In Chapter 2 the chemical characterization of agro-waste materials, batch sorption experiments of Cr (III), desorption of biosorbents with several eluting agents at different temperatures and concentrations, and the Cr (III) sorption mechanism are reported.

In Chapter 3 the content of the main components (hemicelluloses, cellulose, and lignin) of agro-waste materials, the functional groups of each fraction, and the

contribution of the main components on the chromium (III) removal from aqueous solution are discussed.

In Chapter 4 the adsorption kinetics of Cr (III) on agro-waste materials by empirical and diffusion kinetic models, and the effect of external mass transfer and intraparticle diffusion on the overall rate of adsorption are compared and discussed.

In Chapter 5 discussion of the main results of this work is presented.

Finally, Chapter 6 includes the main conclusions of this study as well as future work.

1.9 REFERENCES

[1]. Gadd, G. M., Biosorption: critical review of scientific rationale, environmental importance and significance for pollution treatment. J Chem Technol Biotechnol, 84(1) (2009) 13–28.

[2]. Garg, U., M. P. Kaur, G. K. Jawa, D. Sud and V. K. Garg, Removal of cadmium (II) from aqueous solutions by adsorption on agricultural waste biomass. J Hazard Mater, 154(1-3) (2008) 1149-1157.

[3]. Garg, U. K., M. P. Kaur, V. K. Garg and D. Sud, Removal of hexavalent chromium from aqueous solution by agricultural waste biomass. J Hazard Mater, 140(1-2) (2007) 60-68.

[4]. Krishnani, K. K., X. G. Meng, C. Christodoulatos and V. M. Boddu, Biosorption mechanism of nine different heavy metals onto biomatrix from rice husk. J Hazard Mater, 153(3) (2008) 1222-1234.

[5]. Reddad, Z., C. Gerente, Y. Andres and P. Le Cloirec, Adsorption of several metal ions onto a low-cost biosorbent: Kinetic and equilibrium studies. Environ Sci Technol, 36(9) (2002) 2067-2073.

[6]. Veglio, F. and F. Beolchini, Removal of metals by biosorption: A review. Hydrometallurgy, 44(3) (1997) 301-316.

[7]. Bai, R. S. and T. E. Abraham, Studies on chromium(VI) adsorption-desorption using. immobilized fungal biomass. Bioresour Technol, 87(1) (2003) 17-26.

[8]. Boddu, V. M., K. Abburi, J. L. Talbott and E. D. Smith, Removal of hexavalent chromium from wastewater using a new composite chitosan biosorbent. Environ Sci Technol, 37(19) (2003) 4449-4456.

[9]. Chojnacka, K., Biosorption of Cr(III) ions by wheat straw and grass: a systematic characterization of new biosorbents. Pol J Environ Studies, 15(6) (2006) 845-852.

[10]. Cossich, E. S., E. A. Da Silva, C. R. G. Tavares, L. Cardozo and T. M. K. Ravagnani, Biosorption of chromium(III) by biomass of seaweed Sargassum sp in a fixed-bed column. Adsorption, 10(2) (2004) 129-138.

[11]. Gode, F. and E. Pehlivan, A comparative study of two chelating ion-exchange resins for the removal of chromium(III) from aqueous solution. J Hazard Mater, 100(1-3) (2003) 231-243.

[12]. Gode, F. and E. Pehlivan, Removal of chromium(III) from aqueous solutions using Lewatit S 100: The effect of pH, time, metal concentration and temperature. J Hazard Mater, 136(2) (2006) 330-337.

[13]. Ibanez, J. P. and Y. Umetsu, Uptake of trivalent chromium from aqueous solutions using protonated dry alginate beads. Hydrometallurgy, 72(3-4) (2004) 327-334.

[14]. Mohan, D. and C. U. Pittman, Activated carbons and low cost adsorbents for remediation of tri- and hexavalent chromium from water. J Hazard Mater, 137(2) (2006) 762-811.

[15]. Romero-Gonzalez, J., J. R. Peralta-Videa, E. Rodriguez, M. Delgado and J. L. Gardea-Torresdey, Potential of Agave lechuguilla biomass for Cr(III) removal from aqueous solutions: Thermodynamic studies. Bioresour Technol, 97(1) (2006) 178-182.

[16]. Suwalsky, M., R. Castro, F. Villena and C. P. Sotomayor, Cr(III) exerts stronger structural effects than Cr(VI) on the human erythrocyte membrane and molecular models. J Inorg Biochem, 102(4) (2008) 842-849.

[17]. Yu, L. J., S. S. Shukla, K. L. Dorris, A. Shukla and J. L. Margrave, Adsorption of chromium from aqueous solutions by maple sawdust. J Hazard Mater, 100(1-3) (2003) 53-63.

[18]. Yun, Y. S., D. Park, J. M. Park and B. Volesky, Biosorption of trivalent chromium on the brown seaweed biomass. Environ Sci Technol, 35(21) (2001) 4353-4358.

[19]. Garcia-Reyes, R. B. and J. R. Rangel-Mendez, Contribution of Agro-Waste Materials Main Components (Hemicelluloses, Cellulose, and Lignin) on the Removal of Chromium (III) from Aqueous Solution. J Chem Technol Biotechnol, in press (2009).

[20]. Garcia-Reyes, R. B., J. R. Rangel-Mendez and M. C. A.-D. I. Torre, Chromium (III) Uptake by Agro-Waste Biosorbents: Chemical Characterization, Sorption-Desorption Studies, and Mechanism. J Hazard Mater, in press (2009).

[21]. Kratochvil, D., P. Pimentel and B. Volesky, Removal of trivalent and hexavalent chromium by seaweed biosorbent. Environ Sci Technol, 32(18) (1998) 2693-2698.

[22]. Nriagu, J. O. and J. M. Pacyna, Quantitative assessment of worldwide contamination of air, water and soils by trace metals. Nature, 333(6169) (1988) 134-139.

[23]. MWH, Water treatment principles and design. John Wiley & Sons, New Jersey, pp. 1948 (2005).

[24]. Sud, D., G. Mahajan and M. P. Kaur, Agricultural waste material as potential adsorbent for sequestering heavy metal ions from aqueous solutions - A review. Bioresour Technol, 99(14) (2008) 6017-6027.

[25]. SEMARNAT, NOM-001-SEMARNAT-1996. Secretaría de Medio Ambiente y Recursos Naturales, Mexico (1996).

[26]. SEMARNAT, NOM-002-SEMARNAT-1996 (1996).

[27]. SSA, NOM-127-SSA1-1994. Secretaría de Salud, Mexico (1994).

[28]. WHO, Guidelines for drinking-water quality. World Health Organization, Geneva, Switzerland (2008).

[29]. EPA, National Primary Drinking Water Regulations in EPA 40 CFR Parts 141, 142 and 143. Environmental Protection Agency, USA (1991).

[30]. Kimbrough, D. E., Y. Cohen, A. M. Winer, L. Creelman and C. A. Mabuni, Critical assessment of chromium in the environment. Crit Rev Environ Sci Technol, 29(1) (1999) 1-46.

[31]. Hamerlinck, Y. and D. H. Mertens, Activated Carbon Principles in Separation Technology, ed by E.F. Vansant (Ed.). Elsevier, New York (1994).

[32]. Rangel-Mendez, J. R., Adsorption of toxic metals from water using commercial and modified granular and fibrous activated carbons, in Department of Chemical Engineering Loughborough University, Loughborough, pp. 168 (2001).

[33]. Allen, S. J., L. Whitten and G. McKay, The production and characterization of activated carbons: a review. Dev Chem Eng Min Process, 6(5) (1998) 231–262.

[34]. Yang, R. T., Adsorbents: Fundamentals and Applications John Wiley & Sons, New Jersey, USA, pp. 409 (2003).

[35]. Garten, V. A. and D. E. Weiss, A new interpretation of the acidic and basic structures in carbons .2. the chromene-carbonium ion couple in carbon. Aust J Chem, 10(3) (1957) 309-328.

[36]. Boehm, H. P. and M. Voll, Carbon, 8 (1970) 227.

[37]. Voll, M. and H. P. Boehm, Carbon, 9 (1971) 481.

[38]. Thompson, R. W., Recent advances in the understanding of zeolite synthesis, in Molecular Sieves, ed by Karge HG and Weitkamp J. Springer, Berlin Germany and New York, NY, pp. 1-34 (1998).

[39]. S. Kesraoui-Ouki, C. R. Cheeseman and R. Perry, Natural zeolite utilization in pollution control: a review of application to metal's effluents. J Chem Technol Biotechnol, 59 (1994) 121-126.

[40]. Phillips, D. H., B. Gu, D. B. Watson and C. S. Parmele, Uranium removal from contaminated groundwater by synthetic resins. Water Res, 42 (2008) 260-268.

[41]. Volesky, B., Sorption and Biosorption. BV Sorbex, Inc., Montreal, Canada, pp. 316 (2003).

[42]. Davis, T. A., B. Volesky and A. Mucci, A review of the biochemistry of heavy metal biosorption by brown algae. Water Res, 37 (2003) 4311-4330.

[43]. Fourest, E. and B. Volesky, Contribution of sulfonate groups and alginate to heavy metal biosorption by the dry biomass of Sargassum fluitans. Environ Sci Technol, 30(1) (1996) 277-282.

[44]. Niu, C. H., B. Volesky and D. Cleiman, Biosorption of arsenic (V) with acid-washed crab shells. Water Res, 41(11) (2007) 2473-2478.

[45]. Davila-Rodriguez, J. L., V. A. Escobar-Barrios, K. Shirai and J. R. Rangel-Mendez, Synthesis of a chitin-based biocomposite for water treatment: optimization for fluoride removal. J Fluorine Chem, doi: 10.1016/j.jfluchem.2009.05.012 (2009).

[46]. Kamble, S. P., S. Jagtap, N. K. Labhsetwar, D. Thakare, S. Godfrey, S. Devotta and S. S. Rayalu, Defluoridation of drinking water using chitin, chitosan and lanthanum-modified chitosan. Chemical Engineering Journal, 129(1-3) (2007) 173-180.

[47]. Rojas, G., J. Silva, J. A. Flores, A. Rodriguez, M. Ly and H. Maldonado, Adsorption of chromium onto cross-linked chitosan. Sep Purif Technol, 44(1) (2005) 31-36.

[48]. Reid, J. S. G., Carbohydrate metabolism: structural carbohydrates, in Plant biochemistry, ed by Dey PM and Harborne JB. Academic Press, USA, pp. 205-236 (1997).

[49]. Buchanan, B. B., W. Gruissem and R. L. Jones, Biochemistry and molecular biology of plants. American Society of Plant Physiologist Maryland, USA (2000).

[50]. Paniagua, R., M. Nistal, P. Sesma, M. Álvarez-Uría, B. Fraile, R. Anadón and F. J. Sáez, Citología e histología vegetal y animal. McGraw Hill Interamericana España, S. A. U., España (2002).

[51]. García-Hernández, E. d. R. and C. B. Peña-Valdivia, LA PARED CELULAR COMPONENTE FUNDAMENTAL DE LAS CÉLULAS VEGETALES. Universidad Autónoma de Chapingo, México (1995).

[52]. Cosgrove, D. J., Assembly and enlargement of the primary cell wall in plants. Annu Rev Cell Dev Biol, 13 (1997) 171-201.

[53]. Sriamornsak, P., Chemistry of pectin and its pharmaceutical uses : A review. Silpakorn University International Journal, (2003) 206-228.

[54]. Novosel'skaya, I. L., N. L. Voropaeva, L. N. Semenova and S. S. Rashidova, Trends in the science and applications of pectins. Chemistry of Natural Compounds, 36(1) (2000) 1-10.

[55]. Mukhiddinov, Z. K., D. K. Khalikov, F. T. Abdusamiev and C. C. Avloev, Isolation and structural characterization of a pectin homo and ramnogalacturonan, in XXXIst Colloquium Spectroscopicum Internationale. Elsevier Science Bv, Ankara, Turkey, pp. 171-176 (1999).

[56]. Boerjan, W., J. Ralph and M. Baucher, Lignin biosynthesis. Annu Rev Plant Biol, 54 (2003) 519-546.

[57]. Li, J. P., Q. Y. Lin, X. H. Zhang and Y. Yan, Kinetic parameters and mechanisms of the batch biosorption of Cr(VI) and Cr(III) onto Leersia hexandra Swartz biomass. J Colloid Interface Sci, 333(1) (2009) 71-77.

[58]. Lu, D., Q. Cao, X. Li, X. Cao, F. Luo and W. Shao, Kinetics and equilibrium of Cu(II) adsorption onto chemically modified orange peel cellulose biosorbents. Hydrometallurgy, 95(1-2) (2009) 145-152.

[59]. Riaz, M., R. Nadeem, M. A. Hanif, T. M. Ansari and R. Khalil ur, Pb(II) biosorption from hazardous aqueous streams using Gossypium hirsutum (Cotton) waste biomass. J Hazard Mater, 161(1) (2009) 88-94.

[60]. Sawalha, M. F., J. R. Peralta-Videa, G. B. Saupe, K. M. Dokken and J. L. Gardea-Torresdey, Using FTIR to corroborate the identity of functional groups involved in the binding of Cd and Cr to saltbush (Atriplex canescens) biomass. Chemosphere, 66(8) (2007) 1424-1430.

[61]. Park, D., Y. S. Yun and J. M. Park, XAS and XPS studies on chromium-binding groups of biomaterial during Cr(VI) biosorption. J Colloid Interface Sci, 317(1) (2008) 54-61.

[62]. Tiemann, K. J., J. L. Gardea-Torresdey, G. Gamez, K. Dokken and S. Sias, Use of X-ray absorption spectroscopy and esterification to investigate Cr(III)

and Ni(II) ligands in alfalfa biomass. Environ Sci Technol, 33(1) (1999) 150-154.

[63]. Hu, M.-J., Y.-L. Wei, Y.-W. Yang and J.-F. Lee, X-ray absorption spectroscopy study of chromium recovered from Cr(VI)-containing water with rice husk. J Phys: Condens Matter, 16(33) (2004) S3473-S3478.

[64]. Manceau, A., M. C. Boisset, G. Sarret, R. L. Hazemann, M. Mench, P. Cambier and R. Prost, Direct determination of lead speciation in contaminated soils by EXAFS spectroscopy. Environ Sci Technol, 30(5) (1996) 1540-1552.

[65]. Sawalha, M. F., J. L. Gardea-Torresdey, J. G. Parsons, G. Saupe and J. R. Peralta-Videa, Determination of adsorption and speciation of chromium species by saltbush (Atriplex canescens) biomass using a combination of XAS and ICP-OES. Microchemical Journal, 81(1) (2005) 122-132.

[66]. Leyva-Ramos, R., L. A. Bernal-Jacome and I. Acosta-Rodriguez, Adsorption of cadmium(II) from aqueous solution on natural and oxidized corncob. Sep Purif Technol, 45(1) (2005) 41-49.

[67]. Silverstein, R. M., and Webster, F. X., Spectrometric Identification of Organic Compounds. Wiley & Sons, New York (1998).

[68]. Wade, L. G., QUIMICA ORGANICA. Prentice Hall Hispanoamericana, México (1993).

[69]. Naja, G., C. Mustin, B. Volesky and J. Berthelin, A high-resolution titrator: a new approach to studying binding sites of microbial biosorbents. Water Res, 39(4) (2005) 579-588.

[70]. Boehm, H. P., Chemical identification of surface groups, in Advances in catalysis, ed by Eley DD, Pines H and Weisz PB. Academic Press, New York, USA, pp. 179-274 (1966).

[71]. Cano-Rodríguez, I. P.-G., J. A.; Gutiérrez-Valtierra, M.; Gardea-Torresdey, J. L., REMOCION Y RECUPERACION DE CROMO(III) DE SOLUCIONES ACUOSAS POR BIOMASA DE SORGO. Revista Mexicana de Ingeniería Química, 1 (2002) 97-103.

[72]. Parab, H., S. Joshi, N. Shenoy, A. Lali, U. S. Sarma and M. Sudersanan, Determination of kinetic and equilibrium parameters of the batch adsorption of Co(II), Cr(III) and Ni(II) onto coir pith. Process Biochem, 41(3) (2006) 609-615.

[73]. Reddad, Z., C. Gerente, Y. Andres, M. C. Ralet, J. F. Thibault and P. Le Cloirec, Ni(II) and Cu(II) binding properties of native and modified sugar beet pulp. Carbohydr Polym, 49(1) (2002) 23-31.

[74]. Tarley, C. R. T. and M. A. Z. Arruda, Biosorption of heavy metals using rice milling by-products. Characterisation and application for removal of metals from aqueous effluents. Chemosphere, 54(7) (2004) 987-995.

[75]. Crini, G., Recent developments in polysaccharide-based materials used as adsorbents in wastewater treatment. Progress in Polymer Science, 30(1) (2005) 38-70.

[76]. Dang, V. B. H., H. D. Doan, T. Dang-Vu and A. Lohi, Equilibrium and kinetics of biosorption of cadmium(II) and copper(II) ions by wheat straw. Bioresour Technol, 100(1) (2009) 211-219.

[77]. Zhu, B., T. X. Fan and D. Zhang, Adsorption of copper ions from aqueous solution by citric acid modified soybean straw. J Hazard Mater, 153(1-2) (2008) 300-308.

[78]. Ngah, W. S. W. and M. Hanafiah, Removal of heavy metal ions from wastewater by chemically modified plant wastes as adsorbents: A review. Bioresour Technol, 99(10) (2008) 3935-3948.

[79]. Kurniawan, T. A., G. Y. S. Chan, W.-h. Lo and S. Babel, Comparisons of low-cost adsorbents for treating wastewaters laden with heavy metals. Science of The Total Environment, 366(2-3) (2006) 409-426.

[80]. Baes, C. F. and R. E. Messmer, The hydrolysis of cations. Wiley-Interscience, New York, USA (1976).

[81]. Stumm, W. and J. J. Morgan, Aquatic Chemistry: Chemical Equilibria and Rates in Natural Waters. John Wiley & Sons, New York (1996).

[82]. Gustafsson, J. S., Visual MINTEQ ver 2.61. KTH Department of Land and Water Resources Engineering (2006).

[83]. USGS, U.S. Geological Survey, PHREEQC (Version 2) (2008).

[84]. Lagergren, S., Zur theorie der sogenannten adsorption gelöster stoffe. K Sven Vetenskapsakad Handl, Band 24(No. 4) (1898) 1-39.

[85]. Ho, Y. S. and G. McKay, The kinetics of sorption of divalent metal ions onto sphagnum moss peat. Water Res, 34(3) (2000) 735-742.

[86]. Leyva-Ramos, R. and C. J. Geankoplis, Model simulation and analysis of surface diffusion of liquids in porous solids. Chem Eng Sci, 40(5) (1985) 799-807.

[87]. Leyva-Ramos, R., P. E. Diaz-Flores, J. Leyva-Ramos and R. A. Femat-Flores, Kinetic modeling of pentachlorophenol adsorption from aqueous solution on activated carbon fibers. Carbon, 45 (2007) 2280-2289.

[88]. Namasivayam, C., N. Muniasamy, K. Gayatri, M. Rani and K. Ranganathan, Removal of dyes from aqueous solutions by cellulosic waste orange peel. Bioresour Technol, 57(1) (1996) 37-43.

[89]. Sismanoglu, T., Removal of some fungicides from aqueous solution by the biopolymer chitin. Colloid Surf A-Physicochem Eng Asp, 297(1-3) (2007) 38-45.

[90]. Kandah, M., Zinc adsorption from aqueous solutions using disposal sheep manure waste (SMW). Chemical Engineering Journal, 84(3) (2001) 543-549.

[91]. Furusawa, T. and J. M. Smith, Fluid-Particle and Intraparticle Mass Transport Rates in Slurries. Ind Eng Chem Fundam, 12(2) (1973) 197-203.

[92]. Mathews, A. P. and W. W. J. Jr, Effects of external mass transfer and intraparticle diffusion on adsorption rates in slurry reactors. AIChE J, 73 (1976) 91-98.

[93]. Allen, S. J., L. J. Whitten, M. Murray, O. Duggan and P. Brown, The adsorption of pollutants by peat, lignite and activated chars. J Chem Tech Biotechnol, 68(4) (1997) 442-452.

[94]. Diniz, V. and B. Volesky, Desorption of lanthanum, europium and ytterbium from Sargassum. Sep Purif Technol, 50(1) (2006) 71-76.

[95]. Deng, S. B. and R. B. Bai, Removal of trivalent and hexavalent chromium with aminated polyacrylonitrile fibers: performance and mechanisms. Water Res, 38(9) (2004) 2424-2432.

[96]. Shashirekha, V., M. R. Sridharan and M. Swamy, Biosorption of trivalent chromium by free and immobilized blue green algae: Kinetics and equilibrium studies. Journal of Environmental Science and Health Part A, 43 (2008) 390-401.

[97]. Bishnoi, N. R., R. Kumar, S. Kumar and S. Rani, Biosorption of Cr (III) from aqueous solution using algal biomass *spirogyra spp.* J Hazard Mater, 145 (2007) 142-147.

[98]. Schiewer, S. and B. Volesky, Ionic strength and electrostatic effects in biosorption of divalent metal ions and protons. Environ Sci Technol, 31(9) (1997) 2478-2485.

[99]. Volesky, B., J. Weber and J. M. Park, Continuous-flow metal biosorption in a regenerable Sargassum column. Water Res, 37(2) (2003) 297-306.

[100]. Romero-Gonzalez, J., J. C. Walton, J. R. Peralta-Videa, E. Rodriguez, J. Romero and J. L. Gardea-Torresdey, Modeling the adsorption of Cr(III) from aqueous solution onto Agave lechuguilla biomass: Study of the advective and dispersive transport. J Hazard Mater, 161(1) (2009) 360-365.

[101]. Gode, F. and E. Moral, Column study on the adsorption of Cr (III) and Cr (VI) using Pumice, Yarikkaya brown coal, Chelex-100 and Lewatit MP 62. Bioresour Technol, 99 (2008) 1981-1991.

[102]. Cordero, T., J. Rodriguez-Mirasol, N. Tancredi, J. Piriz, G. Vivo and J. J. Rodriguez, Influence of surface composition and pore structure on Cr(III) adsorption onto activated carbons. Ind Eng Chem Res, 41 (2002) 6042-6048.

[103]. Schneider, R. M., C. F. Cavalin, M. A. S. D. Barros and C. R. G. Tavares, Adsorption of chromium ions in activated carbon. Chemical Engineering Journal, 132 (2007) 355-362.

[104]. Park, D., Y. S. Yun, H. Y. Cho and J. M. Park, Chromium biosorption by thermally treated biomass of the brown seaweed, Ecklonia sp. Ind Eng Chem Res, 43(26) (2004) 8226-8232.

[105]. Gardea-Torresdey, J. L., J. H. Gonzalez, K. J. Tiemann, O. Rodriguez and G. Gamez, Phytofiltration of hazardous cadmium, chromium, lead and zinc ions by biomass of Medicago sativa (Alfalfa). J Hazard Mater, 57(1-3) (1998) 29-39.

[106]. Oliveira, E. A., S. F. Montanher, A. D. Andrade, J. A. Nóbrega and M. C. Rollemberg, Equilibrium studies for the sorption of chromium and nickel from aqueous solutions using raw rice bran. Process Biochem, 40 (2005) 3485-3490.

Chapter 2

CHROMIUM (III) UPTAKE BY AGRO-WASTE BIOSORBENTS: CHEMICAL CHARACTERIZATION, SORPTION-DESORPTION STUDIES, AND MECHANISM

ABSTRACT

Within their complex structure, agro-waste materials such as sorghum straw (SS), oats straw (OS) and agave bagasse (AB) have functional groups (i.e. carboxyl and phenolic) that play a major role in metals sorption. The advantages of these materials include availability, low-cost, and a reasonable metal sorption capacity. These agro-waste materials were chemically characterized by acid-base titrations and ATR-FTIR analyses in order to determine their functional groups, equilibrium constants, and surface charge distribution. Batch experiments were conducted at pH 3 and 4, at 25°C and 35°C to determine the biosorbents chromium (III) sorption capacity. Partially saturated biosorbents were desorbed with HNO_3, NaOH, and EDTA at different concentrations and temperatures (25°C, 35°C, and 55°C). Finally, the chromium (III) sorption mechanism was discussed.

Agro-waste materials functional groups are associated, in part, to carboxyl and hydroxyl groups these oxygen-containing sites play an important role in the chromium (III) removal. The maximum chromium (III) sorption capacity was 6.96, 12.97, and 11.44 mg/g at pH 4 for acid-washed SS, OS, and AB, respectively. The chromium (III) sorption capacity decreased at pH 3 because H^+ ions competed for the same functional groups. On the other hand, an increase in temperature enhanced both the biosorbents chromium (III) sorption capacity and their desorption by EDTA. The most probable chromium (III) sorption mechanisms were ion exchange and complexation.

The agro-waste materials studied herein efficiently remove chromium (III) from aqueous solution and, most importantly, EDTA can efficiently desorb Cr (III) from agro-waste materials at 55 °C.

Keywords: Agricultural residues; functional groups; equilibrium constants; ion exchange; complexation.

Adapted from: Garcia-Reyes Refugio Bernardo, Rangel-Mendez Jose Rene, and Alfaro-De la Torre Ma. Catalina (2009), Chromium (III) uptake by agro-waste biosorbents: chemical characterization, sorption-desorption studies, and mechanism, Journal of Hazardous Materials, 170(2-3) 845-854.

2.1 INTRODUCTION

Heavy metal pollution is of great concern due to the human health problems that heavy metals cause when present in drinking water. In addition, heavy metals are non-biodegradable and can be bio-accumulated by organisms. Non-treated effluents from industries such as metallurgical, electronic, tannery, electro-plating, water cooling systems, among others can contaminate water systems with chromium, and other heavy metals.

This element is present in aqueous solutions mainly in the trivalent and hexavalent oxidation states. It is well known that trivalent chromium (Cr (III)) is an essential nutrient at trace concentration, and hexavalent chromium (Cr (VI)) is highly toxic and carcinogenic, but recently Suwalsky *et al.* [1] demonstrated that Cr (III) ions cause more structural perturbation in human erythrocyte membrane than Cr (VI). This structural perturbation, induced by Cr (III) ions, changes the biological membrane permeability affecting the functions of ion channels, receptors, and enzymes immersed in the erythrocyte membranes. In humans, Cr (III) can decrease immune system activity.

In Mexico, the maximum allowed concentration of chromium in drinking water is 0.05 mg/L [2]. In wastewater effluents, the allowed chromium concentration, on a monthly average, range from 0.05 to 0.1 mg/L depending on the final discharge site (i.e. river, lake, sea, etc.) [3]. Finally, wastewater discharges into municipal drainage can not exceed 0.5 mg/L (monthly average) measured as Cr (VI) [4].

Due to the toxic effects of chromium, it is necessary to eliminate it from the contaminated effluents. Several alternatives to remove Cr (III) from effluents have been reported; for example, chemical precipitation, chemical oxidation-reduction, electro-chemical treatment, membrane separation processes, evaporation, adsorption, ion exchange, biosorption, among others [5-8]. In general, the first five treatment processes have considerable disadvantages such as incomplete metal removal, high priced equipment and/or expensive monitoring systems, high reactive requirements and/or energy, and toxic sludge production that needs to be confined [9-11].

Biosorption processes have advantages such as low-cost and widely available materials in many countries, although these materials are sensible to pH and temperature changes. Some factors that influence the biosorbents metal sorption capacity are electric charge, type and quantity of chemical groups, pore size, surface area, temperature, and solution pH. Various biosorbents used to remove metals in aqueous solution are microorganism biomass [8, 9, 12], marine seaweed [7, 13-18], agricultural by-products [19-24], chitin and chitosan [25-27], among others.

Agro-waste materials are mainly formed by such natural polymers as cellulose, hemi-cellulose, pectin and lignin. These components contain carboxyl functional groups linked together by calcium bridges which can play an important role in metal adsorption. For instance, researchers have found that divalent metal ions are exchanged by calcium ions present in agro-waste materials [28, 29].

Mexico is a producer of sorghum (*Sorghum bicolor)* and oat (*Avena sativa*). The grains are used to prepare balanced food and sometimes the agro-waste materials (straw) are used for livestock. On the other hand, agave bagasse (*Agave salmiana*) is a waste generated in the industry of mezcal that produces ecological problems because it is burned or disposed of inappropriately. These agro-waste materials are locally available and could be used in adsorption processes, for example to remove Cr (III) from aqueous solution, although desorption studies are required to determine if these biosorbents can be regenerated and reused in order to make their application more attractive.

Therefore, the objectives of this research are to chemically characterize sorghum straw (*Sorghum bicolor*), oats straw (*Avena sativa*), and agave bagasse (*Agave salmiana*), and also to explore their application for removing chromium (III) from water by sorption/desorption studies. An additional objective is to propose a sorption mechanism based on ion exchange.

2.2 MATERIALS AND METHODS

2.2.1 Biosorbents

Sorghum straw (SS), oats straw (OS) and agave bagasse (AB) were tested as biosorbents to remove Cr (III) from aqueous solution. Previous to the sorption experiments, the agro-waste materials were ground to obtain particles of about 1 mm, and then washed with de-ionized water (W) or hydrochloric acid (A) 0.01 N to remove soils from biosorbents and, in the case of the acid washing step, to protonate the surface of the biosorbents. After the acid treatment, the biosorbents were washed with de-ionized water until obtaining a neutral pH. Finally, the biosorbents were dried in an oven at 50°C for 24 h, and then stored in desiccators until the experiments were conducted.

Capital letters were used throughout the document to identify each biosorbent; for example, acid-washed agave bagasse is represented as AAB.

2.2.2 Chemicals

A stock solution of 500 mg/L was prepared by using $Cr(NO_3)_3 \cdot 9H_2O$ (A.C.S., Meyer). Appropriate dilutions were prepared to conduct sorption experiments with initial concentration of Cr (III) ranging from 5 to 100 mg/L. An EDTA salt (disodium salt, dehydrate cystal, A.C.S., J.T. Baker) was used to prepare 0.1 M and 0.05 M eluent solutions. In addition, 1.0 N HNO_3 and 1.0 N NaOH (both A.C.S., Fermont) solutions were used to regenerate chromium-loaded biosorbents. De-ionized water was used to prepare all solutions. Finally, chromium, calcium, and magnesium concentrations were measured by using an atomic absorption spectrophotometer, AAS (Perkin Elmer, AAnalyst 400).

2.2.3 Surface charge distribution, functional groups, and equilibrium constants

Potentiometric titrations were conducted to determine the materials surface charge distribution. First, 125 mg of biosorbent were placed in 50 mL polyethylene vials. After that, 20 mL of 0.1 N NaCl (A.C.S, Caledon) were added to the vial containing the biosorbent. Then a different volume of 0.1 N NaOH or 0.1 N HCl (both A.C.S.,

J.T. Baker) was added into each vial. Finally, 0.1 N NaCl solution was used to complete 25 mL. Carbon dioxide free-solution was obtained by stripping with nitrogen gas. In the same way, a blank experiment (without biosorbent) was conducted. Solutions were kept at 25°C and were manually shaken twice a day for a period of 5 days. Finally, the equilibrium pH of each experiment was measured (Thermo, Orion 4 STAR).

Additionally, to estimate the biosorbents functional groups and their equilibrium constants, the experimental data obtained from potentiometric titrations were processed according to the method proposed by Yun *et al.* [18].

2.2.4 Functional groups identification

Attenuated Total Reflection Fourier Transform Infrared (ATR-FTIR) analyses (Thermo-Nicolet, Nexus 470 FT-IR E.S.P.) were used to identify the biosorbents functional groups, before and after the sorption-desorption processes.

Previous to ATR-FTIR analyses, biosorbents were dried at 50°C for 24 hours. Then, the spectra were obtained in the range from 650 to 4000 cm^{-1} with 4 cm^{-1} resolution. The resulting spectra were the average of 32 scans. Finally, the spectra were used to identify the functional groups based on the characteristic transmittance peaks.

2.2.5 Chromium species in aqueous solution

The chromium speciation diagram was computed with the software Visual MINTEQ 2.51 [30]. This diagram was obtained for a chromium concentration of 100 mg/L and 357 mg/L of nitrates.

2.2.6 Adsorption experiments

The biosorbents Cr (III) sorption capacity (Q_e) was determined at different temperatures (25° and 35°C) and pH values (3 and 4) in duplicate and the average values are presented. Samples of 100 mg of biosorbents were added to 100 mL of Cr (III) concentrations of 5 to 100 mg/L. These experiments were continuously stirred at 180 rpm. The solution pH was adjusted daily to pH 3 or 4 by adding 0.1 N

NaOH and/or 0.1 N HNO_3 until the equilibrium was achieved. The equilibrium was considered to be reached when at least 3 consecutive measurements of the Cr (III) concentration were similar in the batch experiments. Aliquots (10 mL) were taken to measure the initial and the equilibrium chromium concentrations (C_e) by AAS.

2.2.7 Metal ions adsorbed and released

It is well known that heavy metal ions are exchanged by other ions (such as calcium, magnesium or H^+) in biosorption processes. To understand the Cr (III) sorption mechanism, batch experiments were conducted in triplicate to determine both the chromium adsorbed and the ions released (such as calcium, magnesium, and H^+) from the agro-waste materials.

Samples of 100 mg of biosorbent were added to 100 mL of Cr (III) solutions (initial concentration 20 mg/L) contained in Erlenmeyer flasks at 25°C. These flasks were closed and continuously stirred at 180 rpm. For experiments with pH control, the solution pH was adjusted daily to pH 4 by adding 0.1 N NaOH and/or 0.1 N HNO_3 until the equilibrium was achieved. For experiments without pH control, the initial pH was fixed to 4 and the final pH was measured at the end of the experiment.

Finally, 10 mL aliquots were taken to measure the initial and final (at equilibrium) chromium, calcium and magnesium concentrations by AAS. The H^+ desorption capacity was calculated based on the initial and final pH measurements. In the same way, blank experiments (without chromium) were conducted to measure calcium, magnesium, and H^+ released.

2.2.8 Desorption experiments

To determine the Cr (III) desorption from agro-waste materials, batch experiments were carried out in duplicate and the average values are reported. Biosorbents were previously exposed to 20 mg/L of Cr (III) at pH 4 and 25°C. Then 5 mL aliquots were taken to determine the initial and final (at equilibrium) concentrations. After that, chromium-loaded biosorbents were filtered and slightly rinsed with de-ionized water (at pH 4) to remove the excess of chromium solution. Then the biosorbent was added to 100 mL of HNO_3 (1.0 N or 0.1 N), NaOH (1.0 N or 0.1 N)

or EDTA (0.1 M or 0.5 M) solutions. Regeneration experiments were continuously stirred at 180 rpm at selected temperatures (25°C, 35°C, or 55°C) for 24 hours. Finally, 5 mL aliquots were taken to measure the equilibrium chromium concentration by AAS.

Regenerated biosorbents were filtered, rinsed with de-ionized water (100 mL), dried at room temperature for 5 days, and weighed to obtain the mass loss after the regeneration step.

2.3 RESULTS AND DISCUSSION

2.3.1 Chemical characterization

Biosorbents have functional groups that play a major role in metal sorption. These groups can be dissociated or protonated depending on the solution pH. Yun *et al.* [18] developed a physical-chemical-based method to estimate the functional groups (b, measure as mmol/g) and their equilibrium constants (pK_a). The experimental data obtained from potentiometric titration were processed according to this method (details are given in Appendix A). In most cases, the determination coefficient (R^2) was greater than 95% indicating that the estimated parameters (b and pK_a) agreed with the experimental results. Table 2.1 shows the functional groups (b) and their equilibrium constants (pK_a). In general, the biosorbents functional group types were similar, although these were present in different amounts.

The functional group with pK_a ranging from 3.6 to 4.1 can be associated to carboxyl groups [18], which can be verified since it is well known that agro-waste materials contain pectin and hemi-celluloses which have carboxyl groups in their chemical structure [29]. The latter was corroborated by ATR-FTIR spectra (Figure 2.1 (A) and Appendix B) since these provided transmittance peaks of around 1745, 1650, 1260, 1160, and 1060 cm^{-1} attributed to carboxyl groups [31-33].

Groups with pK_a varying between 6.6 and 7.2 cannot be associated to a specific group because there are several types of functional groups such as amine, phosphoryl, amide, imidazol, etc., that have pK_a values in this range. The analysis of the ATR-FTIR spectra (see Figure 2.1 (A) and Appendix B) suggested that the

agro-waste materials have amine groups related to transmittance bands at 1610 cm^{-1} [31, 33].

Table 2.1 Functional groups (b, mmol/g) quantity and equilibrium constants (pK_a).

Biosorbent	Functional group	pK_a	b (mmol/g)
WSS	Unknown	7.00 (0)	1.12 (0.3)
	Hydroxyl	10.63 (0)	1.15 (2.0)
ASS	Unknown	6.61 (0)	1.03 (0.2)
	Hydroxyl	10.28 (0)	1.29 (0.1)
WOS	Unknown	7.04 (0)	0.91 (0.2)
	Hydroxyl	9.41 (0)	1.12 (0.3)
AOS	Carboxyl	3.79 (0.4)	0.17 (0.2)
	Unknown	6.33 (0)	0.09 (0.2)
	Hydroxyl	9.86 (0)	1.20 (0.2)
WAB	Unknown	6.90 (0)	0.98 (0.5)
	Hydroxyl	9.06 (0)	0.22 (0.5)
	Hydroxyl	12.58 (0)	0.45 (0.6)
AAB	Carboxyl	4.12 (0.1)	0.31 (0.2)
	Unknown	7.05 (0)	0.58 (0.2)
	Hydroxyl	10.97 (0)	0.57 (0.2)

Standard errors are given in parenthesis.

Finally, a third functional group can be associated to hydroxyl groups (pK_a 9.06 – 12.58), which are present in the agro-waste materials components (e.g. cellulose, hemicelluloses, pectin, lignin, etc.). These groups were confirmed by ATR-FTIR analyses (Figure 2.1 (A) and Appendix B) at transmittance peaks of about 3350 and 1060 cm^{-1} [31-33].

Figure 2.2 shows the surface charge distribution curves of agro-waste materials that are related to the type and quantity of surface functional groups. The slope changes of these curves indicated the dissociation of carboxyl, nitrogen-containing, and hydroxyl groups which is directly related to their pK_a value. Figure 2.2 also shows that the acid treatment applied to the biosorbents changed the pH_{PZC} (point of zero charge) to acid values. For instance, the water-washed SS, OS, and AB had a pH_{PZC} of 6.0, 6.0, and 5.0, respectively, whereas the pH_{PZC} of acid-washed

SS, OS, and AB was 5.5, 3.2, and 3.5, respectively. If the sorption experiments were conducted at a pH higher than the pH_{PZC} (where the net surface charge is negative) of the agro-waste materials, then positively-charged metals ions would easily interact with the biosorbents surface.

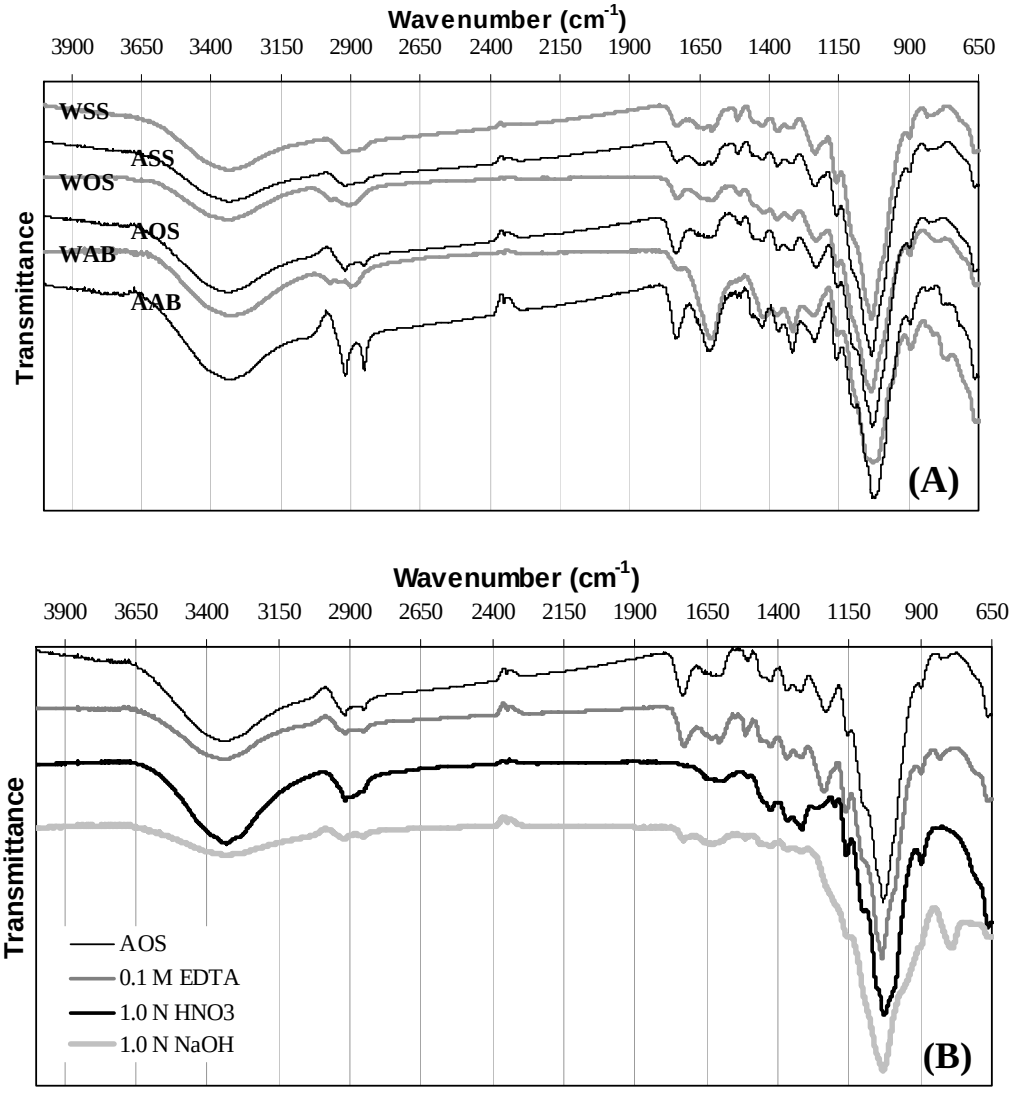

Figure 2.1. (A) ATR-FTIR spectra of water-washed (grey line) and acid-washed (black line) agro-waste materials. **(B)** Acid-washed oats straw (AOS) spectra before and after being regenerated with EDTA, HNO_3, and NaOH.

On the other hand, AOS and AAB contained fewer groups that have pK_a values between 6.6 and 7.2 (see Table 2.1) in comparison with water-washed materials, suggesting salts dissolution. This fact was supported by the ATR-FTIR spectra of the water and acid treated biosorbents (see Figure 2.1 (A) WOS, AOS, WAB, AAB) because changes were observed between them at 1740 cm^{-1}. These can also be related to lower slope at pH 6 to 8 of the surface charge distribution curve (Figure 2.2) of both OS and AB at pH 6 to 8. The acid treatment applied to SS did not significantly affect the slope at pH 6.5 to 7.5 (Figure 2.2) and the ATR-FTIR spectra (Figure 2.1 (A) WSS, ASS).

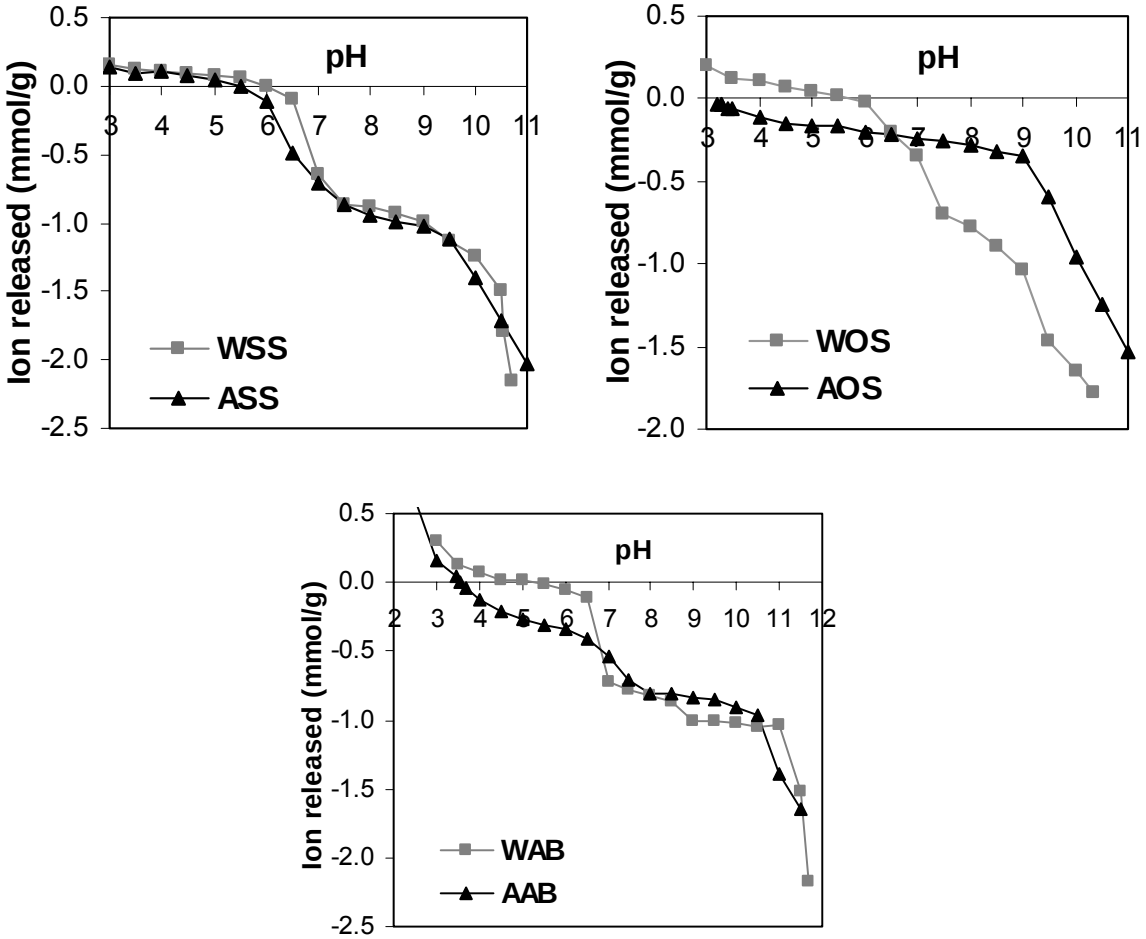

Figure 2.2 Surface charge distribution curves of water-washed (gray) and acid-washed (black) agro-waste materials. The ionic strength was fixed with 0.1 N NaCl.

2.3.2 Chromium species in aqueous solution

The chromium speciation diagram (Figure 2.3) shows the concentration of dissolved species and the pH at which hydrolysis occurs. At pH 3 the estimated dissolved species are Cr^{3+} (87%), $CrOH^{2+}$ (11%) and $Cr_2(OH)_2^{4+}$ (2%), whereas at pH 4 the distribution of these species changes as follows: Cr^{3+} (30%), $CrOH^{2+}$ (40%), $Cr_2(OH)_2^{4+}$ (26%), and $Cr_3(OH)_4^{5+}$ (4%). It is important to note that Cr (III) precipitates at pH 4.6 when the total concentration is 100 mg/L. In order to preserve the metal in solution, adsorption experiments were conducted at pH 3 and 4.

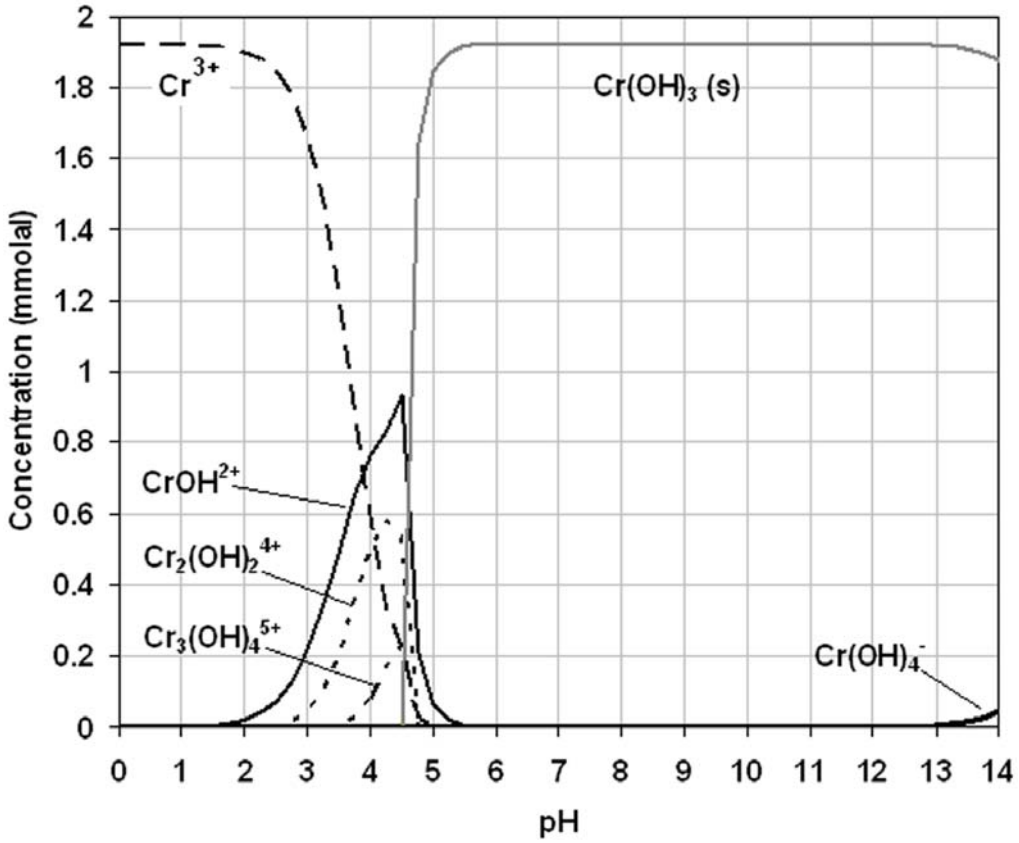

Figure 2.3 Chromium (III) species in aqueous solution computed with VMINTEQ 2.51. This diagram was obtained for a chromium concentration of 100 mg/L and 357 mg/L of nitrates as $Cr(NO_3)_3$.

2.3.3 Adsorption experiments

Both Langmuir and Freundlich isotherms fitted the experimental data adequately (see Appendix C Table C1). In this case Langmuir isotherm, shown as a continuous line on Figures 2.4 and 2.5, was selected to model the experimental results since this model gives useful information such as the maximum chromium sorption capacity (Q_{max}) and the isotherm constant (b) that is related to the affinity of the binding sites for metal ions.

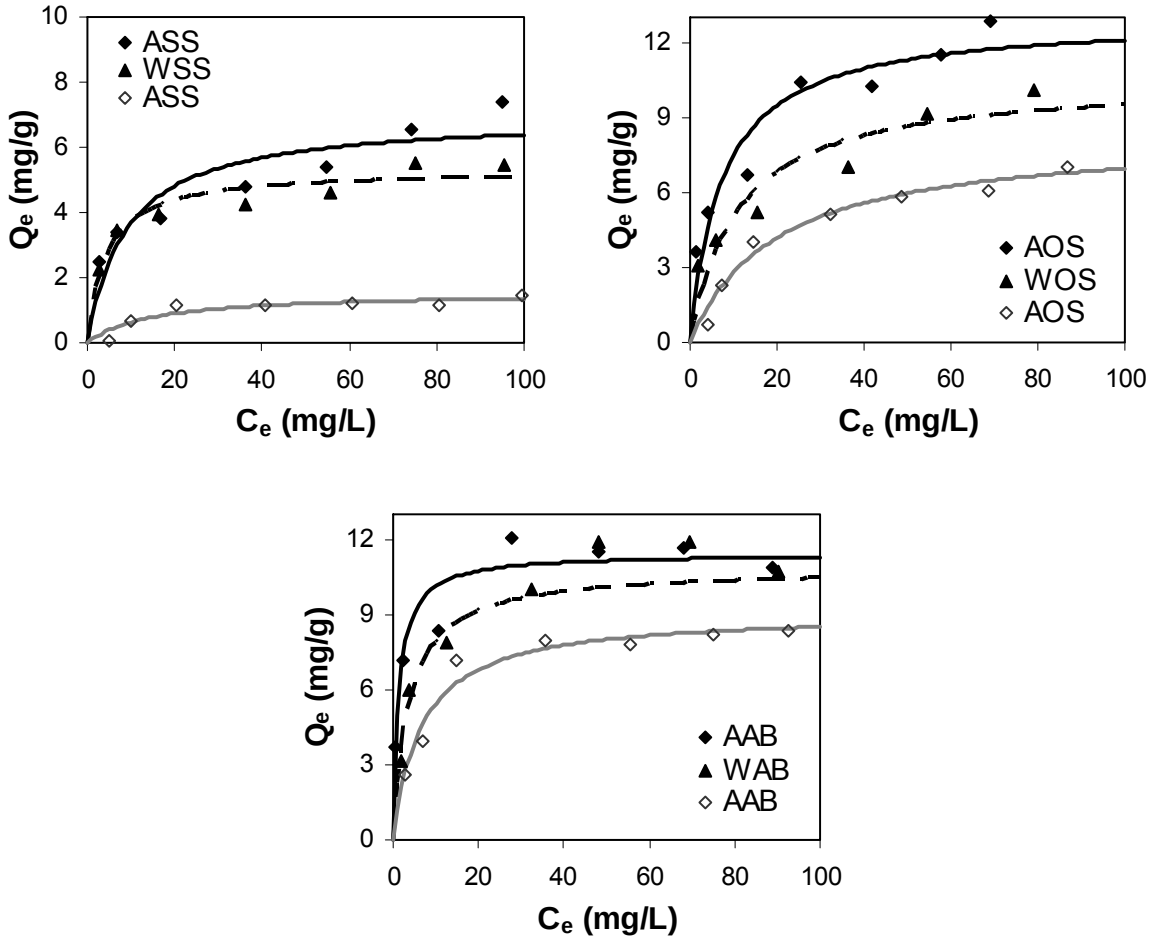

Figure 2.4 Adsorption isotherms of chromium (III) onto agro-waste materials at 25°C, pH 4 (solid symbols), and pH 3 (open symbols). Symbols represent the experimental measurements and the line the Langmuir model.

Figure 2.4 shows the Cr (III) adsorption isotherms onto agro-waste materials at 25°C, pH 4, and pH 3. At pH 4, Q_{max} obtained by the Langmuir model was 5.33 and 6.96 mg/g for WSS and ASS, respectively. Cano-Rodriguez *et al.* [19] reported that protonated sorghum biomass adsorbed 10 mg of chromium (III)/g at pH 4.5-5.0, which is 30% higher than the maximum chromium adsorbed by the ASS (6.96 mg/g) used in this study. This difference could be due to the pH at which the chromium adsorption experiments were conducted. For instance, at pH 5 the biosorbent possesses more dissociated functional groups that can participate in the chromium sorption (i.e. carboxyl sites). In addition, according to the chromium speciation diagram (shown in Figure 2.3) at pH 5, a solid phase would be formed in solution ($Cr(OH)_3$) and hence contribute to the chromium removal.

On the other hand, the maximum chromium sorption capacity for WOS and AOS at pH 4 and 25°C was 10.55 and 12.97 mg/g, respectively. These results demonstrated that chromium sorption capacity was higher for AOS (12.97 mg/g) than ASS (6.96 mg/g). This difference could be due to the presence of available carboxyl groups in AOS (see Table 2.1). These functional groups have been broadly studied and results reported in literature have demonstrated that metal cations have a high affinity for carboxyl sites [18, 23, 34, 35].

In addition, the maximum chromium sorption capacity for WAB and AAB at 25°C and pH 4 was 10.84 and 11.44 mg/g, respectively. Romero-Gonzalez *et al.* [21] reported a sorption capacity of 11.31 mg of chromium (III)/g of protonated Agave *lechuguilla* biomass at pH 4 and 22°C, which agrees with our results although it is a different species.

Comparing the chromium sorption capacity (Q_e) among the agro-waste materials in this study, it is clear that AB and OS have higher Q_e than SS (see Figure 2.4), which is related to the concentration of carboxyl groups (see Table 2.1). Also the ATR-FTIR spectra obtained from AB and OS (Figure 2.1 (A)) showed stronger transmittance bands associated to carboxyl and amine groups (at 1750 and 1620 cm^{-1}) that are likely to be involved in the Cr (III) sorption.

In addition, the chromium sorption capacity of the acid-washed biosorbents was lower at pH 3 than at pH 4 (see Figure 2.4), most probably due to the lower

availability of active sites and the competition between H^+ and Cr (III) ions for the same sorption sites on the materials. This competition has been previously demonstrated in other studies [18, 36].

Several research groups have tested a variety of adsorbents for the chromium (III) removal from aqueous solution, for instance seaweed biomass, agro-waste materials, and ion exchange resins (Table 2.2). Cossich *et al.* [13] reported that the water-washed seaweed *Sargassum* sp. biomass had very high chromium (III) sorption capacity (68.1 mg/g at pH 3.5) because all functional groups were kept in the biomass after being water washed. In contrast, Yun *et al.* [18] reported a lower chromium (III) sorption capacity (20.5 mg/g at pH 3.5) for protonated seaweed biomass that could be due to the acid treatment (2.0 N H_2SO_4). The water-washed or acid-washed agro-waste materials studied herein did not show strong differences in the chromium sorption capacity as the aforementioned seaweed biomass. This was probably due to the mild conditions used in the acid treatment applied (25°C and 0.01 N HCl) in this research.

As shown in Table 2.2, the agro-waste materials have a lower chromium sorption capacity than ion exchange resins and seaweed biomass, but those are locally available and cheaper than ion exchange resins. For example, the cost of agro-waste materials locally is approximately 0.20 USD/kg.

Table 2.2 Maximum chromium (III) sorption capacity (Q_{max}, mg/g) of various adsorbents.

Adsorbent	Conditions	Q_{max} (mg/g)	Reference
Sorghum biomass	pH 4.5-5.0	10.00	[19]
Agave *lechuguilla* biomass	pH 4, 22°C	11.31	[21]
Wheat straw	pH 4, 20°C, C_o=200 mg/L	6.75	[20]
Grass		7.31	
Coir pith	pH 3.3, 27°C, C_o=20 mg/L	9.82	[35]
Brown seaweed Biomass (*Ecklonia* sp.)	pH 3.0, C_o=0 – 500 mg/L	11.00	[18]
	pH 3.5, C_o=0 – 500 mg/L	20.50	
	pH 4, C_o=0 – 500 mg/L	34.10	
Seaweed biomass (*Sargassum* sp.)	pH 3.5, C_o=104 – 624 mg/L	68.12	[13]
Lewatit S 100	pH 3.8, 25°C, C_o=5.2 – 52 mg/L	20.28	[37]
Chelex-100	pH 4.5, 25°C, C_o=5.2 – 52 mg/L	15.08	[36]
Lewatit TP207		17.73	
Sorghum straw	pH 3, 25°C, C_o=5 – 100 mg/L (Acid-washed)	1.55	This study
Oats straw		8.32	
Agave bagasse		9.06	
Sorghum straw	pH 4, 25°C, C_o=5 – 100 mg/L (Water-washed)	5.33	
Oats straw		9.93	
Agave bagasse		10.84	
Sorghum straw	pH 4, 25°C, C_o=5 – 100 mg/L (Acid-washed)	6.96	
Oats straw		12.97	
Agave bagasse		11.44	

Figure 2.5 shows the effect of temperature in the sorption capacity of chromium on acid-washed agro-waste materials. In general, an increase in temperature from 25°C to 35°C enhanced the sorption capacity of the acid-washed agro-waste materials. In the case of AOS, the chromium sorption capacity did not increase at lower concentration than 40 mg/L. Romero-Gonzalez *et al.* [21] demonstrated the endothermic nature ($\Delta H°$=52.77 kJ/mol) of chromium adsorption onto *Agave lechuguilla* biomass which could explain the increasing chromium sorption capacity by raising the temperature.

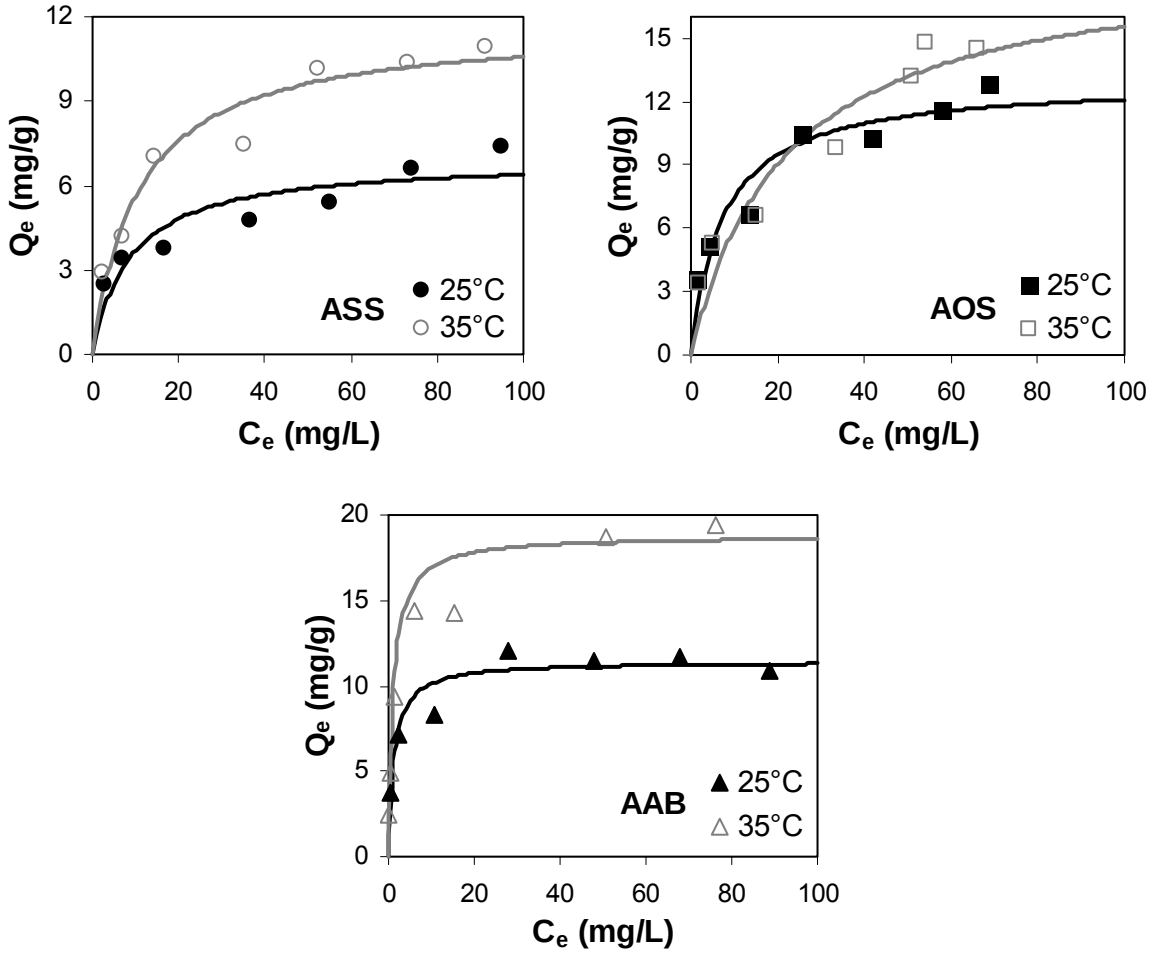

Figure 2.5 Adsorption isotherms of chromium (III) onto acid-washed agro-waste materials at pH 4, 25°C (black), and 35°C (grey). Symbols represent the experimental measurements and the line the Langmuir model.

2.3.4 Adsorption mechanisms

The chromium (III) sorption mechanisms have not been clarified due to the complex nature of the biosorbents. Methodologies such as chemical modifications, FTIR (Fourier Transform Infrared), XPS (X-Ray photoelectron spectra), among others, have been used to determine functional groups and at the same time to elucidate the biosorbents metal sorption mechanism [18, 23, 28, 35, 37]. Some of the functional groups that have been identified in biosorbents include: carboxyl, carbonyl, acetamide, amine, sulfonate, phosphate, phenolic, hydroxyl, etc., and the cations adsorption mechanisms that have been proposed for biosorbents include:

chemical adsorption (complexes formation), ion exchange with cations such as calcium or magnesium, and physical adsorption by electrostatic interaction. For example, Yun *et al.* [18] demonstrated, by using potentiometric titrations and FTIR analyses of protonated brown seaweed *Ecklonia* sp. biomass, that carboxyl groups were the chromium-binding sites. In the same way Sawalha *et al.* [35] showed more evidence, by FTIR analyses, that the trivalent chromium adsorption was mainly due to carboxyl groups of chemically-modified saltbush biomass (*Atriplex canescens*). On the other hand, Ibañez and Umetsu [34] demonstrated that the uptake of trivalent chromium by protonated dry alginate beads was coupled with a release of protons from the carboxyl groups, and the following ion exchange was proposed as the chromium sorption mechanism:

$$3\{\equiv R\text{-}COOH\} + Cr^{3+} \leftrightarrow \{\equiv R\text{-}COO\}_3\text{–}Cr + 3H^+ \quad (1)$$

$$2\{\equiv R\text{-}COOH\} + CrOH^{2+} \leftrightarrow \{\equiv R\text{-}COO\}_2\text{–}CrOH + 2H^+ \quad (2)$$

Moreover, when poly-nuclear chromium species are present at pH 4, reaction (3) has to be considered:

$$n\{\equiv R\text{-}COOH\} + Cr_2(OH)_2^{4+} \leftrightarrow \{\equiv R\text{-}COO\}_n\text{–}[Cr_2(OH)_2]^{(4-n)} + nH^+ \quad (3)$$

In contrast, Krishnani *et al.* [28] found that such divalent metals as Cd^{2+}, Pb^{2+}, Zn^{2+}, Cu^{2+}, Ni^{2+}, Hg^{2+}, Co^{2+}, and Mn^{2+} can be adsorbed onto previously treated rice husks and that the metal adsorption capacity can be explained, in a high percentage, as ion exchange with calcium and, in the case of Cd^{2+}, Pb^{2+}, Hg^{2+} with both calcium and magnesium. Also, Reddad *et al.* [29] demonstrated that the predominant sorption mechanisms for Pb^{2+}, Cu^{2+}, and Zn^{2+} onto sugar beet pulp are both ion exchange with calcium and complexation. However, this ion exchange mechanism has not been studied for trivalent metal ions such as Cr (III).

In order to understand the chromium (III) sorption mechanism, as a whole, on agro-waste materials, batch experiments were conducted to determine the chromium (III) sorption capacity and the concentration of ions released (such as calcium, magnesium and H^+) as a consequence of the ion exchange mechanism.

Poly-galacturonic and hexuronic acids (present in pectin and hemi-celluloses) contain carboxyl groups linked together by calcium bridges, but once calcium is

released to the solution, the carboxyl groups could be used by chromium (III) ions as adsorption sites.

Figure 2.6 (I) shows the chromium (III) adsorbed and the calcium released by agro-waste materials. Calcium released from AAB (0.211 mmol/g) was similar to the amount of Cr (III) adsorbed (0.207 mmol/g). These results suggested that calcium is released from the carboxyl moieties once chromium (III) species were adsorbed on it. In contrast, the calcium released/chromium (III) adsorbed (as a molar ratio) is about 0.64 when WSS, ASS and WOS are used as adsorbent which means that chromium was bound not only to carboxyl groups. The possible chromium (III) sorption mechanism that involves calcium release from carboxyl groups could be:

$$3\{\equiv R\text{-}COO\}_2\text{-}Ca + 2Cr^{3+} \leftrightarrow 2\{\equiv R\text{-}COO\}_3\text{–}Cr + 3Ca^{2+} \quad (4)$$

$$\{\equiv R\text{-}COO\}_2\text{-}Ca + CrOH^{2+} \leftrightarrow \{\equiv R\text{-}COO\}_2\text{–}CrOH + Ca^{2+} \quad (5)$$

$$2\{\equiv R\text{-}COO\}_2\text{-}Ca + Cr_2(OH)_2^{4+} \leftrightarrow \{\equiv R\text{-}COO\}_4\text{–}Cr_2(OH)_2 + 2Ca^{2+} \quad (6)$$

However, the amount of chromium (III) adsorbed onto AOS can not be explained as ion exchange with calcium (molar ratio 0.15). In order to quantify other ions released (e.g. Ca^{2+}, Mg^{2+}, H^+, etc) when chromium is adsorbed onto AOS, experiments in triplicate without pH control were conducted and the results are presented in Figure 2.6 (II). The equilibrium pH was around 3.48 for these experiments. The molar average ratio between H^+ released/chromium (III) adsorbed is 1.95 which could suggest that $CrOH^{2+}$ was preferentially adsorbed onto AOS because of the release of 2 mol of H^+ to the solution according to reaction (2). In these experiments, calcium and magnesium ions were not detected.

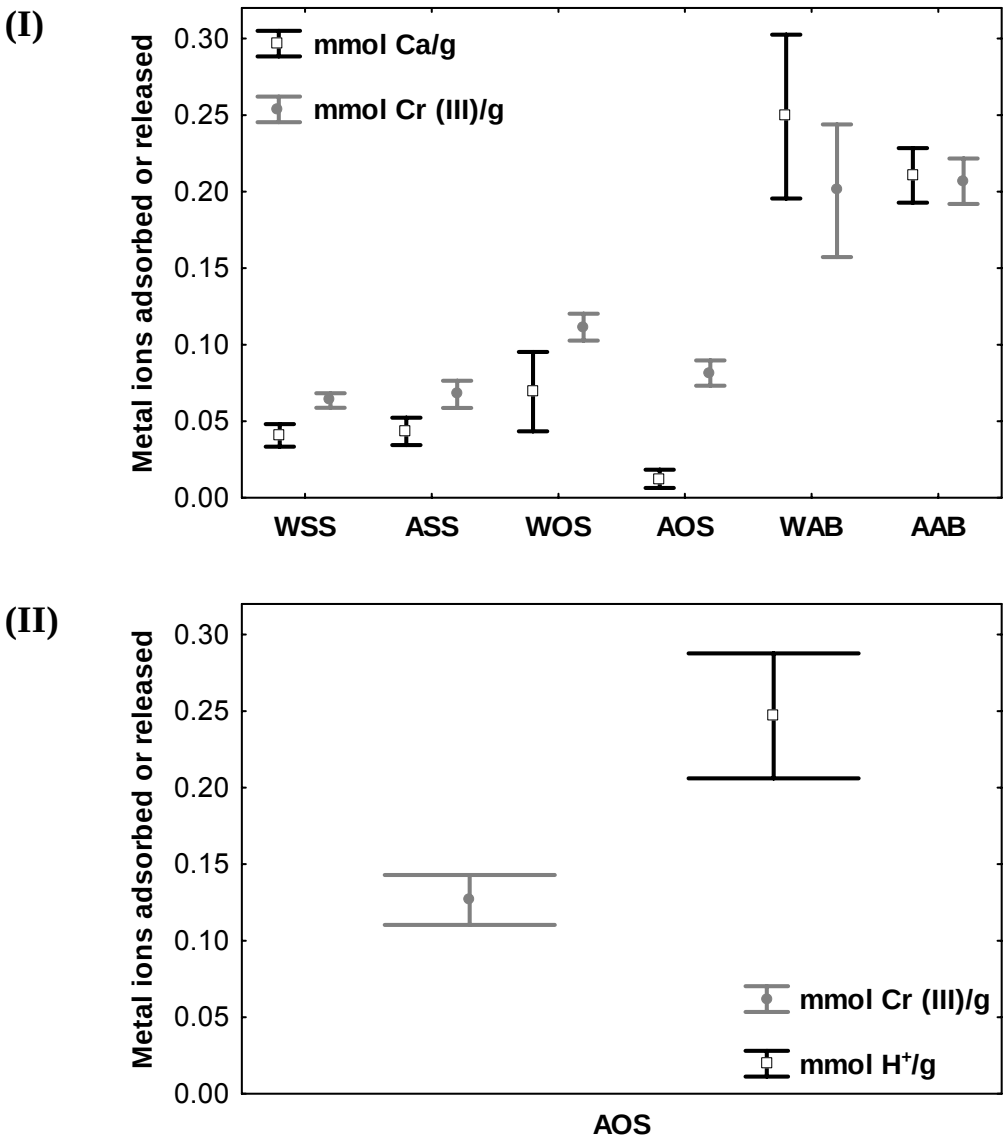

Figure 2.6 Metal ions adsorbed and released when agro-waste materials are used as adsorbents. **(I)** Chromium adsorbed and calcium released from water-washed and acid-washed agro-waste materials at pH 4, 25°C, and C_o=20 mg of Cr (III)/L. **(II)** Chromium adsorbed and H^+ released from acid-washed oats straw (AOS) without pH control at 25°C, initial pH 4, and C_o=120 mg of Cr (III)/L. Symbols represent the average values and bar errors were built with a confidence interval of 95%.

Some studies have confirmed that oxygen-containing groups (e.g. carboxyl and phenolic) are involved in metal adsorption. For example, Manceau *et al.* [38] demonstrated that lead in contaminated soil was complexed to salicylate and catechol-type functional groups of humic substances. In another study, Park *et al.* [17] established that carboxyl and phenolic groups play a major role in the binding of the Cr (III) resulting from the abiotic reduction of Cr (VI) by the seaweed biomass. Yu *et al.* [24] proposed that H^+ ions (present in carboxyl and phenolic groups of maple sawdust) can be exchanged with metal cations (species such as M^{n+} and $M(OH)^{(n-1)+}$) in solution: when carboxyl groups are involved, the mechanisms are similar to reaction (1) and (2), whereas sorption on phenolic groups was reported as:

$$\{\equiv R\text{-}C_6H_5\text{-}OH\} + M^{n+} \leftrightarrow \{\equiv R\text{-}C_6H_5\text{-}O\}\text{–}M^{(n-1)+} + H^+ \quad (7)$$

$$\{\equiv R\text{-}C_6H_5\text{-}OH\} + M(OH)^{(n-1)+} \leftrightarrow \{\equiv R\text{-}C_6H_5\text{-}O\}\text{–}\ M(OH)^{(n-2)+} + H^+ \quad (8)$$

2.3.5 Desorption experiments

Metal desorption from biosorbents has not been well explored and for that reason it is necessary to study this process more in detail. In this research the chromium-loaded agro-waste materials were regenerated. Solutions of HNO_3, NaOH, and EDTA were used as eluents at different concentrations and temperatures (25°C, 35°C, and 55°C). These eluents were selected aiming at an ion exchange process, between H^+ and Na^+ with Cr (III) species, or complexation (EDTA-Cr (III)). Figure 2.7 and Figure 2.8 show the chromium (III) desorption from water-washed and acid-washed agro-waste materials, respectively.

It was thought that if Cr (III) was adsorbed on carboxyl-binding groups by electrostatic interaction, then acid solutions (e.g. HNO_3) would regenerate the chromium-loaded biosorbents since the concentration of H^+ increases (pH decreases and oxygen groups protonates) giving way to ion exchange with the chromium adsorbed as follows:

$$\{\equiv R\text{-}COO\}_3\text{–}Cr + 3H^+ \leftrightarrow 3\{\equiv R\text{-}COOH\} + Cr^{3+} \quad (9)$$

$$\{\equiv R\text{-}COO\}_2\text{–}CrOH + 2H^+ \leftrightarrow 2\{\equiv R\text{-}COOH\} + CrOH^{2+} \quad (10)$$

$$\{\equiv R\text{-}COO\}_4\text{–}Cr_2(OH)_2 + 4H^+ \leftrightarrow 4\{\equiv R\text{-}COOH\} + Cr_2(OH)_2^{4+} \quad (11)$$

However, the low Cr (III) desorption from agro-waste materials at 25°C (lower than 46% for WOS when 1.0 N HNO_3 was used) suggested that chromium ions form more stable chemical bonds (i.e. covalent coordinated bonds) with the biosorbents. This could be related to the increase in sorption capacity when the temperature rises (see Figure 2.5).

For instance, chromium desorption from AAB with 1.0 M HNO_3 was 43%, 47%, and 68% at 25°C, 35°C, and 55°C, respectively (see Figure 2.8). However, the regeneration of AAB with 1.0 M HNO_3 at 55°C caused 30% of weight loss (see Figure 2.9), which suggested that the acid eluent hydrolyzed part of hemi-celluloses and dissolved some salts like calcium present in the agro-waste materials.

Conversely, the chromium desorbed with NaOH (1.0 N) at 25°C varied from 18% to 71% depending on the agro-waste material (see Figure 2.7 and 2.8). However, the weight lost when 1.0 N NaOH was used as eluent was higher (22% to 42%) compared to the regeneration with 1.0 N HNO_3 (see Figure 2.9). These results suggested that some components (mainly lignin and hemicelluloses) present in the biosorbents could be hydrolyzed in an alkaline solution.

The most probable mechanism that could explain the chromium desorption with NaOH is illustrated in the following reactions:

$$2\{\equiv R\text{-}COO\}_3\text{–}Cr + 6Na^+ + 7OH^- \leftrightarrow 6\{\equiv R\text{-}COO\}\text{-}Na + Cr(OH)_4^- + Cr(OH)_{3\,(s)} \quad (12)$$

$$2\{\equiv R\text{-}COO\}_2\text{–}CrOH + 4Na^+ + 5OH^- \leftrightarrow 4\{\equiv R\text{-}COO\}\text{-}Na + Cr(OH)_4^- + Cr(OH)_{3\,(s)} \quad (13)$$

$$\{\equiv R\text{-}COO\}_4\text{–}Cr_2(OH)_2 + 4Na^+ + 5OH^- \leftrightarrow 4\{\equiv R\text{-}COO\}\text{-}Na + Cr(OH)_4^- + Cr(OH)_{3(s)} \quad (14)$$

The main species formed by alkaline regeneration is $Cr(OH)_{3\,(s)}$ due to the high concentration of OH^- (see Figure 2.3), although $Cr(OH)_4^-$ is also formed but to a lesser extent at high pH values. It is important to note that Cr (III) desorption by NaOH may be underestimated due to the presence of chromium precipitate as $Cr(OH)_{3\,(s)}$ (more experiments are needed to clarify this issue).

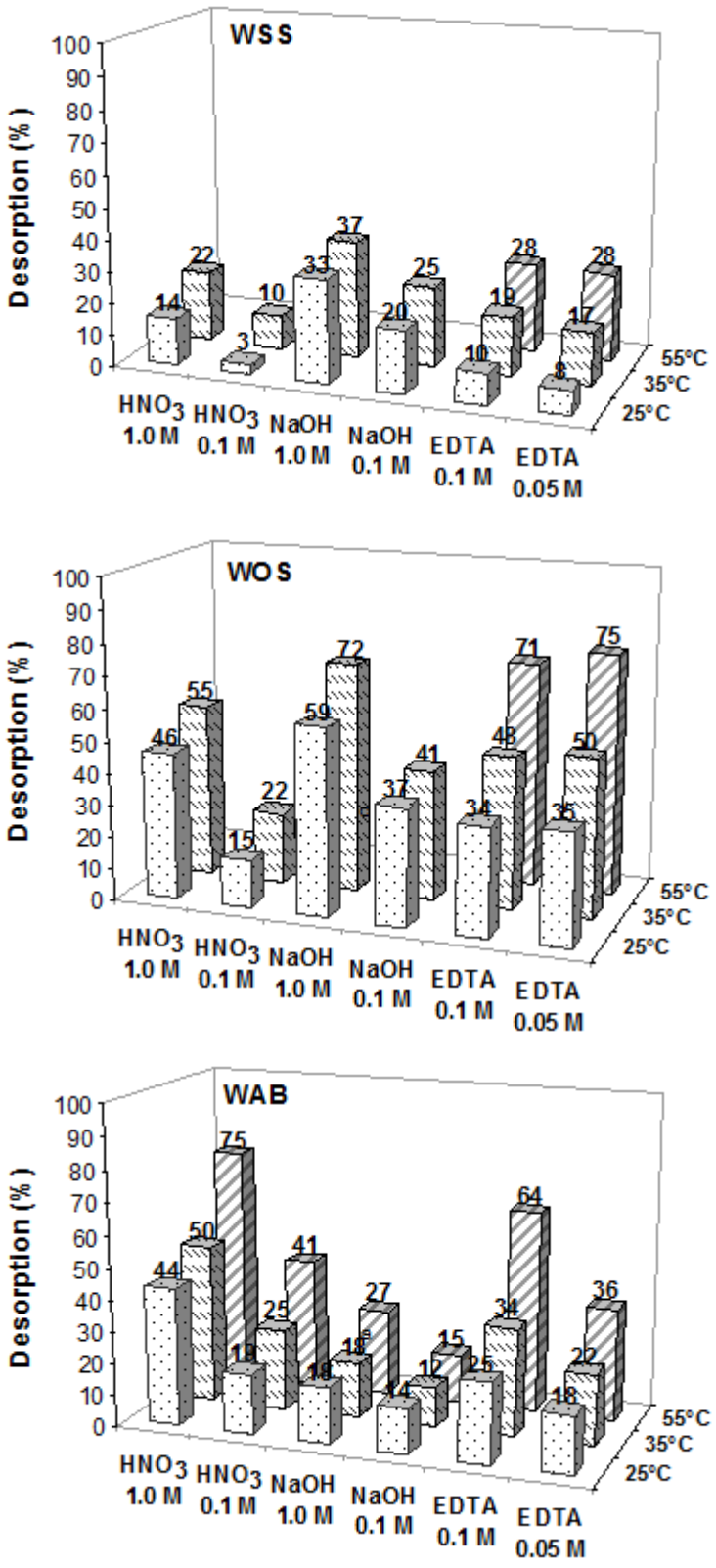

Figure 2.7 Chromium (III) desorption after 24 hours from water-washed agro-waste materials for several eluents and temperatures tested.

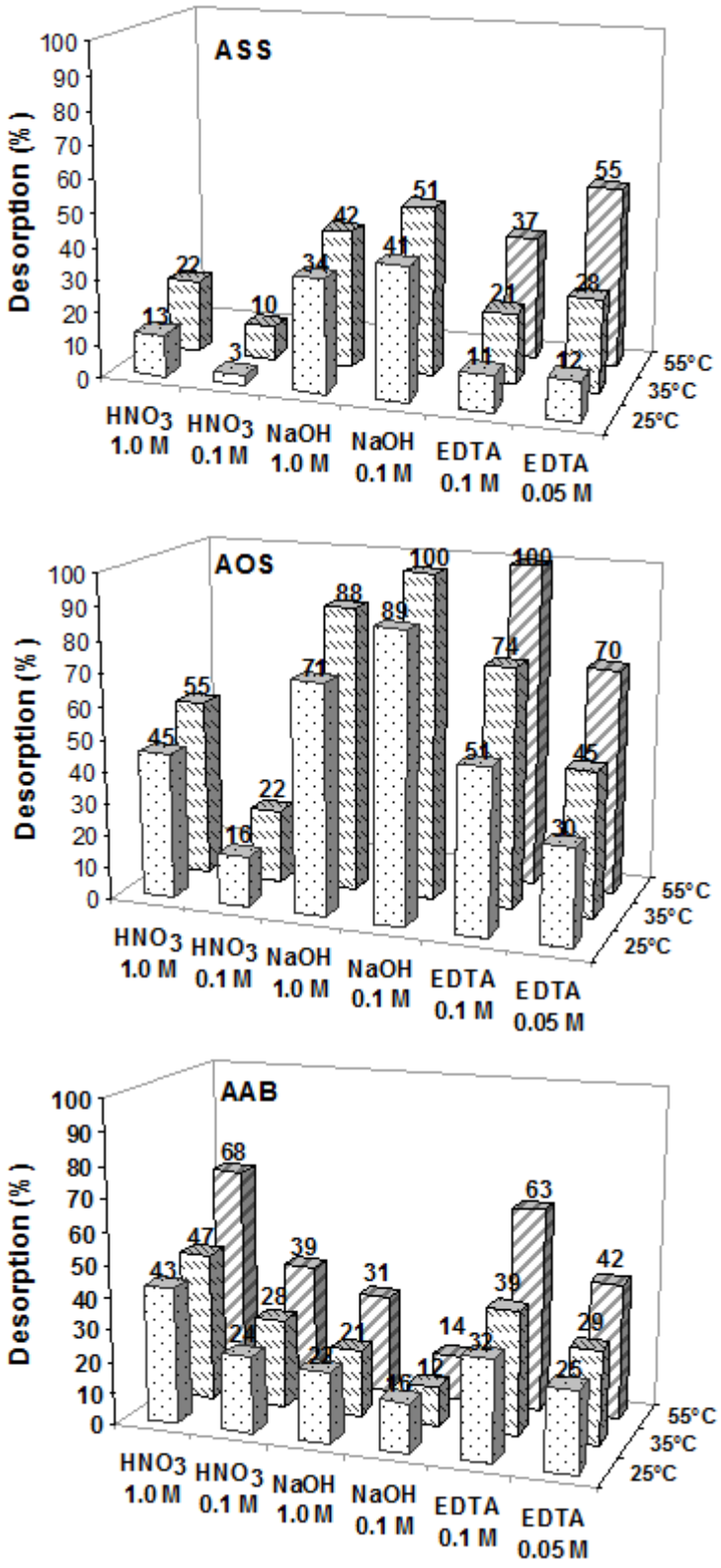

Figure 2.8 Chromium (III) desorption after 24 hours from acid-washed agro-waste materials for several eluents and temperatures tested.

Moreover, it is important to mention that the regeneration effect is lessened when the eluent is diluted. For instance chromium (III) desorption was less than 10% by using mild acid (pH 2 or 3) or alkaline solutions (pH 11 or 12). These findings indicated that the Cr (III) desorption mechanism is not an easy task due to the agro-waste materials complexity.

Solutions of EDTA (0.1 M and 0.05 M) were used to regenerate the chromium-loaded agro-waste materials. This eluent was chosen because it is well known that chromium (III) and EDTA ligand have the highest stability constants for the formation of complexes [39].

From Figure 2.7 and 2.8, it is clearly observed that the regeneration with EDTA was affected by both temperature and the eluent concentration. For instance, the AOS regeneration with 1.0 M EDTA at 25°C and 35°C was 51% and 74%, respectively, but at 55°C this biosorbent was completely regenerated (see Figure 2.8). The higher chromium desorption with 1.0 M EDTA obtained at 55°C suggested that the interaction Cr (III)-EDTA involved a chelate formation and an increase in temperature facilitated the chemical interaction between EDTA and Cr (III). Also when EDTA concentration was 0.05 M, the regeneration was reduced to 70% at 55°C.

The possible chromium desorption mechanism by EDTA (where M^+ represents either Na^+ or H^+) could occur as follows:

$$\{\equiv \text{R-COO}\}_3\text{–Cr} + \text{EDTA}^{4-} + 3M^+ \leftrightarrow 3\{\equiv \text{R-COO}\}\text{-M} + \{\text{Y-Cr}\}^{-1} \quad (15)$$

$$\{\equiv \text{R-COO}\}_2\text{–CrOH} + \text{EDTA}^{4-} + 2M^+ \leftrightarrow 2\{\equiv \text{R-COO}\}\text{-M} + \{\text{Y-CrOH}\}^{2-} \quad (16)$$

$$\{\equiv \text{R-COO}\}_4\text{–Cr}_2(\text{OH})_2 + \text{EDTA}^{4-} + 4M^+ \leftrightarrow 4\{\equiv \text{R-COO}\}\text{-M} + \{\text{Y-Cr}_2(\text{OH})_2\} \quad (17)$$

In addition, the weight loss of acid-washed materials due to the regeneration with 0.1 M EDTA was much lower (0-9%) than that obtained when 1.0 N HNO_3 or 1.0 N NaOH was used as eluent (see Figure 2.9). This fact suggested that EDTA solutions produced fewer structural modifications in the biosorbents than the acid or the alkaline solutions; for example Figure 2.1 (B) shows that acid and alkaline solutions attacked the carboxyl groups (1740 cm^{-1}) conversely to EDTA solutions. In addition, alkaline and acid regeneration produced hydrolysis of the agro-waste materials confirmed by the weight loss, and the biosorbents color change.

Therefore, based on the chromium desorbed and the weight loss, EDTA was the best option to regenerate the chromium-loaded agro-waste materials.

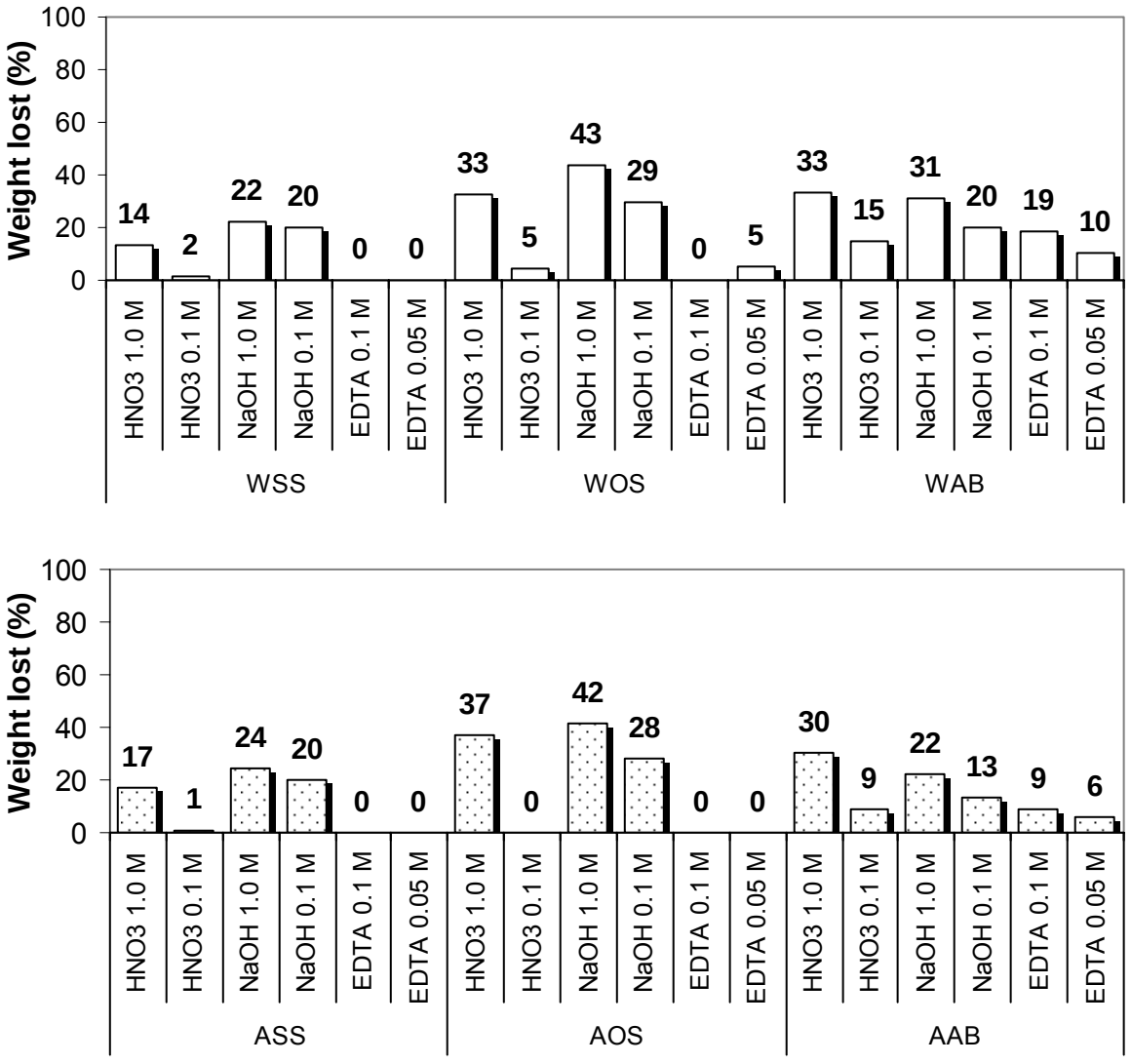

Figure 2.9 Initial weight lost after the regeneration of agro-waste materials at the highest desorption temperature shown in Figure 2.7 and 2.8.

These results have demonstrated that the agro-waste materials studied herein have functional groups capable of removing Cr (III) from water. In addition, these materials will likely remove other heavy metal ions from aqueous solution (e.g. Pb^{2+}, Cu^{2+}, Cd^{2+}, etc.). Besides batch sorption/desorption experiments, sorption

kinetics studies and sorption-desorption cycles in fixed-bed columns must be conducted to explore the feasibility of using these biosorbents in water treatment systems.

2.4 CONCLUSIONS

Functional groups such as carboxyl and hydroxyl are able to bind chromium (III) from aqueous solution. At concentrations below 20 mg of Cr (III)/L, agave bagasse has higher sorption capacity than oats and sorghum straw, which decreases at pH 3 since H^+ and Cr (III) ions compete for the biosorbents sorption groups. In addition, an increase in temperature from 25°C to 35°C enhances the chromium sorption in agro-waste materials because of the endothermic nature of the sorption process. Conversely, partially saturated agro-waste materials can be efficiently regenerated by an EDTA solution at 55°C without apparent modifications on the biosorbents. Finally, based on the chromium sorption-desorption experiments, the possible chromium (III) sorption mechanisms onto agro-waste materials are ion exchange and complexation.

2.5 REFERENCES

[1]. Suwalsky, M., R. Castro, F. Villena, C. P. Sotomayor, Cr(III) exerts stronger structural effects than Cr(VI) on the human erythrocyte membrane and molecular models, J. Inorg. Biochem. 102 (4) (2008) 842-849.

[2]. SSA, NOM-127-SSA1-1994, http://www.salud.gob.mx/unidades/cdi/nom/127ssa14.html

[3]. SEMARNAT, NOM-001-SEMARNAT-1996, http://www.semarnat.gob.mx/leyesynormas/Normas%20Oficiales%20Mexicanas%20vigentes/NOM-001-ECOL.pdf

[4]. SEMARNAT, NOM-002-SEMARNAT-1996, http://www.semarnat.gob.mx/leyesynormas/Normas%20Oficiales%20Mexicanas%20vigentes/NOM-ECOL-002.pdf

[5]. Juang, R. S., R. C. Shiau, Metal removal from aqueous solutions using chitosan-enhanced membrane filtration, J. Membr. Sci. 165 (2) (2000) 159-167.

[6]. Lacour, S., J. C. Bollinger, B. Serpaud, P. Chantron, R. Arcos, Removal of heavy metals in industrial wastewaters by ion-exchanger grafted textiles, Anal. Chim. Acta 428 (1) (2001) 121-132.

[7]. Matheickal, J. T., Q. M. Yu, Biosorption of lead(II) and copper(II) from aqueous solutions by pre-treated biomass of Australian marine algae, Bioresour. Technol. 69 (3) (1999) 223-229.

[8]. Yan, G. Y., T. Viraraghavan, Heavy metal removal in a biosorption column by immobilized M-rouxii biomass. Bioresour. Technol. 78 (3) (2001) 243-249.

[9]. Bai, R. S., T. E. Abraham, Studies on chromium(VI) adsorption-desorption using. immobilized fungal biomass, Bioresour. Technol. 87 (1) (2003) 17-26.

[10]. Benguella, B., H. Benaissa, Effects of competing cations on cadmium biosorption by chitin, Colloid Surf. A-Physicochem. Eng. Asp. 201 (1-3) (2002) 143-150.

[11]. Veglio, F., F. Beolchini, Removal of metals by biosorption: A review, Hydrometallurgy 44 (3) (1997) 301-316.

[12]. Saiano, F., M. Ciofalo, S. O. Cacciola, S. Ramirez, Metal ion adsorption by Phomopsis sp biomaterial in laboratory experiments and real wastewater treatments, Water Res. 39, (11) (2005) 2273-2280.

[13]. Cossich, E. S., E. A. Da Silva, C. R. G. Tavares, L. Cardozo, T. M. K. Ravagnani, Biosorption of chromium(III) by biomass of seaweed Sargassum sp in a fixed-bed column, Adsorption 10 (2) (2004) 129-138.

[14]. Kratochvil, D., P. Pimentel, B. Volesky, Removal of trivalent and hexavalent chromium by seaweed biosorbent, Environ. Sci. Technol. 32 (18) (1998) 2693-2698.

[15]. Park, D., Y. S. Yun, H. Y. Cho, J. M. Park, Chromium biosorption by thermally treated biomass of the brown seaweed, Ecklonia sp., Ind. Eng. Chem. Res. 43 (26) (2004) 8226-8232.

[16]. Park, D., Y. S. Yun, J. H. Jo, J. M. Park, Biosorption process for treatment of electroplating wastewater containing Cr(VI): Laboratory-scale feasibility test, Ind. Eng. Chem. Res. 45 (14) (2006) 5059-5065.

[17]. Park, D., Y. S. Yun, J. M. Park, XAS and XPS studies on chromium-binding groups of biomaterial during Cr(VI) biosorption, J. Colloid Interface Sci. 317 (1) (2008) 54-61.

[18]. Yun, Y. S., D. Park, J. M. Park, B. Volesky, Biosorption of trivalent chromium on the brown seaweed biomass, Environ. Sci. Technol. 35 (21) (2001) 4353-4358.

[19]. Cano-Rodríguez, I., J. A. Perez-Garcia, M. Gutiérrez-Valtierra, J. L. Gardea-Torresdey, REMOCION Y RECUPERACION DE CROMO(III) DE SOLUCIONES ACUOSAS POR BIOMASA DE SORGO, Revista Mexicana de Ingeniería Química 1 (2002) 97-103.

[20]. Chojnacka, K., Biosorption of Cr(III) ions by wheat straw and grass: a systematic characterization of new biosorbents, Pol. J. Environ. Studies 15 (6) (2006) 845-852.

[21]. Romero-Gonzalez, J., J. R. Peralta-Videa, E. Rodriguez, M. Delgado, J. L. Gardea-Torresdey, Potential of Agave lechuguilla biomass for Cr(III) removal from aqueous solutions: Thermodynamic studies, Bioresour. Technol. 97 (1) (2006) 178-182.

[22]. Tarley, C. R. T., M. A. Z. Arruda, Biosorption of heavy metals using rice milling by-products. Characterisation and application for removal of metals from aqueous effluents, Chemosphere 54 (7) (2004) 987-995.

[23]. Tiemann, K. J., J. L. Gardea-Torresdey, G. Gamez, K. Dokken, S. Sias, Use of X-ray absorption spectroscopy and esterification to investigate Cr(III) and Ni(II) ligands in alfalfa biomass, Environ. Sci. Technol. 33 (1) (1999) 150-154.

[24]. Yu, L. J., S. S. Shukla, K. L. Dorris, A. Shukla, J. L. Margrave, Adsorption of chromium from aqueous solutions by maple sawdust, J. Hazard. Mater. 100 (1-3) (2003) 53-63.

[25]. Boddu, V. M., K. Abburi, J. L. Talbott, E. D. Smith, Removal of hexavalent chromium from wastewater using a new composite chitosan biosorbent, Environ. Sci. Technol. 37 (19) (2003) 4449-4456.

[26]. Rojas, G., J. Silva, J. A. Flores, A. Rodriguez, M. Ly, H. Maldonado, Adsorption of chromium onto cross-linked chitosan, Sep. Purif. Technol. 44 (1) (2005) 31-36.

[27]. Zhou, D., L. N. Zhang, J. P. Zhou, S. L. Guo, Cellulose/chitin beads for adsorption of heavy metals in aqueous solution, Water Res. 38 (11) (2004) 2643-2650.

[28]. Krishnani, K. K., X. G. Meng, C. Christodoulatos, V. M. Boddu, Biosorption mechanism of nine different heavy metals onto biomatrix from rice husk, J. Hazard. Mater. 153 (3) (2008) 1222-1234.

[29]. Reddad, Z., C. Gerente, Y. Andres, P. Le Cloirec, Adsorption of several metal ions onto a low-cost biosorbent: Kinetic and equilibrium studies, Environ. Sci. Technol. 36 (9) (2002) 2067-2073.

[30]. Gustafsson, J. S., http://www.lwr.kth.se/English/OurSoftware/vminteq/

[31]. Silverstein, R. M. and F. X. Webster, Spectrometric Identification of Organic Compounds, 6th. ed., Wiley & Sons, New York, 1998.

[32]. Socrates, G., Infrared Characteristic Group Frequencies, 2nd. ed., John Wiley & Sons, New York, 1998.

[33]. Wade, L. G., QUIMICA ORGANICA, 2nd. ed., Prentice Hall Hispanoamericana, México, 1993.

[34]. Ibanez, J. P., Y. Umetsu, Uptake of trivalent chromium from aqueous solutions using protonated dry alginate beads, Hydrometallurgy 72 (3-4) (2004) 327-334.

[35]. Sawalha, M. F., J. R. Peralta-Videa, G. B. Saupe, K. M. Dokken, J. L. Gardea-Torresdey, Using FTIR to corroborate the identity of functional groups involved in the binding of Cd and Cr to saltbush (Atriplex canescens) biomass, Chemosphere 66 (8) (2007) 1424-1430.

[36]. Parab, H., S. Joshi, N. Shenoy, A. Lali, U. S. Sarma, M. Sudersanan, Determination of kinetic and equilibrium parameters of the batch adsorption of

Co(II), Cr(III) and Ni(II) onto coir pith, Process Biochem. 41 (3) (2006) 609-615.

[37]. Garg, U., M. P. Kaur, G. K. Jawa, D. Sud, V. K. Garg, Removal of cadmium (II) from aqueous solutions by adsorption on agricultural waste biomass, J. Hazard. Mater. 154 (1-3) (2008) 1149-1157.

[38]. Manceau, A., M. C. Boisset, G. Sarret, R. L. Hazemann, M. Mench, P. Cambier, R. Prost, Direct determination of lead speciation in contaminated soils by EXAFS spectroscopy, Environ. Sci. Technol. 30 (5) (1996) 1540-1552.

[39]. Stumm, W. and J. J. Morgan, Aquatic Chemistry: Chemical Equilibria and Rates in Natural Waters, 3rd. ed., John Wiley & Sons, New York, 1996.

Chapter 3

CONTRIBUTION OF AGRO-WASTE MATERIALS MAIN COMPONENTS (HEMICELLULOSES, CELLULOSE, AND LIGNIN) TO THE REMOVAL OF CHROMIUM (III) FROM AQUEOUS SOLUTION

ABSTRACT

BACKGROUND: Agro-waste materials can be used as biosorbents of heavy metals in aqueous solution. However, it is necessary to further study the contribution of agro-waste materials components (i.e. hemicelluloses, cellulose, and lignin) to the heavy metal ions removal from aqueous solution to better understand the biosorption mechanism, and also based on the biosorbents main components to predict their potential to remove heavy metals.

RESULTS: Cellulose is contained in major proportion (greater than 46%) in the agro-waste materials reported herein compared to hemicelluloses (from 12% to 26%), lignin (varying from 3% to 10%), and other compounds (22% to 30%) that were removed after the neutral detergent fiber procedure. The identified functional groups in agro-waste materials and their fractions included hydroxyl, carboxyl, and nitrogen-containing compounds. Lignin contributed in higher proportion than hemicelluloses to the Cr (III) adsorption capacity on both sorghum straw and oats straw. On the other hand lignin was the main responsible fraction for Cr (III) adsorption on agave bagasse.

CONCLUSION: Hemicelluloses and lignin mainly contributed to the chromium (III) removal from aqueous solution, and cellulose contained in the agro-waste adsorbents studied herein did not seem to participate.

Keywords: Agro-waste materials, sequential fiber extraction, components, functional groups, adsorption, chromium (III).

Adapted from: Garcia-Reyes Refugio Bernardo and Rangel-Mendez Jose Rene (2009), Contribution of agro-waste materials main components (hemicelluloses, cellulose, and lignin) to the removal of chromium (III) from aqueous solution, Journal of Chemical Technology and Biotechnology, 84(10) 1533-1538.

3.1 NOTATIONS

ATR-FTIR	Attenuated Total Reflection Fourier Transform Infrared
AAS	Atomic absorption spectroscopy
ADF	Acid detergent fiber (cellulose and lignin)
ADL	Acid detergent lignin (lignin)
b	Langmuir isotherm constant, L mg^{-1}
C_e	Equilibrium chromium (III) concentration, mg L^{-1}
k	Freundlich isotherm constant, mg g^{-1} $L^{1/n}$ $mg^{1-1/n}$
n	Freundlich isotherm constant (dimensionless)
NDF	Neutral detergent fiber (hemicelluloses, cellulose and lignin)
Q_e	Chromium (III) sorption capacity, mg g^{-1}
Q_{max}	Maximum chromium (III) sorption capacity, mg g^{-1}
r^2	Correlation coefficient (dimensionless)
WAB	Water-washed agave bagasse
WOS	Water-washed oats straw
WSS	Water-washed sorghum straw

3.2 INTRODUCTION

In recent decades, industrial activities have increased and these have enabled an important economic growth in different countries around the world. However, industrial effluents and their level of contamination have also increased.

Wastewater from industries such as tannery, metal-plating, electronic, pigments and paints, among others, contain heavy metals such as trivalent chromium (Cr (III)). Recently, it has been established that Cr (III) affects to a greater extent than Cr (VI) the human erythrocyte membrane; this perturbation could decrease the immune system activity [1].

Metal-containing effluents are commonly treated by chemical precipitation [2], coagulation–sedimentation [3], membranes systems [4], etc. Nevertheless, the high cost of membranes and chemicals make these processes less viable. Furthermore, the recommended discharge concentrations (RDC) are not always reached by chemical precipitation and coagulation–sedimentation processes

because heavy metals in solutions have a higher minimum solubility than the RDC. For this reason, it is necessary to apply another treatment like adsorption in order to achieve the RDC of heavy metals.

Adsorbents commonly used to remove heavy metals from aqueous solution include activated carbon [5], polymeric ion exchanger resins [6], zeolites [7], etc. But recently some researchers have successfully used biosorbents for removing heavy-metal ions from aqueous solution, for example: seaweed biomass [8, 9], chitin and chitosan [10], alginate beads [11, 12], agro-waste adsorbents [13-18], etc. The main advantages of using biosorbents in adsorption processes are the low cost and the local availability.

In Mexico, agro-waste materials such as sorghum straw (*Sorghum bicolor*), oats straw (*Avena sativa*), and agave bagasse (*Agave salmiana*) can be used to treat metal-containing wastewater. The low cost of these agro-waste materials (< $2 USD/Kg), compared with commercial resins (≤ $17 USD/Kg), increases the possibility of using biosorbents in adsorption processes.

As already mentioned, several studies have demonstrated the potential of using agro-waste materials for removing heavy metal ions from aqueous solution [13-18]. However, it is important to understand and explain more in detail the contribution of the agro-waste materials main components (hemicelluloses, cellulose, and lignin) to the removal of contaminants (e.g. Cr (III)) from aqueous solution in order to elucidate the sorption mechanism and also to predict the potential of these residues as adsorbents based on the content of the components. For this reason the aim of this research is to determine the Cr (III) adsorption capacity of agro-waste materials and their main components to quantify their contribution to the sorption process.

3.3 MATERIALS AND METHODS

3.3.1 Biosorbents

Sorghum straw (SS), oats straw (OS) and agave bagasse (AB) were tested as biosorbents to remove Cr (III) from aqueous solution. Previous to the sorption experiments, the agro-waste materials were ground to obtain particles of about 1

mm, and then washed with de-ionized water (W). Finally, the biosorbents were dried in an oven at 50°C for 24 h, and then stored in desiccators until the experiments were conducted.

To identify the biosorbents, capital letters were used throughout the document; for example, water-washed sorghum straw (WSS), water-washed oats straw (WOS), and water-washed agave bagasse (WAB).

It is important to mention that the agave bagasse used as starting material had being thermally and mechanically processed to produce an alcoholic beverage called 'mezcal'.

3.3.2 Chemicals

A stock solution of 500 mg L^{-1} was prepared by using $Cr(NO_3)_3 \cdot 9H_2O$ (A.C.S., Meyer). Appropriate dilutions were prepared to conduct sorption experiments with initial concentration of Cr (III) ranging from 5 to 100 mg L^{-1}. De-ionized water was used to prepare all solutions. Finally, chromium concentrations were measured by atomic absorption spectroscopy (AAS) by a Perkin Elmer, AAnalyst 400.

3.3.3 Fiber analyses

Agro-waste materials main components (hemicelluloses, cellulose, and lignin) were quantified by difference after obtaining neutral detergent fiber (NDF), acid detergent fiber (ADF), and acid detergent lignin (ADL) by the filter bag technique using an ANKOM 200 Fiber Analyzer [19]. These procedures are based on the sequential extraction methods first proposed by Van Soest [20].

Although the fiber extraction procedures are no totally selective, residues that remain can be related to certain structural biopolymers. For instance, the residues remaining after the NDF procedure consist principally of hemicelluloses, cellulose, and lignin. In the case of the ADF procedure, the residues that remain are rich in cellulose, and lignin. Finally, a fraction rich in lignin is obtained after the ADL procedure. These fractions were used in adsorption experiments.

3.3.4 Functional groups in the agro-waste materials

Attenuated Total Fourier Transform Infrared (ATR-FTIR) spectra were obtained by a Thermo-Nicolet, Nexus 470 FT-IR E.S.P., for agro-waste materials, their fractions, and commercial standards (pectin, cellulose, and lignin). Functional groups were identified based on their characteristic transmittance peaks.

3.3.5 Adsorption experiments

The Cr (III) sorption capacity (Q_e) of the biosorbents was determined at 25°C and pH 4. Samples of biosorbent (10 mg) were added to 10 mL of Cr (III) solutions containing 5 to 100 mg L^{-1} of Cr (III). These experiments were continuously stirred at 180 rpm. The solution pH was adjusted daily to pH 4 by adding 0.1 N NaOH and/or 0.1 N HNO_3 until the equilibrium was achieved. Aliquots were taken to measure the initial and the final (at equilibrium) chromium concentrations (C_e) by AAS. Adsorption isotherm models (Langmuir and Freundlich) were used to adjust the experimental data.

3.4 RESULTS AND DISCUSSION

3.4.1 Fiber analyses

Agro-waste materials are formed of such structural biopolymers as cellulose, hemicelluloses, pectin, and lignin. In addition, these residues contain some waxes, salts, water, starch, tannin, proteins, etc. [21]. The percentage content of main components varies according to the plant age and from one species to another.

Sorghum and oats crops require 3 to 4 months to become an adult plant. In contrast, agave plants require about 5 to 8 years. This age difference suggests dissimilar fiber content in the selected agro-waste materials.

Figure 3.1 shows the percentage of the main components of the agro-waste materials. As can be seen, cellulose is present in major proportion (greater than 46%) compared with hemicelluloses (from 12% to 26%) and lignin (varying from 3% to 10%) for all the biosorbents studied herein. It is important to note that the cellulose percentage is approximately the same for the three agro-waste materials.

The percentage of compounds lost (extractives) after NDF was around 22% for WSS and WOS, but in the case of WAB it was about 30%. This behavior can be due to the thermal and mechanic treatment previously applied to WAB to extract sugars that are fermented to produce mezcal. Additionally, because of this same treatment, WAB hemicelluloses are approximately half (12.8%) of those in WSS and WOS (both about 26%) which were just water washed and dried before being used as adsorbents.

Finally, WAB contained a higher lignin quantity (10.1%) than WSS (3.7%) and WOS (5.7%), which could be attributed to its age. As mentioned the lignin percentage in agro-waste materials increases with age.

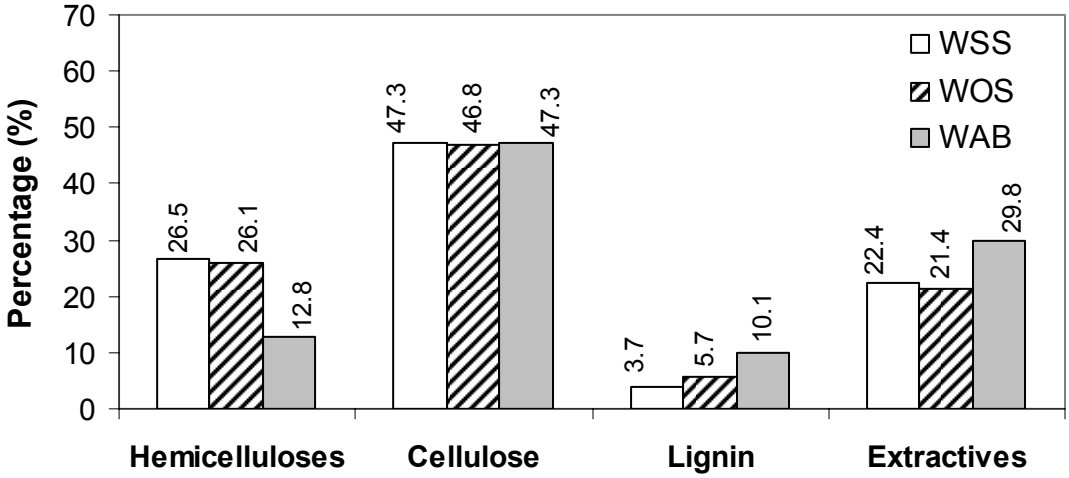

Figure 3.1. Agro-waste materials main components.

3.4.2 Functional groups in agro-waste materials

Structural biopolymers that are present in agro-waste materials have functional groups which are able to link biopolymer chains by hydrogen and calcium bridges to give structural support. Moreover, these functional groups can play a major role in heavy metals adsorption processes. For this reason, it is important to identify these functional groups in order to predict the potential of agro-waste materials for use as adsorbents of heavy metals present in aqueous solution.

Figure 3.2 (A), (B), and (C) show ATR-FTIR spectra of agro-waste materials and their fractions (NDF and ADF). Figure 3.2 (D) shows ATR-FTIR spectra of lignin

obtained from agro-waste adsorbents. Finally, Figure 3.3 shows ATR-FTIR spectra of commercial standard compounds.

Agro-waste materials main components (cellulose, hemicelluloses, pectin, and lignin) have hydroxyl groups [21] that can be confirmed by ATR-FTIR analyses (see Figure 3.2–3.3) at around 3350 cm^{-1} and 1050 cm^{-1} [22, 23]. Broader and more intense peaks appeared around 3350 cm^{-1} after digesting agro-waste materials using the ADF procedure (see Figure 3.2 (A), (B), and (C)). This suggests that cellulose and lignin (which contain a higher density of hydroxyl groups) were more freely vibrated by infrared energy because some compounds were removed (hemicelluloses, pectin, and extractives) from the agro-waste materials. In the case of lignin spectra (Figure 3.2 (D)) obtained for agro-waste materials, the hydroxyl-corresponding band was shifted from 3350 cm^{-1} to 3220 cm^{-1}, and this signal decreased after the ADL procedure suggesting that cellulose was efficiently hydrolyzed. On the other hand, nitrogen-containing groups were identified in lignin residues (see Figure 3.2 (D)) at characteristic peaks around 3060 cm^{-1} [22, 23].

Hemicelluloses, pectin, and lignin contain carboxyl groups [22, 23] that have characteristic infrared bands at around 1740 cm^{-1} and 1660 cm^{-1} when these are associated to aliphatic and aromatic compounds, respectively [22, 23]. These two characteristic bands were observed in both water-washed agro-waste materials and their fractions (see Figure 3.2 (A), (B), (C), and (D)), which can be attributed to pectin and lignin of the agro-waste materials since the infrared spectra of these standards (Figure 3.3) clearly showed carboxyl groups at 1740 cm^{-1} and 1650 cm^{-1}, respectively. Once the agro-waste materials were digested by the ADF procedure, the intensity of the carboxyl-corresponding bands decreased in comparison to those of the water-washed materials. This behavior can be attributed to the pectin and hemicelluloses hydrolysis.

Regarding the lignin spectra obtained from agro-waste materials (see Figure 3.2 (D)), the carboxyl characteristic bands (1740 cm^{-1} and 1650 cm^{-1}) were more intense than those obtained for water-washed agro-waste materials and their fractions (NDF and ADF) as shown on Figure 3.2 (A), (B), and (C). These carboxyl-

corresponding groups could be formed due to the strong acid digestion carried out by H_2SO_4 (24 N) to obtain lignin fraction.

Nitrogen-containing functional groups (e.g. amine and amide) show infrared characteristic bands around 1610 cm^{-1} [23]. These functional groups were identified in agro-waste materials and their fractions (see Figure 3.2 (A), (B), (C), and (D)). However, the signal in this band was stronger for lignin (Figure 3.2 (D)) which suggests higher density of nitrogen-containing groups. Nevertheless it should be considered that part of this behavior could be attributed to the ADF procedure since acid detergent (cetyl trimethyl ammonium bromide, CTAB) contains amines. Likewise, proteins contain amide groups that can be associated to lignin biopolymers: these proteins can increase the characteristic bands around 1610 cm^{-1}.

Finally, methyl groups regularly present characteristic bands at around 2962 cm^{-1} and 2872 cm^{-1} for asymmetrical and symmetrical vibrations, respectively [22]. Such bands were detected in the spectra shown on Figure 3.2 ((A), (B), (C), and (D)). In addition, methylene groups show characteristic bands at about 2926 cm^{-1} and 2853 cm^{-1} for asymmetrical and symmetrical vibrations, respectively [22]. These methylene groups were confirmed in lignin fraction of agro-waste materials spectra (see Figure 3.2 (D)), which suggests that the acid treatment (24 N H_2SO_4) to obtain the lignin fraction favored the appearance of the methylene group. This acid digestion also increased the content of sulfate groups on the lignin fraction and can be identified around 1450 cm^{-1} in the ATR-FTIR spectra (Figure 3.3 (D)). Sulfate groups can be used as adsorption sites of metal cations.

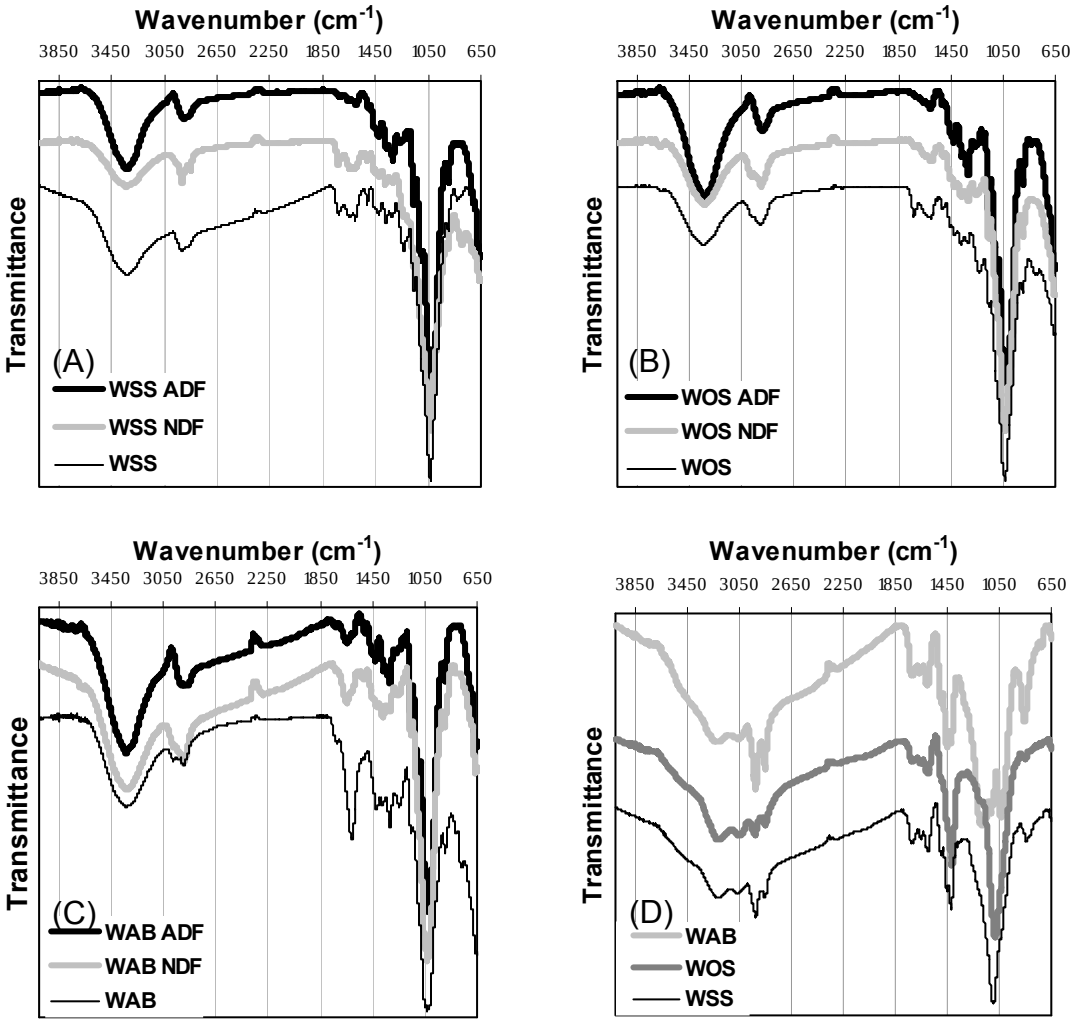

Figure 3.2. ATR-FTIR spectra of agro-waste materials and their fractions: (A) WSS, (B) WOS, (C) WAB, and (D) ADL.

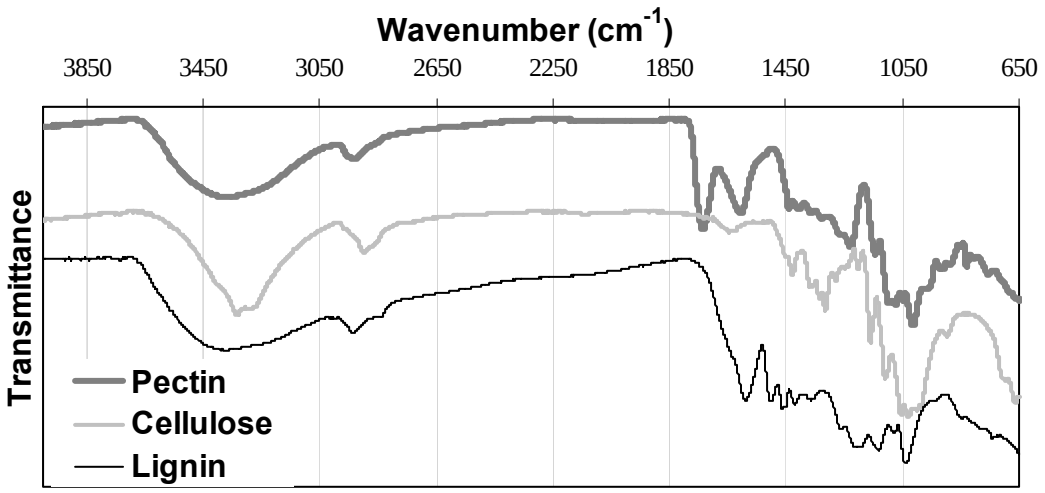

Figure 3.3. ATR-FTIR spectra of commercial standards.

3.4.3 Adsorption experiments

Chromium (III) adsorption isotherms of agro-waste materials and their fractions are shown on Figure 3.4. Although the Freundlich model fitted the experimental adsorption data better than the Langmuir model (see Table 1), based on the correlation coefficient (r^2), these models are used only to predict the tendency of the experimental results and to compare the isotherm estimated parameters between adsorbents for a given metal. The maximum Cr (III) sorption capacity (Q_{max}) of both agro-waste materials and their fractions calculated by the Langmuir model was in the range of 5.6–14.5 mg g^{-1} (see Table 1). Some of these Q_{max} values are similar to those reported for polymeric resins namely Lewatit S-100 (20.3 mg g^{-1}) and Chelex-100 (15.1 mg g^{-1}) [6]. Moreover, the Langmuir isotherm constant (b) is related to the affinity of the binding sites for the metals. The low values of parameter b (0.02–2.82 L mg^{-1}) indicate that both agro-waste adsorbents and their fractions have high affinity for Cr (III). Nevertheless these values are higher than those reported for Chelex-100 resins (0.002 L mg^{-1}) and Lewatit S-100 (0.001 L mg^{-1}) [6].

3.4.4 Adsorption experiments on NDF residues (hemicelluloses, cellulose, and lignin)

Chromium (III) adsorption capacity of NDF residues both from WSS (Figure 3.4 (I) ○) and WOS (Figure 3.4 (II) ○) was 9.8 and 12.2 mg g^{-1}, respectively, for an initial Cr (III) concentration of 100 mg L^{-1} and pH 4. As can be observed on Figure 3.4 (I) and (II), NDF residues had a higher Cr (III) sorption capacity than both water-washed biosorbents (♦) and the ADF fraction (▲: cellulose and lignin). The latter suggests that the NDF procedure removed some compounds from WSS and WOS that decreased the Cr (III) sorption capacity of NDF residues. Such compounds hydrolyzed during the NDF procedure could be waxes, inorganic salts, starch, tannin, among others.

In contrast, Figure 3.4 (III) (♦) shows that WAB had higher Cr (III) adsorption capacity (14.8 mg g^{-1} for an initial Cr (III) concentration of 100 mg L^{-1} at pH 4) than their fractions (○NDF, ▲ADF, and □ADL). This suggests that the fiber sequential extraction procedures applied to the WAB materials caused stronger structural modifications, as can be seen in the corresponding ATR-FTIR spectra (around 1650 cm^{-1}) presented on Figure 3.2 (C). These structural modifications reduced the Cr (III) sorption capacity probably due to carboxyl group hydrolysis.

Table 3.1. Isotherm parameters estimated from experimental data at pH 4 and 25°C.

Biosorbent	LANGMUIR			FREUNDLICH		
	Q_{max}	b	r^2	k	n	r^2
WSS	11.60	0.02	0.89	0.73	1.97	0.94
WSS NDF	9.30	0.11	0.82	2.02	2.93	0.93
WSS ADF	9.12	0.02	0.96	0.40	1.67	0.97
WSS ADL	n.a.	n.a.	n.a.	4.13	-90.42	0.45
WOS	6.26	0.67	0.85	3.47	6.93	0.90
WOS NDF	12.18	0.10	0.75	3.03	3.32	0.92
WOS ADF	10.41	0.02	0.99	0.44	1.66	0.99
WOS ADL	5.93	2.16	0.59	4.12	10.25	0.80
WAB	12.08	0.74	0.93	5.00	4.23	0.97
WAB NDF	5.64	2.82	0.84	3.61	8.13	0.91
WAB ADF	14.48	0.01	0.91	0.35	1.48	0.93
WAB ADL	8.05	0.05	0.84	1.25	2.65	0.94

n.a.=not avalaible; Q_{max} (mg g^{-1}); b (L mg^{-1}); k (mg g^{-1} $L^{1/n}$ $mg^{1-1/n}$); b, r^2 (dimensionless).

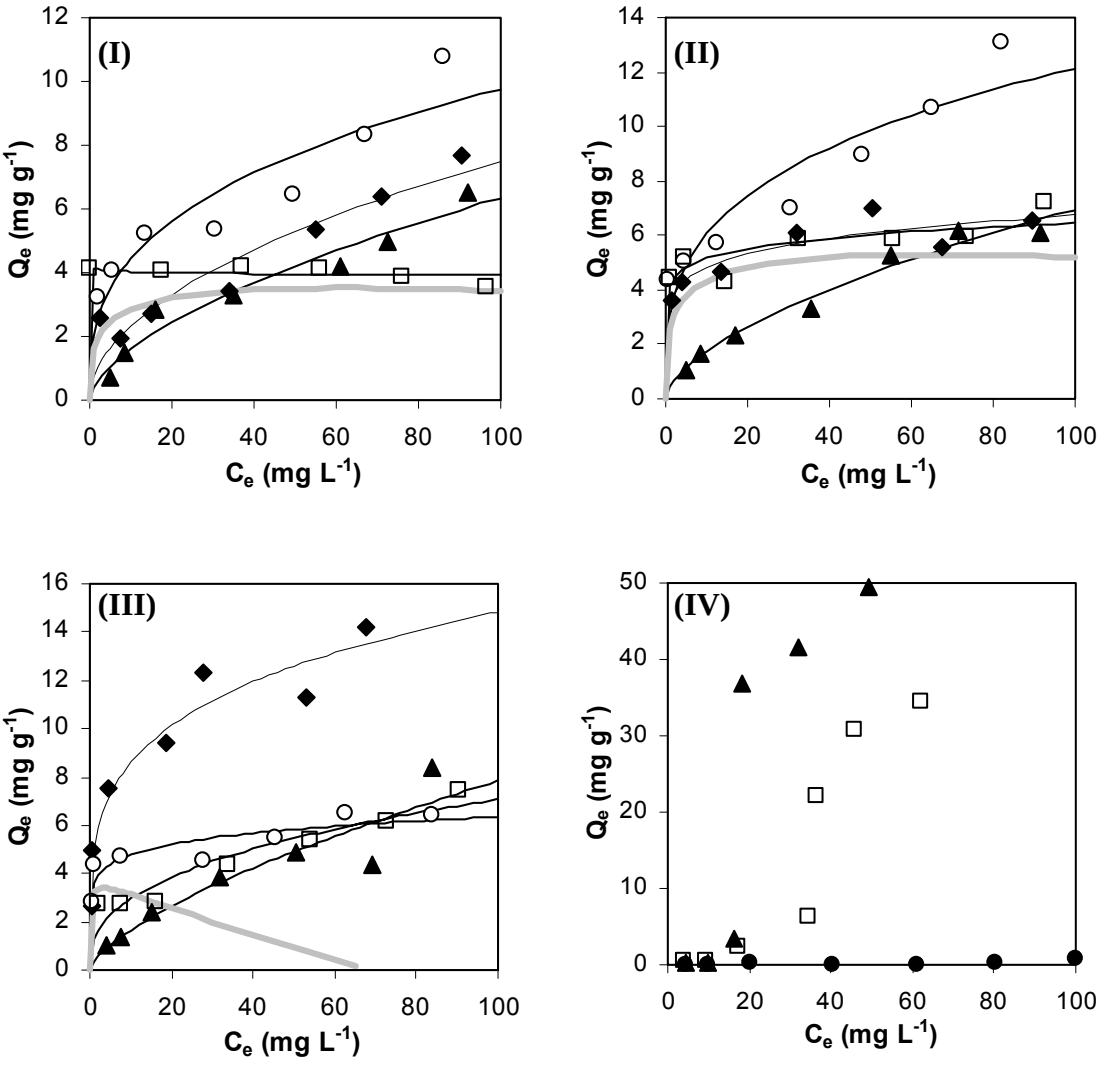

Figure 3.4. Chromium (III) adsorption isotherms of water-washed (♦) agro-waste materials [(I) WSS, (II) WOS, and (III) WAB], their fractions (○NDF, ▲ADF, □ADL), and commercial standards [(IV): ● Cellulose, □ Pectin, and ▲Lignin] at pH 4 and 25°C. The lines represent the Freundlich model. The contribution of hemicelluloses in chromium adsorption capacity is shown on (I), (II), and (III) as a gray line.

3.4.5 Adsorption experiments on ADF residues (cellulose and lignin)

The Cr (III) adsorption capacity of ADF residues for both WSS (Figure 3.4 (I) ▲) and WOS (Figure 3.4 (II) ▲) decreased in comparison to NDF residues (○). Similar

results were obtained for ADF residues of WAB (Figure 3.4 (III) ▲) but at lower Cr (III) initial concentrations than 80 mg L^{-1}. This behavior is likely due to the removal of hemicelluloses from the NDF residues after the ADF procedure. As was mentioned, hemicelluloses and pectin have carboxyl groups (as hexuronic and poly-galacturonic acids, respectively) that play an important role in adsorption of positively-charged heavy metal ions in aqueous solution [9, 11, 18].

3.4.6 Adsorption experiments on ADL residues (lignin)

Regarding the Cr (III) adsorption capacity of ADL residues of WOS (Figure 3.4 (II) □), a lower Q_e than NDF residues of WOS (Figure 3.4 (II) ○) but higher than ADF residues of WOS (Figure 3.4 (II) ▲) was obtained. This suggests that the hemicelluloses and lignin of WOS were major contributors to Cr (III) removal. These results are supported by the Cr (III) adsorption capacity of pectin and lignin, commercial standard compounds, shown on Figure 3.4 (IV).

Based on the results shown on Figure 3.4 (III) (□), the Cr (III) adsorption capacity of ADL residues of WAB was approximately equal to that found for ADF residues of WAB (Figure 3.4 (III) ▲) which indicates that cellulose did not participate in the Cr (III) adsorption capacity, and that lignin was mainly responsible for the Cr (III) removal. Figure 3.4 (IV) (●) also demonstrates that cellulose did not contribute in the removal of Cr (III). These results are in agreement with those reported in the literature which have demonstrated that lignin plays an important role in heavy metal removal [24] and that cellulose does not adsorb heavy metal ions [25].

On the other hand, Cr (III) sorption capacity of ADL residues of both WSS and WOS, (Figure 3.4 (I) □, and (II) □), remained approximately constant at low initial Cr (III) concentration which means that chromium ions had a high affinity for functional groups on lignin fractions. Nevertheless this behavior is quite different for ADL residues of WAB (Figure 3.4 (III) □) perhaps because of its high lignin content (see Figure 3.1), which enhanced the sorption capacity as the initial chromium concentration increased.

In addition, 40% and 55% of the Cr (III) adsorption capacity at C_e=100 mg L^{-1} of NDF residues of WSS and WOS, respectively, could be attributed to the lignin

fraction. On the other hand, at the same equilibrium concentration, the lignin fraction of WAB was mainly responsible for Cr (III) adsorption.

3.4.7 Adsorption capacity of hemicelluloses in agro-waste materials

Figure 3.4 ((I), (II), and (III)) shows the hemicelluloses contribution to the Cr (III) adsorption capacity (represented as a gray line) at pH 4 and 25°C. This Cr (III) adsorption capacity was calculated from the difference between NDF residues and the ADF residues adsorption capacity predicted by the Freundlich model.

Figure 3.4 (I) and (II) clearly show that hemicelluloses of agro-waste materials contributed in high proportion to the Cr (III) adsorption capacity. For example, the Cr (III) adsorption capacity of hemicelluloses from WSS (Figure 3.4 (I)) was in the range of 1.6 to 3.4 mg g^{-1} for Cr (III) initial concentration of 1 to 100 mg L^{-1}, respectively. In contrast, the Cr (III) adsorption capacity attributed to hemicelluloses from WOS was in the range of 2.6 to 5.2 mg g^{-1} depending again on the Cr (III) initial concentration. From these results it can be deduced that 35% and 43% of the Cr (III) adsorption capacity of NDF residues (at C_e=100 mg Cr (III) L^{-1}) could be attributed to the hemicelluloses from WSS and WOS, respectively.

For WAB (Figure 3.4 (III)), at C_e>65 mg Cr (III) L^{-1}, hemicelluloses did not seem to contribute to Cr (III) removal. In addition, at C_e>65 mg Cr (III) L^{-1}, the Cr (III) adsorption capacity can be attributed to the lignin fraction. This suggests that chromium (III) is preferentially bound to the lignin fraction of WAB. The higher percentage of lignin in WAB (see Figure 3.1) could explain why Cr (III) was preferentially bound to this fraction contrary to the other agro-waste materials studied.

Due to the complex composition of the agro-waste materials, it is difficult to assign the contribution of their main components (cellulose, hemicelluloses, and lignin) to the chromium (III) removal. Nevertheless it can be concluded that hemicelluloses and lignin in agro-waste materials are the major contributors to the removal of Cr (III) from aqueous solution.

3.5 CONCLUSIONS

The agro-waste materials studied have the following contents: cellulose (greater than 46%), hemicelluloses (from 12% to 26%), lignin (varying from 3% to 10%), and compounds removed after NDF (22% to 30%).

Functional groups identified on agro-waste materials and their fractions include hydroxyl, carboxyl, and nitrogen-containing compounds. These functional groups are affected by the procedure applied in order to separate the agro-waste materials main fractions (NDF, ADF, and ADL).

NDF fraction (residues rich in cellulose, hemicelluloses, and lignin) from both WSS and WOS has higher Cr (III) adsorption capacity than water-washed biosorbents which means that the removed compounds (waxes, inorganic salts, starch, and tannin, etc.) restrict the interaction between NDF fraction and the Cr (III) species in aqueous solution. In contrast, WAB has higher Cr (III) adsorption capacity than its fractions (NDF, ADF, and ADL) probably to fiber extraction procedures, source, composition, and treatment of this biosorbent.

Chromium (III) adsorption capacity decreases after the ADF procedure on WSS and WOS because hemicelluloses are removed from the NDF residues; this biopolymer contains carboxyl groups that play an important role in adsorption of positively-charged heavy metal ions from aqueous solution.

Hemicelluloses and lignin contribute in higher proportion in Cr (III) adsorption capacity on WSS and WOS. For example, the contribution of hemicelluloses and lignin of WSS to the Cr (III) adsorption capacity was 35% and 40%, respectively. Lignin is the major constituent responsible for the removal of Cr (III) in WAB.

In summary, lignin was more important than hemicelluloses in the removal of Cr (III) from aqueous solution, and cellulose contained in all the agro-waste materials studied does not seem to participate in Cr (III) adsorption capacity.

3.6 REFERENCES

[1]. Suwalsky, M., R. Castro, F. Villena, and C. P. Sotomayor, Cr(III) exerts stronger structural effects than Cr(VI) on the human erythrocyte membrane and molecular models. J. Inorg. Biochem., 102(4) (2008) 842-849.

[2]. Matlock, M. M., B. S. Howerton, and D. A. Atwood, Chemical precipitation of heavy metals from acid mine drainage. Water Res., 36(19) (2002) 4757-4764.

[3]. Qin, G., M. J. McGuire, N. K. Blute, C. Seidel, and L. Fong, Hexavalent Chromium Removal by Reduction with Ferrous Sulfate, Coagulation, and Filtration: A Pilot-Scale Study. Environ. Sci. Technol., 39(16) (2005) 6321-6327.

[4]. Qin, J. J., M. N. Wai, M. H. Oo, and F. S. Wong, A feasibility study on the treatment and recycling of a wastewater from metal plating. J. Membr. Sci., 208(1-2) (2002) 213-221.

[5]. Schneider, R. M., C. F. Cavalin, M. A. S. D. Barros, and C. R. G. Tavares, Adsorption of chromium ions in activated carbon. Chem. Eng. J., 132(1-3) (2007) 355-362.

[6]. Gode, F. and E. Pehlivan, Removal of chromium(III) from aqueous solutions using Lewatit S 100: The effect of pH, time, metal concentration and temperature. J. Hazard. Mater., 136(2) (2006) 330-337.

[7]. Pansini, M., C. Colella, and M. De Gennaro, Chromium removal from water by ion exchange using zeolite. Desalination, 83(1-3) (1991) 145-157.

[8]. Kratochvil, D., P. Pimentel, and B. Volesky, Removal of trivalent and hexavalent chromium by seaweed biosorbent. Environ. Sci. Technol., 32(18) (1998) 2693-2698.

[9]. Park, D., Y. S. Yun, and J. M. Park, XAS and XPS studies on chromium-binding groups of biomaterial during Cr(VI) biosorption. J. Colloid Interface Sci., 317(1) (2008) 54-61.

[10]. Rojas, G., J. Silva, J. A. Flores, A. Rodriguez, M. Ly, and H. Maldonado, Adsorption of chromium onto cross-linked chitosan. Sep. Purif. Technol., 44(1) (2005) 31-36.

[11]. Ibanez, J. P. and Y. Umetsu, Uptake of trivalent chromium from aqueous solutions using protonated dry alginate beads. Hydrometallurgy, 72(3-4) (2004) 327-334.

[12]. Silva, R. M. P., J. P. H. Manso, J. R. C. Rodrigues, and R. J. L. Lagoa, A comparative study of alginate beads and an ion-exchange resin for the removal of heavy metals from a metal plating effluent. J. Environ. Sci. Health Part A-Toxic/Hazard. Subst. Environ. Eng., 43(11) (2008) 1311-1317.

[13]. Cano-Rodríguez, I. P.-G., J. A.; Gutiérrez-Valtierra, M.; Gardea-Torresdey, J. L., Remoción y recuperación de cromo(III) de soluciones acuosas por biomasa de sorgo. Rev. Mex. Ing. Quim., 1 (2002) 97-103.

[14]. Chojnacka, K., Biosorption of Cr(III) ions by wheat straw and grass: a systematic characterization of new biosorbents. Pol. J. Environ. Studies, 15(6) (2006) 845-852.

[15]. Krishnani, K. K., X. G. Meng, C. Christodoulatos, and V. M. Boddu, Biosorption mechanism of nine different heavy metals onto biomatrix from rice husk. J. Hazard. Mater., 153(3) (2008) 1222-1234.

[16]. Reddad, Z., C. Gerente, Y. Andres, and P. Le Cloirec, Adsorption of several metal ions onto a low-cost biosorbent: Kinetic and equilibrium studies. Environ. Sci. Technol., 36(9) (2002) 2067-2073.

[17]. Romero-Gonzalez, J., J. R. Peralta-Videa, E. Rodriguez, M. Delgado, and J. L. Gardea-Torresdey, Potential of Agave lechuguilla biomass for Cr(III) removal from aqueous solutions: Thermodynamic studies. Bioresour. Technol., 97(1) (2006) 178-182.

[18]. Sawalha, M. F., J. R. Peralta-Videa, G. B. Saupe, K. M. Dokken, and J. L. Gardea-Torresdey, Using FTIR to corroborate the identity of functional groups involved in the binding of Cd and Cr to saltbush (Atriplex canescens) biomass. Chemosphere, 66(8) (2007) 1424-1430.

[19]. ANKOM and Technology. 2005 [cited 2009 January 19]; Available from: http://www.ankom.com/.

[20]. Van Soest, P. J., Use of detergents in the analysis of fibrous feeds. II. A rapid method for the determination of fiber and lignin. J. Ass. Offic. Agr. Chem., 46 (1963) 829-835.

[21]. Buchanan, B. B., Gruissem, W., Jones, R. L., Biochemistry & Molecular Biology of Plants. 2000, Maryland, USA: American Society of Plant Physiologists.

[22]. Silverstein, R. M., and Webster, F. X., Spectrometric Identification of Organic Compounds. 6th. ed. 1998, New York: Wiley & Sons.

[23]. Wade, L. G., QUIMICA ORGANICA. 2nd. ed. 1993, México: Prentice Hall Hispanoamericana.

[24]. Lee, B. G. and R. M. Rowell, Removal of heavy metal ions from aqueous solutions using lignocellulosic fibers. J. Nat. Fibers, 1(1) (2004) 97-108.

[25]. Marshall, W. E., D. E. Akin, L. H. Wartelle, and P. A. Annis, Citric acid treatment of flax, cotton and blended nonwoven mats for copper ion absorption. Industrial Crops and Products, 26(1) (2007) 8-13.

Chapter 4

ADSORPTION KINETICS OF CHROMIUM (III) IONS ON AGRO-WASTE MATERIALS

ABSTRACT

Besides equilibrium studies, adsorption kinetics of pollutants onto adsorbents are very important to design appropriate packed columns to be used as adsorbers and to determine the rate-controlling step in the mass transfer process. A number of models are available to predict the concentration decay curves. The aim of this research is to compare the empirical (pseudo-first and pseudo-second order models) and diffusion models (film diffusion, film – pore volume diffusion, and film – surface diffusion models) in predicting the adsorption kinetics of chromium (III) (Cr (III)) on water-washed agro-waste materials (sorghum straw, SS; oats straw, OS; and agave bagasse, AB).

These biosorbents were physically characterized by calculating the solid density, surface area and pore volume distribution. Equilibrium adsorption experiments of Cr (III) on agro-waste materials were conducted in batch systems at pH 4 and 25°C. A rotating-basket reactor was used to obtain the adsorption kinetics of Cr (III) on agro-waste materials at initial pH of 4, 25°C, two initial Cr (III) concentrations and different stirring speeds.

The equilibrium adsorption results were adequately predicted by both Langmuir and Freundlich isotherm models. The maximum Cr (III) sorption capacity, calculated by the Langmuir models was 9.4, 12.1, and 22.4 mg/g for SS, OS, and AB, respectively; these biosorbents have a great potential for removing metal cations from aqueous solutions even at low metal concentrations. The adsorption rate of Cr (III) on agro-waste materials studied herein increased when increasing the initial Cr (III) concentration or the stirring speed. The concentration decay curves can be predicted by using either empirical or diffusion kinetic models.

However, the film diffusion model seems to be the most appropriate one based on the low deviation between the experimental and the predicted data, and the physical properties (low porosity (0.004–0.007), low surface area (0.6–1.2 m^2 g^{-1}) and low pore volume (0.003–0.004 cm^{-3} g^{-1}) of the selected agro-waste materials, which support the idea that intraparticle diffusion may be neglected. Furthermore, the external mass transfer coefficient estimated with the film diffusion has a physical meaning that helps to explain the diffusion of solutes across the film resistance in agro-waste biosorbents.

The film diffusion model predicted adequately the concentration decay curves of Cr (III) on agro-waste materials suggesting that the adsorption of Cr (III) is mainly limited by the film resistance surrounding the adsorbent particle.

Keywords: Diffusion models, film resistance, intraparticle diffusion, adsorption, chromium, biosorbents.

4.1 NOTATIONS

A	Outer surface area of particle per unit mass of adsorbent ($cm^2\ g^{-1}$)
AAS	Atomic absorption spectroscopy
AB	Agave bagasse
b	Langmuir isotherm constant ($L\ mg^{-1}$)
C	Concentration of solute in solution ($mg\ L^{-1}$)
C_0	Initial concentration of solute in solution ($mg\ L^{-1}$)
C_e	Equilibrium concentration of Cr (III) ($mg\ L^{-1}$)
C_{Exp}	Experimental Cr (III) concentration in solution ($mg\ g^{-1}$)
C_{Pred}	Predicted Cr (III) concentration in solution ($mg\ g^{-1}$)
C_S	Equilibrium concentration of solute at the surface of adsorbent ($mg\ L^{-1}$)
$C_{S,r}$	Concentration of adsorbate in pore volume at distance r ($mg\ L^{-1}$)
$D_{e,p}$	Effective pore diffusivity ($cm^2\ s^{-1}$)
D_p	Average pore diameter calculated by the N_2-BJH method (nm)
D_S	Surface diffusivity ($cm^2\ s^{-1}$)
%D	Average absolute percentage deviation (dimensionless)
h	Initial sorption rate calculated with parameters of the pseudo-second order model, $h \equiv k q_e^2$ ($mg\ g^{-1}\ min^{-1}$)
k	Freundlich isotherm constant ($mg\ g^{-1}\ L^{1/n}\ mg^{1-1/n}$)
k_1	Rate constant of the pseudo-first order model (min^{-1})
k_2	Rate constant of the pseudo-second order model ($g\ mg^{-1}\ min^{-1}$)
k_L	External mass transfer coefficient ($cm\ s^{-1}$)
m	Mass of adsorbent (g)
n	Freundlich isotherm constant (dimensionless)
N	Number of experimental data (dimensionless)
OS	Oats straw
$\bar{q}$	Average adsorbate concentration in the adsorbent particle ($g\ g^{-1}$)
q_e	Amount of metal ions adsorbed at equilibrium of the pseudo-second order model ($mg\ g^{-1}$)
Q_e	Cr (III) sorption capacity ($mg\ g^{-1}$)

Q_{max}	Maximum chromium (III) sorption capacity of the Langmuir model (mg g^{-1})
q_t	Amount of metal ion adsorbed at time t of the pseudo-second order model (mg g^{-1})
r	Radial co-ordinate (cm)
R	Radius of adsorbent particle (cm)
r^2	Correlation coefficient (dimensionless)
S	Surface area determined by the N_2-BET method (m^2 g^{-1})
SS	Sorghum straw
t	Time (s or min)
V	Volume of solution (cm^3)
V_p	Average pore-volume calculated by the N2-BJH method (cm^3 g^{-1})
WAB	Water-washed agave bagasse
WOS	Water-washed oats straw
WSS	Water-washed sorghum straw
X	Adsorption capacity at equilibrium of the pseudo-first order model (mg g^{-1})
x	Adsorption capacity at time t of the pseudo-first order model (mg g^{-1})
ε_p	Void fraction or porosity of the adsorbent (dimensionless)
ρ_p	Density of the adsorbent particle (g cm^{-3})
ρ_S	Solid density of adsorbent (g cm^{-3})

4.2 INTRODUCTION

Heavy metals pollution is of great concern because of the human health hazards associated with this kind of contaminants. Due to their persistence in nature, these pollutants could be dispersed in water, accumulated in plants and animals, and finally in human beings through the food chain or by consumption of contaminated water, causing serious health hazards [1]. Non-treated effluents from industries such as leather tannery, metal finishing, electroplating, stainless steel production, textile industries, etc., could contaminate water with chromium and other heavy metals.

Chromium mainly exists in the environment in its hexavalent (Cr (VI)) and trivalent form (Cr (III)). Although it is well known that Cr (VI) is more toxic than Cr (III),

prolonged exposure to Cr (III) species could also cause skin allergies and cancer in human beings [2]. In addition, Cr (III) can under certain conditions be oxidized to the state of more carcinogenic and mutagenic Cr (VI) by some bacteria or manganese oxide present in the environment [3].

Several research studies have demonstrated that heavy metal ions can be removed from aqueous solutions by adsorption processes in a full treatment facility as a polishing step. Adsorbents commonly used to remove Cr (III) include activated carbons [4], ion exchangers (i.e. polymeric resins) [5, 6], and biosorbents [1, 2, 7-13], among others. Biosorption is an emerging technology that uses biological materials as adsorbents of heavy metal ions, for example: seaweed biomass [2, 7, 10, 11], chitin/chitosan wastes [14, 15], microorganism biomass [8, 11, 16], lignocellulosic materials [1, 9, 12, 17-24], etc.

The agro-waste materials have a Cr (III) sorption capacity [25] similar to commercial ion exchangers and hence these residues can be used as adsorbents of heavy metals from aqueous solution. Nevertheless, it is necessary to conduct adsorption kinetic experiments, by using agro-waste materials, in order to design appropriate packed columns to be used as adsorbers. In addition, adsorption kinetic experiments can be used to better understand the rate-controlling step of the mass transfer process. The overall rate of adsorption on adsorbents can be described by a mechanism of three consecutive steps [26-29]:

(i) External mass transfer of solutes from bulk solution through the boundary layer to the surface of the adsorbent (film diffusion), which is commonly identified as an external mass transfer resistance.

(ii) Diffusion of solute through the adsorbent solid matrix (intraparticle diffusion), associated to intraparticle mass transfer resistance (pore volume diffusion or surface diffusion).

(iii) Adsorption of solute molecules at the active sites. This step evaluates the overall rate of adsorption of a solute by an adsorption reaction model.

According to Helfferich [26] the third step is very fast and the solute adsorption rate is limited by diffusion in porous materials. Steps (i) and (ii) are shown schematically in Figure 4.1.

The main objective of this research is to compare the empirical and the diffusion kinetic models in predicting the adsorption kinetics of Cr (III) on agro-waste materials. In addition, it is important to assess the effect of external mass transfer and intraparticle diffusion on the overall rate of adsorption to determine the controlling-rate step of this process.

4.2.1 MODELING OF ADSORPTION KINETICS OF METALS IN BATCH SYSTEMS

In designing adsorption processes, information of adsorption kinetics is required. As mentioned, the adsorption rate-controlling step may be due to various mass transfer resistances (film diffusion, intraparticle diffusion, and reaction in the adsorption sites). Several authors have proposed different models for describing adsorption kinetics based on those mass transfer resistances, for example: empirical adsorption rate models (pseudo-first order [30] or pseudo-second order [31] reaction models), film diffusion models [32, 33], intraparticle diffusion models [27, 28, 34] or a combination of these last two models (film and intraparticle diffusion models) [33].

Empirical adsorption rate models have been widely used, however the major shortcomings of these models are that film and intraparticle diffusion are neglected even though these steps are very important in mass transfer processes as occurs in adsorption.

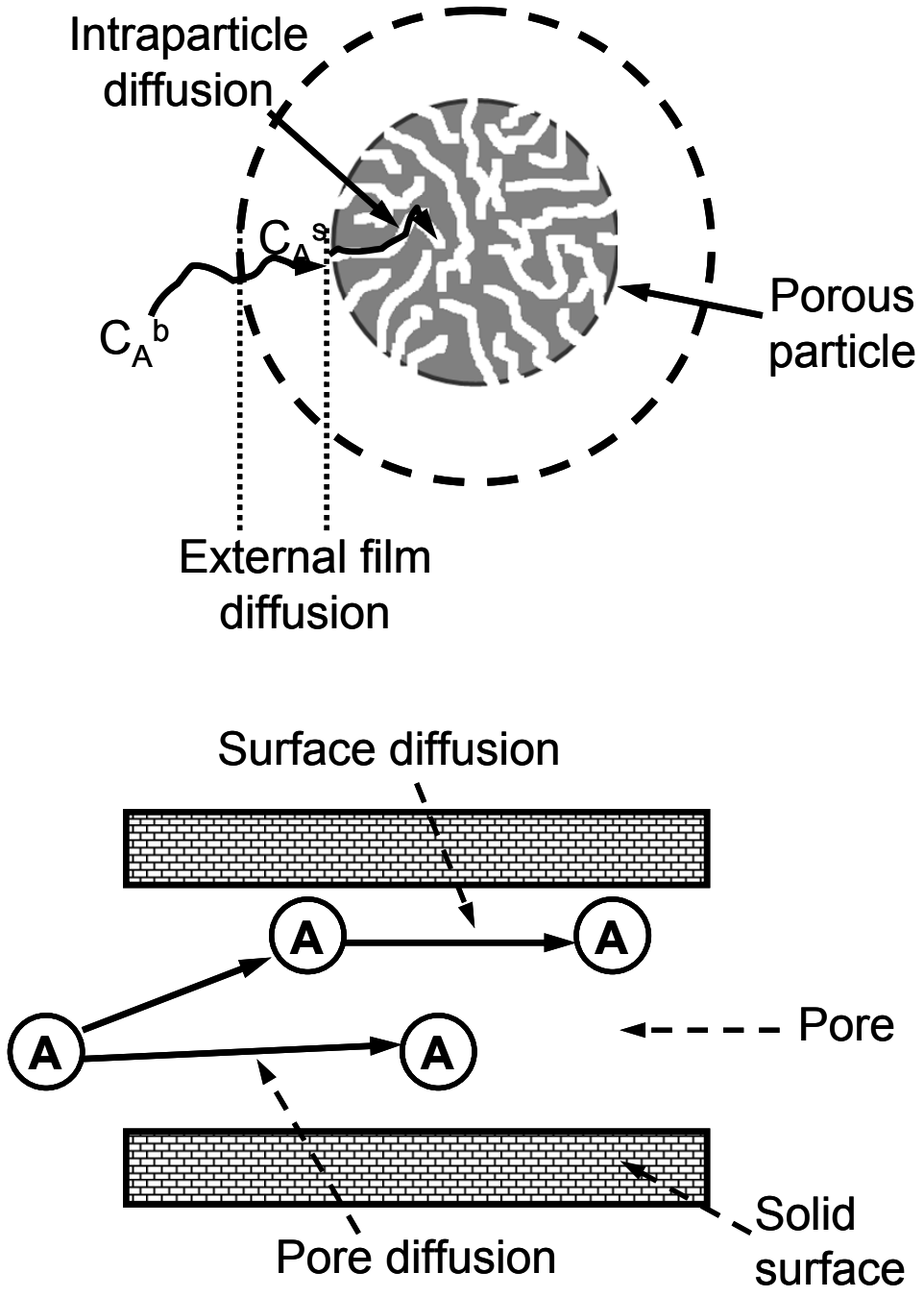

Figure 4.1. Schematic illustration of mass transfer resistances on porous adsorbents [29]. Upper image shows the external resistance due to the boundary layer. Lower image depicts intraparticle diffusion due to a gradient concentration (pore-volume diffusion) or hopping mechanism (surface diffusion).

4.2.1.1 Empirical adsorption rate models

Several researchers have predicted the overall rate of adsorption of a solute by an empirical adsorption reaction model. This rate can be considered to follow pseudo-first order or pseudo-second order reactions based on the amount of solute adsorbed on the adsorbent. The adsorption kinetics of several metals follow the pseudo-second order model, for instance: Co (II), Fe (II), and Cu (II), on modified and unmodified maize cob [19]; Cr (III) on both *Leersia hexandra Swartz* biomass [1] and blue green algae (*Spirulina platensis*) [35]; Pb (II), Cu (II) and Ni (II) onto sphagnum moss peat [31]; Pb (II), Cu (II), Zn (II), Cd (II), and Ni (II) on water-washed sugar-beet pulp [36]; Cd (II) and Cu (II) on acid- and alkali-washed wheat straw [37]; Co (II), Cr (III) and Ni (II) on coir pith [9], etc.

4.2.1.1.1 *Pseudo-first order reaction model*

The kinetics equation proposed by Lagergren [30] has been used to describe the adsorption of an adsorbate from an aqueous solution. The pseudo-first order reaction equation for the liquid-solid adsorption system has been expressed as follows:

$$\frac{dx}{dt} = k_1(X - x) \qquad (1)$$

where X and x (mg g^{-1}) are the adsorption capacities at equilibrium and time t, respectively, and k_1 (min^{-1}) is the rate constant of this adsorption model. Integrating equation (1) with the boundary conditions t = 0 to t = t and x = 0 to x = x it gives:

$$\ln\left(\frac{X}{X - x}\right) = kt \qquad (2)$$

Rearranging Eq. (2) to the linear form gives:

$$\ln(X - x) = \ln(X) + kt \qquad (3)$$

A straight line of ln (X - x) versus t suggests the applicability of this empirical model. The values of X and k_1 are calculated from the intercepts and the slopes of the straight line.

4.2.1.1.2 *Pseudo-second order reaction model*

Ho and Mckay [31] proposed an expression of pseudo-second order rate for the adsorption kinetics of divalent metal ions on *sphagnum* moss peat. This biosorbent contains polar functional groups (P^- and HP) which could be involved in chemical bonding and are responsible for the cation exchange capacity of peat. Therefore, the peat-copper reaction may be represented in two ways [38]:

$$2P^- + Cu^{2+} \leftrightarrow CuP_2 \quad (4)$$

and

$$2HP + Cu^{2+} \leftrightarrow CuP_2 + 2H^+ \quad (5)$$

To represent the adsorption of divalent metals onto peat during agitation, it was assumed that the process may be second-order and that chemisorption occurs involving valence forces through sharing or the exchange of electrons between adsorbent and adsorbate as covalent forces [31]. The rate of second-order reaction may be dependent on the amount of divalent metal ions on the surface of the peat, and the amount of divalent metal ions adsorbed at equilibrium. The rate expressions for the reactions shown in Eq. (4) and (5) are:

$$\frac{d(P)_t}{dt} = k_2\left[(P)_0 - (P)_t\right]^2 \quad (6)$$

and

$$\frac{d(HP)_t}{dt} = k_2\left[(HP)_0 - (HP)_t\right]^2 \quad (7)$$

where $(P)_t$ and $(HP)_t$ are the number of active sites occupied on the peat at time t, and $(P)_0$ and $(HP)_0$ are the number of equilibrium sites available on the peat.

The driving force, $(q_e - q_t)$, is proportional to the available fraction of active sites, then the kinetic rate equations can be rewritten as follows [31]:

$$\frac{dq_t}{dt} = k_2(q_e - q_t)^2 \quad (8)$$

where k_2 (g mg^{-1} min^{-1}) is the rate constant of sorption, q_e and q_t are the amount of divalent metal ion (mg g^{-1}) sorbed at equilibrium and at any time, respectively. Integrating equation (4) with boundary conditions t = 0 to t = t and q_t = 0 to $q_t = q_t$, gives:

$$\frac{1}{(q_e - q_t)} = \frac{1}{q_e} + k_2 t \quad (9)$$

which has a linear form of:

$$\frac{t}{q_t} = \frac{1}{k_2 q_e^2} + \frac{1}{q_e} t \quad (10)$$

The parameters of this model (k_2 and q_e) can be determined experimentally by plotting t/q_t against t. The initial sorption rate is given as $h=k_2 q_e^2$ (mg g^{-1} min^{-1}); h represents the amount of metal adsorbed per unit mass of adsorbent and unit of time. This value (h) can be used to compare the initial sorption rate of metals on various adsorbents at similar conditions (pH, solid/liquid ratio, initial metal concentrations, etc.).

4.2.1.2 *Film diffusion model*

To evaluate the external mass transfer coefficient, two models are commonly used: Furusawa and Smith model [39] and Mathews and Weber model [40]. The first model is limited to the linear region of the Langmuir isotherm model and the second one takes into account the first two points of the decay curve when time tends to zero. Although these models give a rough estimated value of the external mass transfer coefficient (k_L), these could still be used to determine whether the adsorption of solutes is limited by the film resistance surrounding the adsorbent particle (see Figure 4.1).

Allen *et al.* [32, 33] reported that the film diffusion model [39, 40] predicted very well the experimentally obtained concentration decay curves of metal cations on peat, particularly at high solid/liquid proportions. Under these conditions, film diffusion seems to be the rate-controlling step in the adsorption of metal ions (such as Pb^{2+}, Cd^{2+}, Cu^{2+}, Zn^{2+} and Al^{3+}) by peat. However, the effect of internal mass transfer resistance is more important at low biosorbent doses.

When using the mathematical equations for film diffusion model, the following assumptions must be considered:

a) External mass transfer is the only controlling adsorption process,
b) Adsorbent particles are spherical,

c) The concentration of the solute in the adsorbent and mass of adsorbate in the adsorbent are not dependent on the radial position,
d) Adsorption rate at an active site is instantaneous, and
e) Average mass of solute adsorbed on adsorbent can be represented by the Langmuir isotherm equation.

The movement of solute from the liquid phase to the adsorbent particle is given by:

$$m\frac{d\bar{q}}{dt} = mAk_L(C - C_S) \quad (11)$$

The right side of Eq. (11) is related to the accumulation of adsorbate in the outer surface of the adsorbent particle. The left side of Eq (11) indicates the rate of mass transfer leaving the solution and entering the adsorbent. The initial condition is given by:

$$t = 0,\ C = C_0 \quad (12)$$

The mass balance for the batch system is represented by the following equation:

$$V\frac{dC}{dt} = m\frac{d\bar{q}}{dt} \quad (13)$$

Because local equilibrium exists between the solute concentration on the surface of the adsorbent (C_S) and the amount of solute adsorbed on the external surface of the adsorbent ($\bar{q}$), the Langmuir adsorption isotherm provides the mathematical relationship involving C_S and $\bar{q}$ as follows:

$$\bar{q} = \frac{Q_{max}bC_S}{1 + bC_S} \quad (14)$$

To obtain the external mass transfer coefficient (k_L), the film model equations (Eq. 11–14) must be simultaneously solved by numerical methods (see Appendix E). The value of k_L that adequately fits the experimental data is considered as a mass transfer coefficient for that particular experiment.

4.2.1.3 *Intraparticle diffusion models*

According to Al-Duri and McKay [41], the mechanism of intraparticle diffusion depends on several factors including the structure of the adsorbent, chemical and physical properties of solute and adsorbent, equilibrium behavior and conditions of

adsorption systems. Intraparticle diffusion in liquid-porous solid systems may be governed by pore volume diffusion or surface diffusion or a combination of both.
Pore volume diffusion refers to diffusion of solute molecules through the liquid filled pores to the adsorption sites (Figure 4.1). Moreover, solid diffusion refers to the adsorption that occurs at the outer surface of the adsorbent and at the inner pore wall through a surface-hopping mechanism (Figure 4.1).

4.2.1.3.1 *Pore-volume diffusion model* with external mass transfer resistance

Although pore volume diffusion plays an important role in the adsorption rate of metal ions in porous adsorbents, it has not been well explored and more detailed studies are required for better understanding of intraparticle diffusion by using biosorbents. Leyva-Ramos *et al.* [27, 28, 34] have developed and applied a diffusion model in order to determine the effective pore volume diffusivity of cadmium and zinc on activated carbon and pentachlorophenol on activated carbon fibers. This model considers the following assumptions:

- Intraparticle diffusion is only due to pore volume diffusion,
- Adsorbent particles are spherical,
- Adsorption rate at an active site is instantaneous, and
- Average mass of solute adsorbed on the adsorbent can be represented by the Langmuir isotherm equation.

The model was derived by making a mass balance in the liquid solution and in the adsorbent as previously shown in Eq. 11–14. In addition, a mass balance of adsorbate in a differential element of an adsorbent particle [27] gives:

$$\varepsilon_p \frac{\partial C_{s,r}}{\partial t} + \rho_p \frac{\partial q}{\partial t} = \frac{1}{r^2}\frac{\partial}{\partial r}\left[r^2 \left(D_{e,p} \frac{\partial C_{s,r}}{\partial r} \right) \right] \qquad (15)$$

The two terms on the left in Eq. (15) represent the accumulation of adsorbate on the pore volume and the pore surface. The term on the right represents the effective pore volume diffusion. The initial and boundary conditions are:

$$C_{S,r} = 0 \quad t = 0 \quad 0 \le r \le R \tag{16}$$

$$\left.\frac{\partial C_{S,r}}{\partial r}\right|_{r=0} = 0 \tag{17}$$

$$D_{e,p}\left.\frac{\partial C_{S,r}}{\partial r}\right|_{r=R} = k_L\left(C - C_S\right) \tag{18}$$

The ordinary and partial differential equations (11–18) of this model were numerically solved (see Appendix E) and further details about the solution have been reported [27, 42].

4.2.1.3.2 *Homogeneous solid diffusion model (HSDM) with external mass transfer resistance*

This model considers a dual mass transport mechanism across the hydrodynamic boundary layer surrounding the adsorbent particle and intraparticle resistance within the particle in the form of surface diffusion [27]. Mathematical equations are similar to (11)-(14), although a mass balance of adsorbate in a differential element of an adsorbent particle is required:

$$\rho_p \frac{\partial q}{\partial t} = \frac{1}{r^2}\frac{\partial}{\partial r}\left[r^2\left(D_S \frac{\partial q}{\partial r}\right)\right] \tag{19}$$

The term on the left in equation (19) represent the accumulation of adsorbate on the pore surface. The term on the right represents the surface diffusion. The initial and boundary conditions are:

$$t = 0 \quad 0 \le r \le R \quad q = 0 \tag{20}$$

$$t > 0 \quad r = 0 \quad \frac{\partial q}{\partial r} = 0 \tag{21}$$

$$t > 0 \quad r = 0 \quad \rho_p D_S\left.\left(\frac{\partial q}{\partial r}\right)\right|_{r=R} = k_L\left(C - C_S\right) \tag{22}$$

The liquid-phase surrounding the adsorbent particle is considered uniform and the equilibrium between liquid phase and solid phase is assumed to occur at the surface of the adsorbent particle. The above equations need to be solved simultaneously (see Appendix E). The values of k_L and D_S can be determined by best fit correlation of the dynamic model with the experimental data [27].

4.3 MATERIALS AND METHODS

4.3.1 Biosorbents

Sorghum straw (SS), oats straw (OS) and agave bagasse (AB) were tested as biosorbents to remove Cr (III) from aqueous solution. Previous to the equilibrium and adsorption kinetic experiments, the agro-waste materials were ground to obtain particles in the range of 0.25 to 0.50 mm, washed with de-ionized water (20 g of biosorbents per liter of water for 24 h at 25°C and 150 min^{-1}), filtered off, rinsed, and dried in an oven at 50°C for 24 h, and then stored in desiccators until the experiments were conducted.

To identify the biosorbents, capital letters were used throughout the document; for example, water-washed sorghum straw (WSS), water-washed oats straw (WOS), and water-washed agave bagasse (WAB).

4.3.2 Physical properties of agro-waste materials

Physical characteristics of adsorbents are indispensable in predicting the adsorption kinetics of metals by diffusion models. Table 4.1 shows the physical properties of the selected agro-waste materials. The surface area (S) was determined by the N_2 BET method, the average pore-volume (V_p) and the average pore diameter (D_p) was determined by the N_2 BJH method by using a surface analyzer (Micromeritics ASAP 2020). The solid density (ρ_s) of agro-waste materials was calculated by the helium displacement method by using a Helium Picnometer (Micromeritics Accupic 1330).

The apparent density (ρ_p), the void fraction or porosity (ε_p), and the outer surface area of particle (A) of the biosorbents are also required for predicting the adsorption rate of metals by using diffusion models. These parameters (ρ_p, ε_p, and A) were estimated as follows:

$$\rho_p = \frac{\rho_s}{1 + V_p\ \rho_s} \tag{23}$$

$$\varepsilon_p = \frac{V_p}{V_p + 1/\rho_s} \tag{24}$$

$$A = \frac{3\ m}{\rho_p\ R\ (1-\varepsilon_p)} \qquad (25)$$

Table 4.1. Physical properties of agro-waste biosorbents.

Biosorbent	ρ_s (g cm^{-3})	ρ_p (g cm^{-3})	S (m^2 g^{-1})	V_p (cm^{-3} g^{-1})	D_p (nm)	ε_p (–)
WSS	1.5319	1.5216	1.2047	0.004428	13.542	0.0067
WOS	1.5362	1.5294	0.9399	0.002905	11.688	0.0044
WAB	1.5131	1.5216	0.5823	0.003133	19.590	0.0047

ρ_s: Solid density; ρ_p: Particle density; S: BET Surface area; V_p: BJH average pore volume; D_p: BJH average pore width; ε_p: Porosity (dimensionless).

4.3.3 Chemicals

A stock solution of 500 mg L^{-1} was prepared by using $Cr(NO_3)_3{\cdot}9H_2O$ (A.C.S., Meyer). Appropriate dilutions were prepared to conduct equilibrium adsorption experiments with an initial concentration of Cr (III) ranging from 5 to 100 mg L^{-1}. Deionized water was used to prepare all solutions. Finally, chromium concentration was measured by atomic absorption spectroscopy (AAS) by using a Perkin Elmer spectrometer, AAnalyst 400.

4.3.4 Equilibrium adsorption experiments

The Cr (III) sorption capacity (Q_e) of agro-waste materials was determined at 25°C and pH 4. Samples of 50 mg of biosorbent were added to 50 mL of Cr (III) solutions containing 5 to 100 mg L^{-1}. These experiments were continuously stirred at 150 rpm. The solution pH was adjusted daily to pH 4 by adding 0.1 N NaOH and/or 0.1 N HNO_3 until the equilibrium was achieved. Aliquots were taken to measure the initial and the final (at equilibrium) chromium concentrations by AAS. Adsorption isotherm models (Langmuir and Freundlich) were used to adjust the experimental data.

4.3.5 Adsorption kinetic experiments

A rotating basket adsorber was used to carry out the adsorption kinetic experiments. The adsorber was equipped with four equally spaced baffles for complete mix. The adsorber was partially immersed in a 25°C water bath to keep the temperature of the working adsorption solution constant. Figure 4.2 shows the components of the rotating basket adsorber.

Previous to the kinetic experiments, samples of biosorbents (250±1 mg) were hydrated in deionized water (100 mL) at initial pH of 4.0 for 24 h. After that, hydrated biosorbents were filtered off and slightly rinsed with deionized water at pH 4. Next, hydrated biosorbents were transferred to the basket and it was attached to the shaft of the stirrer in the adsorber. Afterwards, 750 cm^3 of deionized water (at pH 4) were poured into the adsorber, the stirrer was turned on, at 400 rpm for 30 minutes, and the pH was adjusted to 4. Then the stirrer was turned off, 250 cm^3 of a solution of known concentration of Cr (III) (80 or 200 mg L^{-1} at pH 4) were added rapidly, and the timer and the motor of the stirrer were turned on immediately. Once the experiments were initiated, the contents were mixed at the chosen stirring speed (200, 300, or 400 min^{-1}). Samples of the solution were taken at selected intervals of time and the solution pH was also measured: the total volume withdrawn was less than 2% of the initial volume solution. The collected samples were analyzed to determine the Cr (III) concentration by AAS.

It is important to mention that the configuration and dimensions of the reactor (Figure 4.2) are based on the appropriate design parameters namely basket/vessel diameter ratio, baffle dimensions, vessel height/basket depth ratio, etc. This configuration seems to be adequate in order to obtain adsorption kinetic curves which, in turn, are useful to determine film or intraparticle diffusion parameters. A few studies have successfully used this reactor configuration [28, 42-44] to predict adsorption kinetics of metals on various adsorbents.

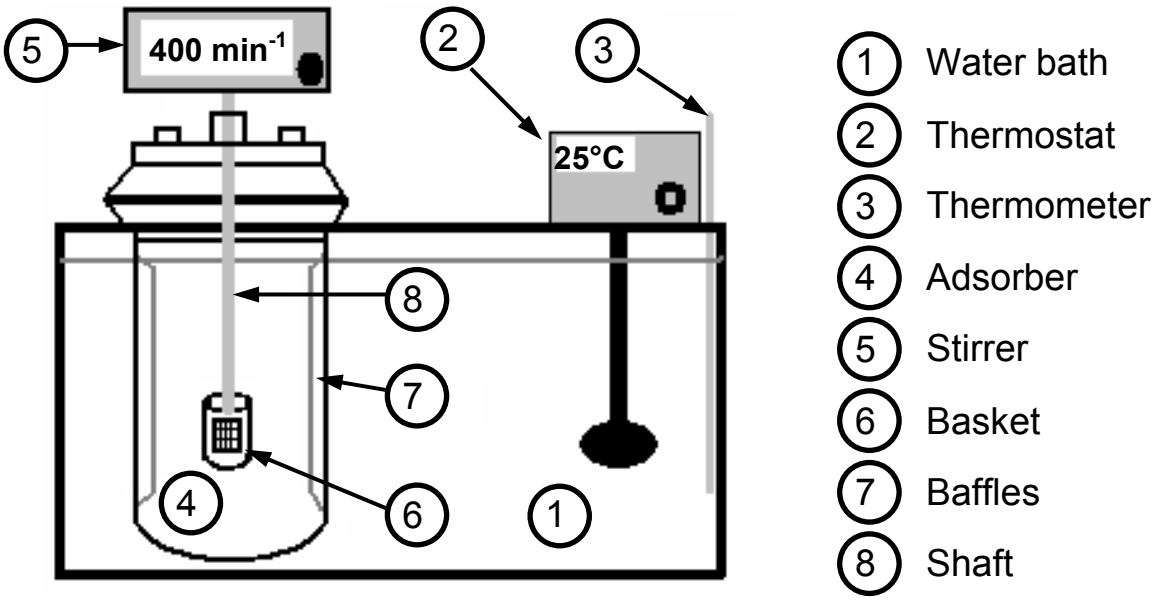

Figure 4.2. Schematic representation of the rotating basket adsorber used to conduct adsorption kinetic experiments.

Most of the published research has not used this reactor configuration and some mistakes have been made in determining diffusion kinetic parameters. Rangel-Mendez [43] conducted adsorption kinetic experiments of Cd (II) on activated carbon under the same conditions, but using a rotating-basket adsorber and only just an impeller for mixing the suspension (i.e. liquid and adsorbent). He reported that a higher sorption rate was obtained with a rotating-basket adsorber than when only just an impeller was used. In the first two minutes, 58% of the sorption capacity at equilibrium was attained with a rotating-basket adsorber while only 12% was obtained using an impeller [43].

Besides the reactor configuration, it is difficult to compare the results of adsorption kinetics for a given metal because of the experimental conditions (e.g. temperature, pH, solid/liquid ratio, particle size, initial concentration, stirring speed, etc.) and the physical-chemical properties of adsorbents (i.e. porosity, density, surface area, pore size and volume, functional groups, etc.). Nevertheless some comparisons could be made but still taking into account the previously exposed facts.

4.3.6 Error analysis

To compare how far the predicted values are from the experimental results and to select also the best parameters in diffusion models, the average absolute percentage deviation (%D) was calculated for each model according to the following equation:

$$\%D = \left(\frac{1}{N} \sum_{i=1}^{N} \left| \frac{C_{Exp} - C_{Pred}}{C_{Exp}} \right| \right) * 100 \qquad (25)$$

where N is the number of kinetic data points, C_{Exp} and C_{Pred} is the experimental and predicted Cr (III) concentration (mg g^{-1}), respectively.

4.4 RESULTS AND DISCUSSION

4.4.1 Equilibrium adsorption experiments

Both Langmuir and Freundlich isotherms predicted the experimental data well, based on their correlation coefficient (r^2). The equilibrium data of Cr (III) adsorption onto WSS and WOS were predicted very well with the Langmuir isotherm (for WSS and WOS, r^2 was 0.96 and 0.99, respectively). However, the Freundlich isotherm fitted better (r^2=0.98) than the Langmuir isotherm (r^2=0.93) the equilibrium results obtained by using WAB. This dissimilarity could be attributed to the differences between the agro-waste materials. WAB had being thermally and mechanically processed to produce an alcoholic beverage called ‘mezcal’, contains less hemicelluloses and lignin than WSS and WOS [45]. Table 4.2 shows the estimated isotherm parameters of these models. Langmuir isotherm parameters are going to be used in diffusion models to predict the adsorption kinetics of Cr (III) because the Langmuir model fitted well two of the three agro-waste materials.

Tabla 4.2. Isotherm parameters estimated from experimental data of Cr (III) adsorption on agro-waste materials at pH 4 and 25°C.

Biosorbent	Langmuir			Freundlich		
	Q_{max}	b	r^2	k	n	r^2
WSS	9.35	0.12	0.96	2.30	3.32	0.90
WOS	12.10	0.10	0.99	2.66	3.05	0.97
WAB	22.38	0.32	0.93	7.91	3.95	0.98

Q_{max} (mg g^{-1}); b (L mg^{-1}); k (mg g^{-1} $L^{1/n}$ $mg^{1-1/n}$); n, r^2 (dimensionless).

The maximum adsorption capacity (Q_{max}) of Cr (III) on agro-waste materials, calculated by the Langmuir model, varies from 9.35 to 22.38 mg g^{-1} (see Table 4.2). The Q_{max} value obtained for WAB is higher than for WSS, WOS and those reported for coir pith (11.6 mg g^{-1}) [9], alfalfa biomass (10.7 mg g^{-1}) [46], aquatic weeds (reed mat, 7.18 mg g^{-1}) [7], lignin (17.9 mg g^{-1}) [47], but lower than other biosorbents such as plant biomass (*Leersia hexandra Swartz*, 28.6 mg g^{-1}) [1], seaweed biomass (*Ecklonia* sp., 34.1 mg g^{-1}) [2], etc. Nonetheless, the agro-waste materials reported herein have a reasonable Cr (III) adsorption capacity which suggests that these biosorbents could be used for the removal of metals from water.

Figure 4.3 shows the adsorption isotherms of Cr (III) onto agro-waste materials at pH 4 and 25°C. At equilibrium concentration (C_e) of 20 mg L^{-1}, the adsorption capacity of Cr (III) on WSS, WOS, and WAB, predicted by the Langmuir model, was 6.5, 8.2, and 19.3 mg g^{-1}, respectively, whereas at C_e=50 mg L^{-1} reached 8.0, 10.2, and 21.5 mg g^{-1}, respectively. These results indicate that at C_e>50 mg L^{-1}, the sorption capacity of Cr (III) on the agro-waste materials studied remained almost constant (see Figure 4.3). These results also suggest that agave bagasse contained more functional groups for metal adsorption compared with both sorghum straw (WSS) and oats straw (WOS). Garcia-Reyes et al. [25] reported that agave bagasse contains almost two times more carboxyl groups in comparison to oats straw: this may be the reason for a higher sorption capacity.

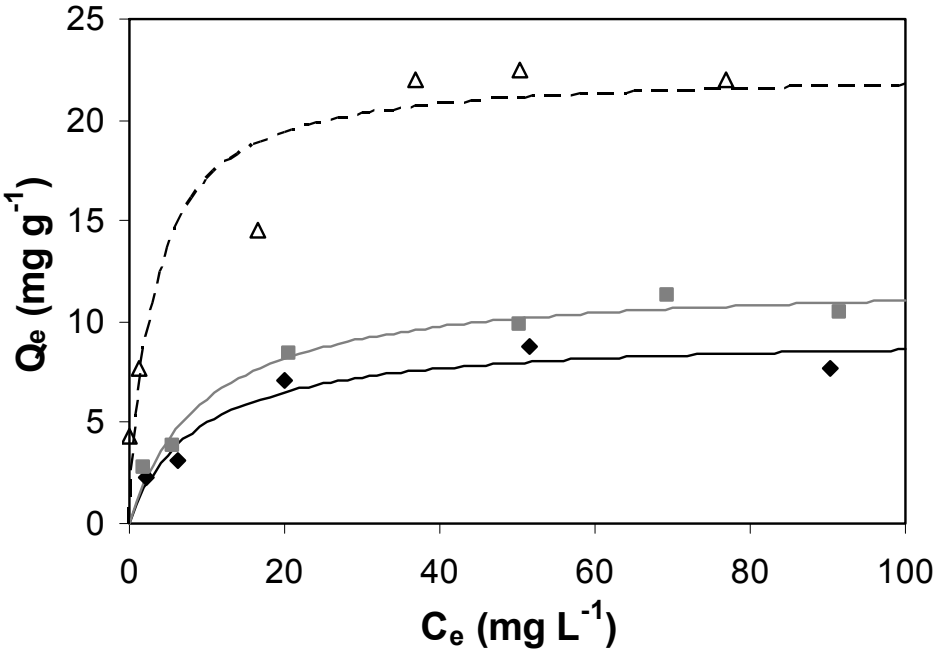

Figure 4.3. Adsorption isotherms of Cr (III) on agro-waste materials at pH 4 and 25°C (♦ WSS, ■ WOS, and Δ WAB). Symbols represent the experimental data and the lines indicate the Langmuir model.

The removal of Cr (III) ions from water has been also reported using polymeric resins namely Lewatit S 100 and Chelex-100 [5]. Lewatit S 100 is a strongly acidic gel-like cation-exchange resin, with sulfonic acid groups as adsorption sites, and beads of uniform size based on crosslinked polystyrene. Chelex-100 is a weakly acidic cation-exchange macroporous resin based on polystyrene-divinylbenzene with carboxyl groups (i.e. iminodiacetic acid) as the exchange site. The Q_{max} of Cr (III) on Lewatit S 100 and Chelex-100, calculated by the Langmuir model, was 20.3 and 15.1 mg g^{-1}, respectively [5]. These Q_{max} values are 9.3% and 32.5% lower than the Q_{max} obtained with WAB. In addition, all agro-waste materials presented in this study had a greater sorption capacity for Cr (III) compared to polymeric resins at low metal concentrations. For example, the sorption capacity of WAB at C_e=20 mg L^{-1}, predicted by the Langmuir model, was 19.3 mg g^{-1} (see Figure 4.3) whereas for Lewatit S-100 it was 0.48 mg g^{-1} [5].

These findings evidently suggest that the agro-waste materials evaluated in this research (in particular WAB) have a great potential for removing metal cations from aqueous solutions even at low metal concentrations. However, to select the most appropriate biosorbent, adsorption kinetic experiments are needed to design appropriate packed columns to be used as adsorber. This topic is going to be discussed in the following section.

4.4.2 Adsorption kinetic experiments

Just a few diffusion models had been previously applied to describe the adsorption rate of metals on biosorbents. Most of the research studies reported in literature have used the empirical rate models (pseudo-first or pseudo-second order reaction models) to predict the overall rate of adsorption, although these models do not consider the mass transfer resistances (namely film and intraparticle diffusion) that control the adsorption rate of metals in any of the adsorbents. Results and discussion of the empirical and the diffusion kinetic models are presented in the subsequent section.

4.4.2.1 Empirical rate models

Both the pseudo-first (Eq. 1) and the pseudo-second (Eq. 8) order reaction models were used to predict the adsorption kinetics of Cr (III) on agro-waste materials. Table 4.3 shows the adsorption rate constants of the pseudo-second order reaction model and Table D1 (Appendix D) shows the parameters of the pseudo-first order model.

The pseudo-first order reaction model did not adequately predict the experimental results based on the percentage average deviation (0.6<%D<6.6). In contrast, the pseudo-second order reaction model did predict well (0.8<%D<2.3) the adsorption kinetics of Cr (III) at different stirring speeds and concentrations (see Table 4.3). Similar results have been reported: the adsorption kinetics of Cr (III) on lignocellulosic materials (such as *Leersia hexandra Swartz* biomass, coir pith, and rice bran) followed a pseudo-second order model instead of a pseudo-first order model [1, 9, 48].

As an example, Figure 4.4 shows the experimental results of the adsorption kinetics of Cr (III) ions on WAB and the predicted values with the pseudo-second order model. The Cr (III) removal increased with time and attained equilibrium at about 600 minutes, except at stirring speed of 200 min^{-1} that required twice the time (Figure 4.4 A). A higher adsorption rate is presented in the beginning of the experiments; this may be due to the greater number of adsorption sites in the external surface of the adsorbent. Afterwards, the adsorption rate decreased suggesting intraparticle diffusion of metal ions to the adsorption sites.

As previously mentioned, although it is difficult to directly compare the adsorption kinetic results with those reported in the literature because of the reactor configuration, adsorbent characteristics and experimental conditions, some comparisons still could be made. For instance, the initial adsorption rate of Cr (III) on the agro-waste materials selected in this study was higher ($0.22<h<5.09$ mg g^{-1} min^{-1}) than those reported on various lignocellulosic biosorbents ($0.074<h<1.523$ mg g^{-1} min^{-1}) [1, 9, 48]. Nevertheless, this conclusion could be due to the use of the rotating basket adsorber which enhanced the mass transfer to the adsorbent particles as reported by Rangel-Mendez [43].

It is important to mention that the initial metal concentration and stirring speed played an important role in the adsorption of metals. The initial metal concentration, determines both the equilibrium concentration and the adsorption rate of metal ions, whereas stirring speed only affects the adsorption kinetics. In this research, an increase of the initial metal concentration from 20 to 55 mg L^{-1} reduced by three times the time to achieve 90% of the adsorption capacity of Cr (III) on WAB (Figure 4.4 B). It is well known that the concentration gradient (the driving force) facilitates the film and intraparticle diffusion of Cr (III) ions to the adsorbent particles resulting in an increase in the adsorption rate. Likewise, to achieve 90% of the adsorption capacity of Cr (III) on WAB, the time was reduced 3.5 times by increasing the stirring speed from 200 to 400 min^{-1}, both at C_o=20 mg L^{-1} (Figure 4.4 A). This result may be due to the reduction of the external resistance: metal ions are transferred faster to the film or inside the adsorbent particles to be adsorbed. Consequently the time required to reach the 90% of the

equilibrium sorption capacity is reduced. It is also important to note that similar adsorption kinetics of Cr (III), on all agro-waste biosorbents studied in this research, were obtained at 400 min^{-1} and 300 min^{-1} for C_o=20 mg L^{-1}. These results suggest that the film resistance was reduced to a minimum and therefore a further increase in the stirring speed was not necessary to improve the adsorption kinetics. For this reason, adsorption kinetics of Cr (III) at C_o≈53 mg L^{-1} was only conducted at a stirring speed of 400 min^{-1}.

Table 4.3. Empirical and diffusion model parameters estimated by using experimental data of the adsorption kinetics of Cr (III) on agro-waste materials at pH 4 and 25°C.

Biosorbent	C_o (mg L^{-1})	Stirring speed (min^{-1})	Pseudo-second order			Film diffusion		Film – Pore-volume diffusion			Film – Surface diffusion		
			k_2 (g mg^{-1} min^{-1})	q_e (mg g^{-1})	%D	k_L (cm s^{-1})	%D	k_L (cm s^{-1})	$D_{e,p}$ (cm^2 s^{-1})	%D	k_L (cm s^{-1})	D_s (cm^2 s^{-1})	%D
WSS	22.05	200	0.0057	6.139	1.63	0.003	1.60	0.05	2.5E-06	2.38	0.01	5.0E-04	2.15
	21.69	300	0.0337	6.752	1.01	0.005	1.31	0.05	2.0E-06	2.44	0.01	1.5E-03	2.18
	20.52	400	0.0142	7.728	1.12	0.005	1.05	0.05	3.5E-06	1.67	0.01	1.0E-03	1.32
	53.00	**400**	**0.0669**	**8.718**	**0.91**	**0.005**	**0.82**	**0.05**	**6.5E-06**	**1.09**	**0.01**	**1.0E-03**	**2.31**
WOS	21.77	200	0.0452	7.077	0.85	0.003	1.74	0.05	3.0E-06	2.34	0.01	1.0E-05	2.91
	22.74	300	0.0493	9.107	0.95	0.006	0.45	0.05	7.0E-06	2.61	0.01	8.0E-05	2.93
	22.86	400	0.0085	8.547	2.09	0.006	1.99	0.05	7.0E-06	3.48	0.01	2.0E-05	2.66
	52.26	**400**	**0.0068**	**10.142**	**0.83**	**0.0007**	**0.82**	**0.05**	**7.5E-05**	**0.70**	**0.001**	**3.0E-06**	**0.58**
WAB	19.75	200	0.0011	14.045	1.92	0.0005	4.04	0.05	5.0E-07	3.15	0.002	1.0E-08	1.72
	19.57	300	0.0034	14.925	2.32	0.003	5.84	0.05	2.5E-06	2.98	0.005	1.5E-07	1.02
	20.02	400	0.0044	13.889	1.44	0.003	5.33	0.05	3.0E-06	2.72	0.005	1.5E-07	1.03
	55.25	**400**	**0.0096**	**22.989**	**1.08**	**0.005**	**0.88**	**0.05**	**1.5E-05**	**0.91**	**0.005**	**2.0E-07**	**1.07**

C_o: Initial metal concentration; %D: Percentage average deviation (dimensionless).

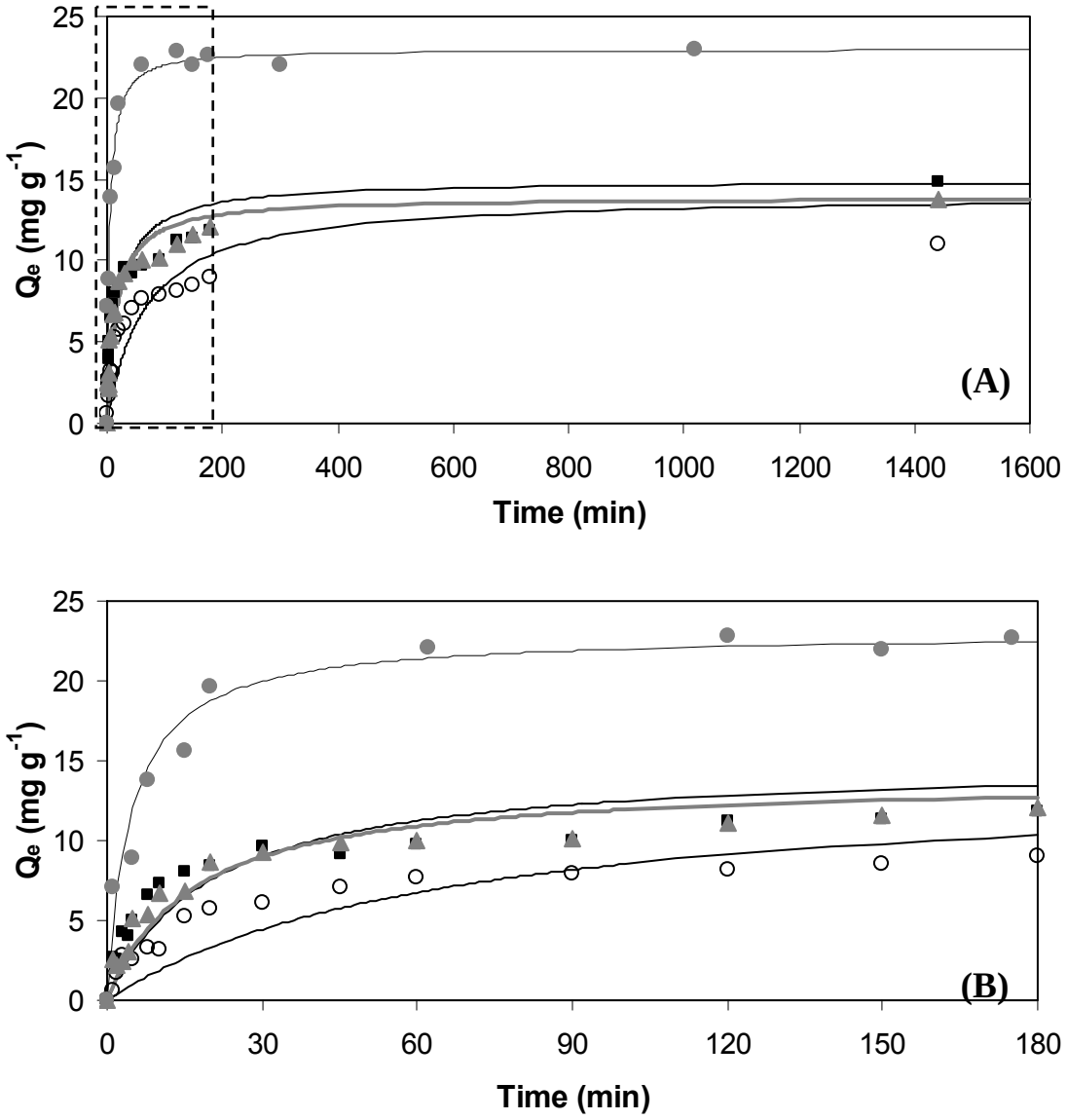

Figure 4.4. Adsorption kinetics of Cr (III) ions on WAB at pH 4, 25°C, using 250 mg of biosorbent in 1 L and different stirring speed and initial Cr (III) concentration (○ 200 min^{-1} and 19.8 mg L^{-1}; ■ 300 min^{-1} and 19.6 mg L^{-1}; ▲ 400 min^{-1} and 20.0 mg L^{-1}; ● 400 min^{-1} and 55.3 mg L^{-1}). Dashed square in (A) is enlarged in (B) for better clarity. Symbols represent the experimental results and the lines the predicted values by the pseudo-second order reaction model.

4.4.2.2 Film diffusion model

Table 4.3 also shows the external mass transfer coefficient (k_L) of the film diffusion model (see section 4.2.1.2) estimated with the experimental data of the adsorption kinetics of Cr (III) on agro-waste materials. It can be observed that this parameter (k_L) is affected by both the stirring speed and the initial metal concentration. For example, in the adsorption of Cr (III) on WAB at $C_o \approx 19.8$ mg L^{-1}, an increase in the stirring speed from 200 min^{-1} to 400 min^{-1}, increased the k_L value up to 83% (for WSS and WOS, k_L increased up to 40% and 50%, respectively). In addition, it is important to note that there is no difference in the k_L value estimated at 300 min^{-1} and 400 min^{-1} (see Table 4.3). This means that the external mass transfer resistance was reduced as much as possible; therefore a further increase in stirring speed is not expected to enhance the external mass diffusion. Similar results were reported by Allen et al. [33] in the adsorption of copper onto peat: the external mass transfer coefficient increased as the stirring speed increased and remained constant at the higher stirring speed.

Regarding the effect of the initial metal concentration on the external mass transfer coefficient, it can be seen that the k_L value increases 40% with increasing the initial Cr (III) concentration from 20 to 55 mg L^{-1} for WAB, whereas for WSS it remained constant (see Table 4.3). A quite different behavior is observed for WOS: k_L value was reduced around 88% with increasing the initial concentration from 23 to 52 mg L^{-1}. This opposing result may be attributed to the heterogeneity of this biosorbent; therefore more experiments with this biosorbent are needed to clarify this issue, since the external mass transfer coefficient should have increased or remained constant when the stirring speed or the initial concentration increases.

A single resistance model predicted adequately ($0.5<\%D<5.8$) the concentration decay curve, at the initial concentrations and stirring speed tested, for some experiments even better than the pseudo-second order reaction model ($0.8<\%D<2.3$). The best predicted curve, with the film diffusion model, was obtained with the highest initial concentration (around 53 mg L^{-1}) compared with the lowest initial concentration (≈ 21 mg L^{-1}). For example, when predicting the concentration decay curve of WAB at $C_o \approx 19.8$ mg L^{-1}, the film diffusion model had

high deviation (%D=5.3) opposite to that obtained at $C_o \approx 55.3$ mg L^{-1} (%D=0.9), both at 400 min^{-1} (see Figures 4.5 and 4.6, in Appendix D Figures D1, D2, D3 and D4). Similar behavior was observed in the other agro-waste materials: low deviation at the high initial concentration (for WSS, %D=0.9; for WOS, %D=0.8) in comparison with the low initial concentration (for WSS, %D=1.1; for WOS, %D=2.2). This behavior could be attributed to the fact that the film diffusion model depends on the isotherm parameters (for the Langmuir model: b and q_{max}). In this research, equilibrium concentrations in the region of the asymptote (or plateau) show less deviation from the experimental data (see Figure 4.3). Consequently, as expected, less deviation is obtained by using the film diffusion model.

Summarizing, it is clear from these results that a film diffusion model predicted adequately the adsorption kinetics of Cr (III) on agro-waste materials for the several experimental conditions tested in this research (see Table 4.3 and Figures 4.5 and 4.6, in Appendix D Figures D1, D2, D3 and D4). Moreover this model helps to understand the mass transfer rate from the solution to the adsorbent. The results obtained by using this model suggested that the adsorption of Cr (III) is limited by film resistance surrounding the adsorbent particle. This conclusion is not surprising due to the low surface area ($0.58<S<1.21$ m^2 g^{-1}), the low porosity ($0.004<\varepsilon_p<0.007$), low pore volume ($0.003<V_p<0.004$ cm^{-3} g^{-1}), and average pore width (mainly consisting of mesopores and macropores) of these biosorbents (see Table 4.1, and in Appendix D Figure D5). Absolute average deviations might be due to both the heterogeneity of the biosorbents and the deviations of the experimental data and estimated values of the isotherm models (see Figure 4.3) since this model depends on the isotherm parameters to estimate the external mass transfer coefficient.

4.4.2.3 Film – Pore-volume diffusion model

To describe the adsorption kinetics of Cr (III) on agro-waste materials, a two resistance model was also applied. This model considers that the mass transfer is limited by two resistances: external (film diffusion) and intraparticle (pore volume diffusion) resistances (see section 4.2.1.3.1).

For all the experimental conditions and biosorbents tested (see Table 4.3), the external mass transfer coefficient remained constant (k_L=0.05 cm s^{-1}). This result suggests that the external film diffusion can describe the first minutes of the adsorption kinetics of Cr (III) on agro-waste adsorbents (see Figures 4.5 and 4.6, in Appendix D Figures D1, D2, D3 and D4). Afterwards, the adsorption rate is limited by the effective pore volume diffusion ($D_{e,p}$) which is highly affected by the stirring speed and the initial metal concentration. For example, the $D_{e,p}$ of Cr (III) on WAB, increased around 80% with increasing either the stirring speed from 200 min^{-1} to 400 min^{-1} or by rising the initial concentration from 20 mg L^{-1} to 55 mg L^{-1}. This could be explained based on the reduction of the external film resistance by increasing the stirring speed and also because the concentration gradient determines the intraparticle diffusion towards the adsorbent.

Similar to the film diffusion model, film – pore-volume diffusion model also depends on the isotherm model parameters; consequently errors of experimental and theoretical results of the isotherm model affect the performance in predicting the adsorption kinetic curves. Nevertheless, the film – pore-volume diffusion model predicted satisfactorily (0.7<%D<3.5) the concentration decay curves of Cr (III) on agro-waste materials. In general and similar to the film diffusion model, at high initial concentration (C_o≈55.3 mg L^{-1}) the lowest deviation (0.7<%D<1.1) was obtained. On the contrary, at low concentration (C_o≈21.2 mg L^{-1}) it was obtained the highest deviation (1.7<%D<3.5).

In conclusion, these results suggest that the concentration gradient (the driving force) as well as the stirring speed play an important role in the adsorbate mass transfer. Moreover, although these biosorbents have a low surface area and low porosity (see Table 4.1), both film and intraparticle diffusion seem to contribute to the adsorption kinetics of Cr (III).

4.4.2.3 Homogeneous solid diffusion model (HSDM) with external mass transfer resistance

Two resistances are considered in this model: external film and intraparticle diffusion (see section 4.2.1.3.2). The first resistance is due to the external mass

transfer and the second resistance is due to a surface-hopping mechanism (see Figure 4.1). Table 4.3 shows the parameters of this model (k_L and D_s) estimated by using the experimental results of the adsorption rate of Cr (III) on agro-waste biosorbents.

For WAB, the stirring speed affected the parameters of this model (k_L and D_s). The k_L value increased up to 60% with increasing the stirring speed from 200 min^{-1} to 300 min^{-1}. Nonetheless, k_L remained constant (0.005 cm s^{-1}) above 300 min^{-1} regardless of the initial metal concentration (see Table 4.3). In addition, D_s increased 93% when the stirring speed was changed from 200 to 300 min^{-1} at C_o=19.8 mg L^{-1}, whereas at 400 min^{-1}, D_s increased 95% due to a change in C_o from 19.8 to 55.3 mg L^{-1}. These findings also suggested that film and intraparticle diffusion are greatly affected by the stirring speed and the concentration gradient as expected and concluded with the other diffusion kinetic models.

The homogeneous solid diffusion model (HSDM) with external mass transfer resistance predicted very well the adsorption kinetics of Cr (III) based on the low deviation (0.6<%D<2.9) between the experimental and predicted values (see Figures 4.5 and 4.6, in Appendix D Figures D1, D2, D3 and D4). Two slopes are clearly identified by using this model: the first slope is associated to the external mass transfer and the second slope is related to the surface diffusion. The external mass transfer coefficient, estimated with this model for WAB, predicted adequately the concentration decay curves the first 20 minutes, although the subsequent time had a higher deviation associated to the surface diffusion. The HSDM model with external mass transfer resistance did not improve the prediction of the adsorption kinetics of Cr (III) on the agro-waste materials selected in this research.

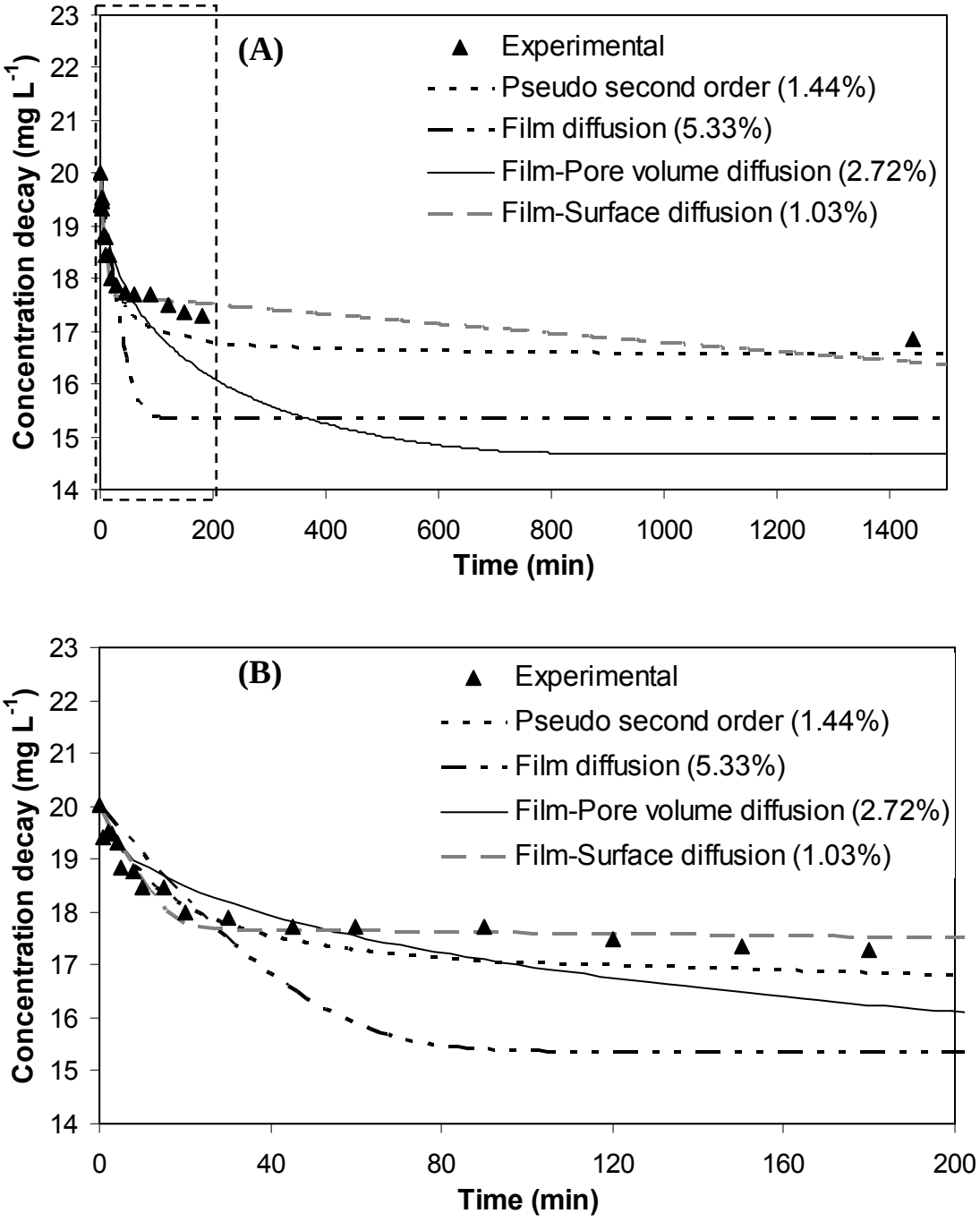

Figure 4.5. Adsorption kinetics of Cr (III) ions on WAB at pH 4, 25°C, using 250 mg of biosorbent in 1 L, 400 min^{-1}, and C_o=20 mg L^{-1}. Dashed square in (A) is enlarged in (B) for better clarity. Symbols represent the experimental results and the lines the predicted value by the models. Percentage deviations are given in parentheses.

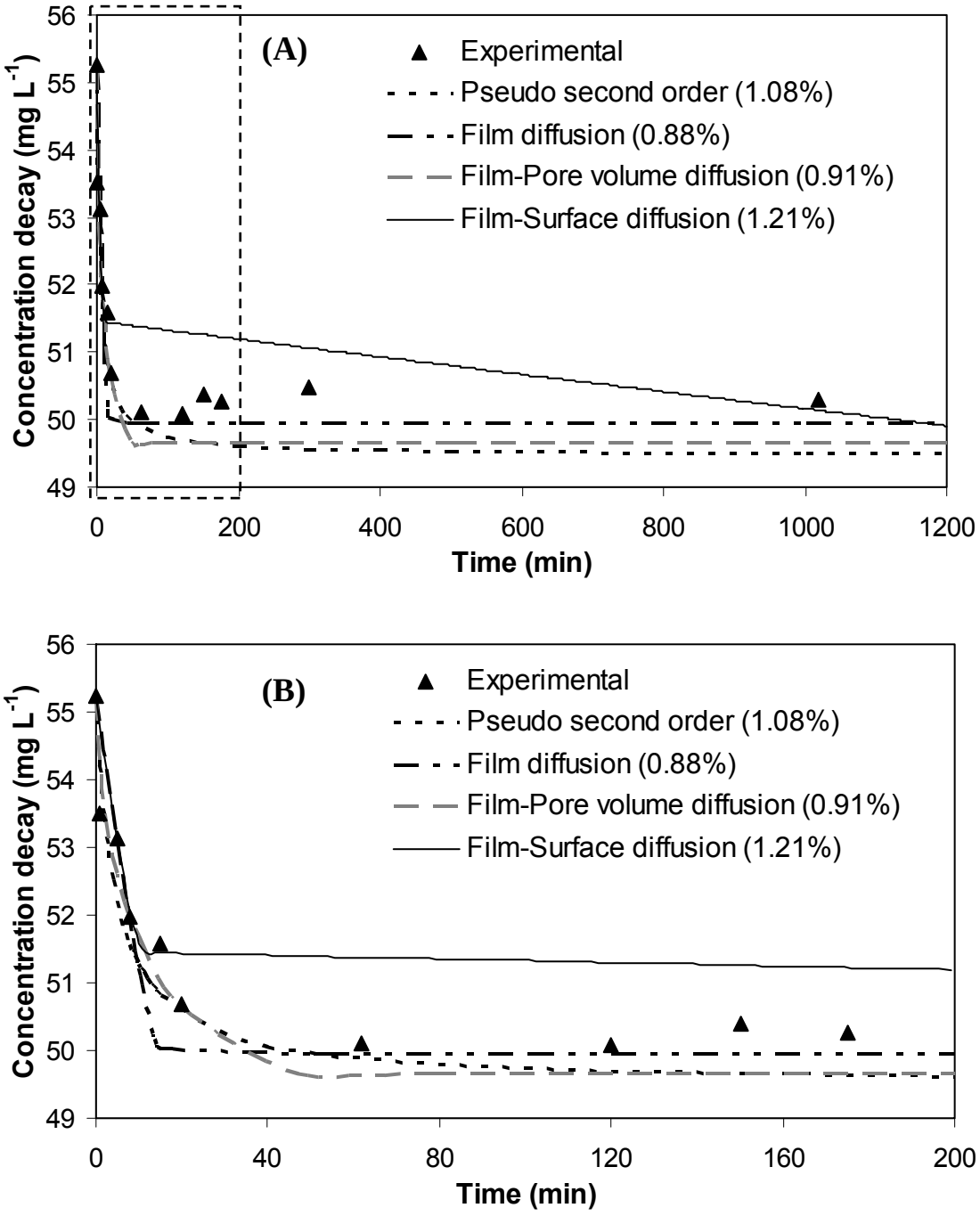

Figure 4.6. Adsorption kinetics of Cr (III) ions on WAB at pH 4, 25°C, using 250 mg of biosorbent in 1 L, 400 min^{-1}, C_o=55.25 mg L^{-1}. Dashed square in (A) is enlarged in (B) for better clarity. Symbols represent the experimental results and the lines the predicted values by the models. Percentage deviations are given in parentheses.

4.4.3 Comparisons of empirical and diffusion models for predicting the adsorption kinetics of Cr (III) on agro-waste materials

Among all the existing models (i.e. empirical and diffusion) to describe adsorption kinetics of pollutants onto any adsorbent, empirical models are the most often used because these are easily applied. In contrast, diffusion models are not commonly used in part because these models require more effort in solving the differential equations. Nevertheless, diffusion models are helpful to understand the adsorbate mass transfer to the adsorbent particle contrary to empirical models.

For predicting the adsorption kinetics of Cr (III) on agro-waste materials, the film diffusion model seems to be the most appropriate among all the models tested. This conclusion is based on various facts. Firstly, the low deviation between the experimental and predicted concentrations indicated that this model fits adequately the concentration decay curve (Table 4.3). Secondly, the physical properties (i.e. low porosity, surface and pore volume area) of these biosorbents (see Table 4.1) suggested that the contribution of intraparticle diffusion is lower than the film diffusion. Moreover, by using two-resistance models (i.e. film – pore-volume diffusion or film – surface diffusion) did not significantly enhance the prediction of the concentration decay curve. Finally, and not less important, the external mass transfer coefficient (k_L) of the film diffusion model has a physical meaning that helps to explain the diffusion of solutes throughout the film resistance.

4.5 CONCLUSIONS

The maximum Cr (III) sorption capacity of agro-waste materials, calculated by the Langmuir model, varies from 9.3 to 22.6 mg g^{-1}. WAB has higher sorption capacity (22.6 mg g^{-1}) than WSS (9.4 mg g^{-1}), WOS (12.1 mg g^{-1}), and polymeric resins (Lewatit S-100 (20.3 mg g^{-1}) and Chelex-100 (15.1 mg g^{-1})). Moreover WAB could be used to remove metals because of the high Cr (III) adsorption capacity (even at low metal concentration) as well as the low cost and availability.

The external film resistance is reduced to a minimum at the highest stirring speed. On the contrary, the external mass transfer coefficient increases with increasing the initial concentration. Therefore, when increasing the stirring speed or the

concentration gradient, metal ions are transferred faster to the film or inside the adsorbent particles to be adsorbed; consequently the adsorption rate increases.

In summary, the adsorption kinetics of Cr (III) on the agro-waste materials studied herein can be described by using either empirical or diffusion kinetic models. However, the film diffusion model seems to be the most appropriate based on the low deviation between the experimental and the predicted data, and the physical properties (low porosity, low surface area and low pore volume) of the agro-waste materials, which support the idea that intraparticle diffusion may be neglected. Moreover, a single resistance model (i.e. film diffusion model) has a physical meaning that explains the mass transfer process towards the adsorbent particle as well as the effects of stirring speed and the initial concentration.

4.6 REFERENCES

[1]. Li, J., Q. Lin, X. Zhang, and Y. Yan, Kinetic parameters and mechanisms of the batch biosorption of Cr(VI) and Cr(III) onto *Leersia hexandra Swartz* biomass. J. Colloid Interface Sci., 333(1) (2009) 71-77.

[2]. Yun, Y. S., D. Park, J. M. Park, and B. Volesky, Biosorption of trivalent chromium on the brown seaweed biomass. Environ. Sci. Technol., 35(21) (2001) 4353-4358.

[3]. Sethunathan, N., M. Megharaj, L. Smith, S. P. B. Kamaludeen, S. Avudainayagam, and R. Naidu, Microbial role in the failure of natural attenuation of chromium(VI) in long-term tannery waste contaminated soil. Agric. Ecosyst. Environ., 105(4) (2005) 657-661.

[4]. Deng, S. B. and R. B. Bai, Removal of trivalent and hexavalent chromium with aminated polyacrylonitrile fibers: performance and mechanisms. Water Res., 38(9) (2004) 2424-2432.

[5]. Gode, F. and E. Pehlivan, Removal of chromium(III) from aqueous solutions using Lewatit S 100: The effect of pH, time, metal concentration and temperature. J. Hazard. Mater., 136(2) (2006) 330-337.

[6]. Rengaraj, S., C. K. Joo, Y. Kim, and J. Yi, Kinetics of removal of chromium from water and electronic process wastewater by ion exchange resins: 1200H, 1500H and IRN97H. J. Hazard. Mater., 102(2-3) (2003) 257-275.

[7]. Elangovan, R., L. Philip, and K. Chandraraj, Biosorption of chromium species by aquatic weeds: Kinetics and mechanism studies. J. Hazard. Mater., 152(1) (2008) 100-112.

[8]. Elmaci, A., T. Yonar, and N. Ozengin, Biosorption characteristics of copper (II), chromium (III), nickel (II), andlead (II) from aqueous solutions by chara sp. and cladophora sp. Water Environ. Res., 79(9) (2007) 1000-1005.

[9]. Parab, H., S. Joshi, N. Shenoy, A. Lali, U. S. Sarma, and M. Sudersanan, Determination of kinetic and equilibrium parameters of the batch adsorption of Co(II), Cr(III) and Ni(II) onto coir pith. Process Biochem., 41(3) (2006) 609-615.

[10]. Park, D., Y. S. Yun, C. K. Ahn, and J. M. Park, Kinetics of the reduction of hexavalent chromium with the brown seaweed Ecklonia biomass. Chemosphere, 66(5) (2007) 939-946.

[11]. Park, D., Y. S. Yun, J. H. Jo, and J. M. Park, Mechanism of hexavalent chromium removal by dead fungal biomass of Aspergillus niger. Water Res., 39(4) (2005) 533-540.

[12]. Sawalha, M. F., J. R. Peralta-Videa, G. B. Saupe, K. M. Dokken, and J. L. Gardea-Torresdey, Using FTIR to corroborate the identity of functional groups involved in the binding of Cd and Cr to saltbush (Atriplex canescens) biomass. Chemosphere, 66(8) (2007) 1424-1430.

[13]. Schmuhl, R., H. M. Krieg, and K. Keizer, Adsorption of Cu(II) and Cr(VI) ions by chitosan: Kinetics and equilibrium studies. Water Sa, 27(1) (2001) 1-7.

[14]. Justi, K. C., V. T. Favere, M. C. M. Laranjeira, A. Neves, and R. A. Peralta, Kinetics and equilibrium adsorption of Cu(II), Cd(II), and Ni(II) ions by chitosan functionalized with 2[-bis-(pyridylmethyl)aminomethyl]-4-methyl-6-formylphenol. J. Colloid Interface Sci., 291(2) (2005) 369-374.

[15]. Zhou, L. M., Y. P. Wang, Z. R. Liu, and Q. W. Huang, Characteristics of equilibrium, kinetics studies for adsorption of Hg(II), Cu(II), and Ni(II) ions by

thiourea-modified magnetic chitosan microspheres. J. Hazard. Mater., 161(2-3) (2009) 995-1002.

[16]. Murphy, V., H. Hughes, and P. McLoughlin, Cu(II) binding by dried biomass of red, green and brown macroalgae. Water Res., 41(4) (2007) 731-740.

[17]. Altundogan, H. S., N. E. Arslan, and F. Tumen, Copper removal from aqueous solutions by sugar beet pulp treated by NaOH and citric acid. J. Hazard. Mater., 149(2) (2007) 432-439.

[18]. Hardin, A. M. and W. Admassu, Kinetics of heavy metal uptake by vegetation immobilized in a polysulfone or polycarbonate polymeric matrix. J. Hazard. Mater., 126(1-3) (2005) 40-53.

[19]. Igwe, J. C. and A. A. Abia, Adsorption kinetics and intraparticulate diffusivities for bioremediation of Co (II), Fe (II) and Cu (II) ions from waste water using modified and unmodified maize cob. International Journal of Physical Sciences, 2(5) (2007) 119-127.

[20]. Kumar, U. and M. Bandyopadhyay, Sorption of cadmium from aqueous solution using pretreated rice husk. Bioresour. Technol., 97(1) (2006) 104-109.

[21]. Lu, D. D., Q. L. Cao, X. M. Li, X. J. Cao, F. Luo, and W. J. Shao, Kinetics and equilibrium of Cu(II) adsorption onto chemically modified orange peel cellulose biosorbents. Hydrometallurgy, 95(1-2) (2009) 145-152.

[22]. Veglio, F., F. Beolchini, and M. Prisciandaro, Sorption of copper by olive mill residues. Water Res., 37(20) (2003) 4895-4903.

[23]. Xuan, Z. X., Y. R. Tang, X. M. Li, Y. H. Liu, and F. Luo, Study on the equilibrium, kinetics and isotherm of biosorption of lead ions onto pretreated chemically modified orange peel. Biochemical Engineering Journal, 31(2) (2006) 160-164.

[24]. Zhang, Y. J., J. R. Chen, X. Y. Yan, and Q. M. Feng, Equilibrium and kinetics studies on adsorption of Cu(II) from aqueous solutions onto a graft copolymer of cross-linked starch/acrylonitrile (CLSAGCP). J. Chem. Thermodyn., 39(6) (2007) 862-865.

[25]. Garcia-Reyes, R. B., J. R. Rangel-Mendez, and M. C. A.-D. l. Torre, Chromium (III) Uptake by Agro-Waste Biosorbents: Chemical Characterization, Sorption-Desorption Studies, and Mechanism. J. Hazard. Mater., in press(doi:10.1016/j.jhazmat.2009.05.046) (2009).

[26]. Helfferich, F., Ion exchange. 1995, New York: Dover Publications. 624.

[27]. Leyva-Ramos, R. and C. J. Geankoplis, Model simulation and analysis of surface diffusion of liquids in porous solids. Chem. Eng. Sci., 40(5) (1985) 799-807.

[28]. Leyva-Ramos, R., J. R. Rangel-mendez, L. A. Bernal-Jacome, and M. S. B. Mendoza, Intraparticle diffusion of cadmium and zinc ions during adsorption from aqueous solution on activated carbon. J. Chem. Technol. Biotechnol., 80(8) (2005) 924-933.

[29]. Valsaraj, K. T., Elements of environmental engineering: termodynamics and kinetics. 2nd. ed. 2000, Boca Raton, Florida: Lewis Publisher. 679.

[30]. Lagergren, S., Zur theorie der sogenannten adsorption gelöster stoffe. K. Sven. Vetenskapsakad. Handl., Band 24(No. 4) (1898) 1-39.

[31]. Ho, Y. S. and G. McKay, The kinetics of sorption of divalent metal ions onto sphagnum moss flat. Water Res., 34(3) (2000) 735-742.

[32]. Allen, S., P. Brown, G. McKay, and O. Flynn, An evaluation of single resistance transfer models in the sorption of metal ions by peat. J. Chem. Technol. Biotechnol., 54(3) (1992) 271-276.

[33]. Allen, S., L. Whitten, M. Murray, O. Duggan, and P. Brown, The Adsorption of Pollutants by Peat, Lignite and Activated Chars. J. Chem. Technol. Biotechnol., 68(4) (1997) 442-452.

[34]. Leyva-Ramos, R., P. E. Diaz-Flores, J. Leyva-Ramos, and R. A. Femat-Flores, Kinetic modeling of pentachlorophenol adsorption from aqueous solution on activated carbon fibers. Carbon, 45(11) (2007) 2280-2289.

[35]. Shashirekha, V., M. R. Sridharan, and M. Swamy, Biosorption of trivalent chromium by free and immobilized blue green algae: Kinetics and equilibrium studies. J. Environ. Sci. Health, Part A: Toxic/Hazard. Subst. Environ. Eng., 43(4) (2008) 390-401.

[36]. Reddad, Z., C. Gerente, Y. Andres, and P. Le Cloirec, Adsorption of several metal ions onto a low-cost biosorbent: Kinetic and equilibrium studies. Environ. Sci. Technol., 36(9) (2002) 2067-2073.

[37]. Dang, V. B. H., H. D. Doan, T. Dang-Vu, and A. Lohi, Equilibrium and kinetics of biosorption of cadmium(II) and copper(II) ions by wheat straw. Bioresour. Technol., 100(1) (2009) 211-219.

[38]. Coleman, N. T., A. C. McClung, and D. P. Moore, Formation constants for Cu(II)-peat complexes. Science, 123 (1956) 330-331.

[39]. Furusawa, T. and J. M. Smith, Fluid-Particle and Intraparticle Mass Transport Rates in Slurries. Ind. Eng. Chem. Fundam., 12(2) (1973) 197-203.

[40]. Mathews, A. P. and W. J. J. Weber, Effects of external mass transfer and intraparticle diffusion on adsorption rates in slurry reactors. AIChE J., 73 (1976) 91-98.

[41]. Al-Duri B. and Mckay G., Comparison in theory and application of several mathematical models to predict kinetics of single component batch adsorption systems. Trans IChemE, 68(Part B) (1990) 245-310.

[42]. Rangel-Mendez, J. R., *Adsorción y difusión intraparticular de Cadmio (II) en solución acuosa sobre carbón activado*, in *Facultad de Ciencias Químicas*. 1997, Universidad Autónoma de San Luis Potosí: San Luis Potosí, México. p. 129.

[43]. Rangel-Mendez, J. R., *Adsorption of toxic metals from water using commercial and modified granular and fibrous activated carbons*, in *Department of Chemical Engineering*. 2001, Loughborough University: Loughborough. p. 168.

[44]. DeMarco, M. J., A. K. Sengupta, and J. E. Greenleaf, Arsenic removal using a polymeric/inorganic hybrid sorbent. Water Res., 37(1) (2003) 164-176.

[45]. Garcia-Reyes, R. B. and J. R. Rangel-Mendez, Contribution of agro-waste material main components (hemicelluloses, cellulose,and lignin) to the removal of chromium (III) from aqueous solution. J Chem. Technol. Biotechnol., DOI 10.1002/jctb.2215 (2009).

[46]. Tiemann, K. J., J. L. Gardea-Torresdey, G. Gamez, K. Dokken, and S. Sias, Use of X-ray absorption spectroscopy and esterification to investigate Cr(III) and Ni(II) ligands in alfalfa biomass. Environ. Sci. Technol., 33(1) (1999) 150-154.

[47]. Wu, Y., S. Zhang, X. Guo, and H. Huang, Adsorption of chromium(III) on lignin. Bioresour. Technol., 99(16) (2008) 7709-7715.

[48]. Oliveira, E. A., S. F. Montanher, A. D. Andrade, J. A. Nobrega, and M. C. Rollemberg, Equilibrium studies for the sorption of chromium and nickel from aqueous solutions using raw rice bran. Process Biochem., 40(11) (2005) 3485-3490.

Chapter 5

5.1 GENERAL DISCUSSION

Agro-waste materials are able to sequester metal ions such as chromium (III) from aqueous solution. Furthermore these biosorbents can also be used to remove other metal cations such as lead (II), cadmium (II), zinc (II), nickel (II), copper (II), etc., from water.

The chromium (III) sorption mechanisms are not easily elucidated due to the complex nature of the biosorbents. Methodologies such as chemical modifications, acid-base titrations, FTIR (Fourier Transform Infrared), XPS (X-Ray photoelectron spectroscopy), among others, have been used to determine functional groups and at the same time to elucidate metal sorption mechanism of biosorbents. Some of the functional groups that have been identified in biosorbents include: carboxyl, carbonyl, acetamide, amine, sulfate, phosphate, phenolic, hydroxyl, etc., and the adsorption mechanisms of cations that have been proposed for biosorbents include: chemical adsorption (complexes formation), ion exchange with cations such as calcium or magnesium, and physical adsorption by electrostatic interaction. In this thesis, it has been demonstrated that the sorption mechanism of Cr (III) is coupled with the release of calcium or hydrogen ions (see Figure 2.6). Poly-galacturonic and hexuronic acids (present in pectin and hemicelluloses) contain carboxyl groups linked together by calcium bridges, but once calcium is released to the solution, the carboxyl groups could be used by chromium (III) ions as adsorption sites. In the same way, protonated carboxyl groups of poly-galacturonic and hexuronic acids could exchange hydrogen ions by Cr (III) ions. Nevertheless, complexation of metals could also take place on oxygen-containing groups (i.e. carboxyl and hydroxyl). Carboxyl groups on agro-waste materials are the main binding-sites on chromium (III) removal. However, hydroxyl groups are capable of complexing metal cations too.

Metal desorption from biosorbents has not been well explored and for that reason it is necessary to study this process more in detail. In this thesis, desorption of chromium-loaded agro-waste materials with solutions of HNO_3, NaOH, and EDTA at different concentrations and temperatures (25°C, 35°C, and 55°C) is reported (see Figure 2.7 and 2.8). These eluents were selected by aiming at an ion exchange process, between H^+ and Na^+ with Cr (III) species, or complexation (EDTA-Cr (III)). It was thought that if Cr (III) was adsorbed on carboxyl-binding groups by electrostatic interaction, then acid solutions (e.g. HNO_3) would regenerate the chromium-loaded biosorbents since the concentration of H^+ increases (pH decreases and oxygen groups protonates) giving place to ion exchange with the chromium adsorbed. However, the low Cr (III) desorption from agro-waste materials at 25°C (lower than 46% for WOS when 1.0 N HNO_3 was used) suggested that chromium ions form more stable chemical bonds (i.e. covalent coordinated bonds) with the functional groups of biosorbents. An increase in temperature enhanced the amount of desorbed metal for instance the chromium desorption from AAB with 1.0 M HNO_3 was 43%, 47%, and 68% at 25°C, 35°C, and 55°C, respectively (see Figure 2.8). Nonetheless, the regeneration of AAB with 1.0 M HNO_3 at 55°C caused 30% of weight loss (see Figure 2.9), which suggested that the acid eluent hydrolyzed part of hemi-celluloses and pectin present in the agro-waste materials. Conversely, the chromium desorbed with NaOH (1.0 N) at 25°C varied from 18% to 71% depending on the agro-waste material (see Figure 2.7 and 2.8). However, the weight lost when 1.0 N NaOH was used as eluent was higher (22% to 42%) compared to the regeneration with 1.0 N HNO_3 (see Figure 2.9). These results suggested that some components (mainly lignin and hemicelluloses) present in the biosorbents could be hydrolyzed in alkaline solutions. The main species formed by alkaline regeneration is $Cr(OH)_{3(s)}$ due to the high concentration of OH^- (see Figure 2.3), although $Cr(OH)_4^-$ is also formed but to a lesser extent at high pH values. It is important to note that Cr (III) desorption by NaOH may be underestimated due to the presence of chromium precipitate as $Cr(OH)_{3\ (s)}$ (more experiments are needed to clarify this issue). Solutions of EDTA (0.1 M and 0.05 M) were also used to regenerate the chromium-

loaded agro-waste materials. This eluting-agent was chosen because it is well known that chromium (III) and EDTA ligand have the highest stability constants for the formation of complexes. Regeneration with EDTA was affected by both temperature and the eluent concentration. For instance, the AOS regeneration with 1.0 M EDTA at 25°C and 35°C was 51% and 74%, respectively, but at 55°C this biosorbent was completely regenerated (see Figure 2.8). The higher chromium desorption with 1.0 M EDTA obtained at 55°C suggested that the interaction Cr (III)-EDTA involved a chelate formation and an increase in temperature facilitated the chemical interaction between EDTA and Cr (III). Also when the EDTA concentration was 0.05 M, the regeneration was reduced to 70% at 55°C. In addition, the weight loss of acid-washed materials due to the regeneration with 0.1 M EDTA was much lower (0-9%) than that obtained when 1.0 N HNO_3 or 1.0 N NaOH was used as eluent (see Figure 2.9). This fact suggested that EDTA solutions produced apparently fewer structural modifications in the biosorbents than the acid or the alkaline solutions; for example Figure 2.1 (B) shows that acid and alkaline solutions attacked the carboxyl groups (1740 cm^{-1}) conversely to EDTA solutions. In addition, alkaline and acid regenerations produced hydrolysis of the agro-waste materials confirmed by the weight loss, and the color change of biosorbents. Therefore, based on the chromium desorbed and the initial weight loss, EDTA seems to be a promising alternative to regenerate chromium-loaded agro-waste materials without apparent modifications of the biosorbents in contrast to either acid or alkaline eluting-agents which hydrolyze the biopolymer components to a greater extent. However, more experiments are required to confirm that regeneration with EDTA do not affect the Cr (III) binding sites of agro-waste materials.

Several studies have demonstrated the potential of using lignocellulosic materials for removing heavy metal ions from aqueous solution. In this thesis, for the first time, the contribution of the main components (hemicelluloses, cellulose, and lignin) of the agro-waste materials to the removal of contaminants (e.g. Cr (III)) from aqueous solution is reported. This knowledge will help to understand and explain more in detail the sorption mechanism and also to predict the potential of

these residues as adsorbents based on the content of the components. It was found that cellulose is present in greater proportion (>46%) compared with hemicelluloses (from 12% to 26%) and lignin (varying from 3% to 10%) for all the biosorbents studied herein; it is important to note that the cellulose percentage is approximately the same for the three agro-waste materials selected (see Figure 3.1 in Chapter 3). The percentage of lost compounds (extractives) after procedure of neutral detergent fiber was around 22% for WSS and WOS, but in the case of WAB it was about 30%. This behavior can be due to the thermal and mechanical treatment previously applied to WAB to extract sugars that are fermented to produce 'mezcal'. Additionally, because of the same treatment, WAB hemicelluloses are approximately half (12.8%) of those in WSS and WOS (both about 26%) which were just water-washed and dried before being used as adsorbents. WAB contained a higher lignin quantity (10.1%) than WSS (3.7%) and WOS (5.7%), which could be attributed to its age: the lignin content in agro-waste materials increases with age and time of storage. Functional groups identified on agro-waste materials and their fractions by ATR-FTIR analyses include hydroxyl, carboxyl, and nitrogen-containing compounds (see Figure 3.2). These functional groups are affected by the procedure applied in order to separate the agro-waste materials main fractions (NDF, ADF, and ADL). It was also found that the NDF procedure removed some compounds from WSS and WOS that decreases the Cr (III) sorption capacity of NDF residues (hemicelluloses, cellulose, and lignin). Such compounds hydrolyzed during the NDF procedure could be waxes, inorganic salts, starch, tannin, among others. In contrast, chromium (III) adsorption capacity decreases after the ADF procedure on WSS and WOS because hemicelluloses are removed from the NDF residues; this biopolymer contains carboxyl groups that play an important role in adsorption of positively-charged heavy metal ions from aqueous solution. Furthermore, the Cr (III) adsorption capacity of ADF (cellulose and lignin) and ADL (lignin) is not significantly different which suggests that cellulose does not contribute to the removal of Cr (III). Similar results were found by using a standard of cellulose and lignin (Figure 3.4). Among all the structural components of agro-waste materials involved in metal adsorption, taking into

account that sequential extraction methods are not totally selective and may affect the composition of biopolymers on agro-waste biosorbents, in general hemicelluloses and lignin are the major contributors to the removal of Cr (III) from aqueous solutions. In addition, cellulose apparently does not participate in the removal of metal cations. These findings also support the idea of adsorption of metal cations on carboxyl groups of agro-waste biosorbents. However, metal cations can also be adsorbed by electrostatic interaction with ionized sulfate groups (due to the acid digestion) attached to the lignin fraction of the residues (cellulose and lignin) that remain after the ADF procedure. Likewise, metal cations can also form coordinated bonds with hydroxyl groups in lignin.

On the other hand, although empirical models have been extensively used in predicting the adsorption kinetics of metals, diffusion models can adequately predict the concentration decay data of Cr (III) on agro-waste materials and also help to explain the mass transfer process occurring in the adsorption phenomena. The film diffusion model (a single-resistance model) predicts very well the adsorption kinetics of Cr (III) on agro-waste adsorbents for some experiments even better or similar to the pseudo second order reaction model (see Table 4.3 in Chapter 4). These results clearly demonstrate that adsorption of metal cations on agro-waste biosorbents is limited by an external mass transfer resistance since the agro-waste materials have a low porosity, low surface area and low pore volume (Table 4.1) and hence the intraparticle diffusion may be neglected. The complexity to solve two-resistance models (film-pore volume diffusion and HSDM) increases since a system of ordinary and partial differential equations must be simultaneously solved. On the contrary, a single-resistance model is easy to solve and can be used to predict the concentration decay curves of adsorption of metals on low porous adsorbents such as agro-waste materials.

To determine diffusion kinetic parameters adequately and also to compare adsorption kinetics for a given metal, it is necessary to conduct adsorption rate experiments by using a rotating-basket reactor as the one used in this research (Figure 4.2). Nevertheless, some differences can be found due to the experimental conditions (e.g. temperature, pH, solid/liquid ratio, particle size, initial

concentration, stirring speed, etc.) and the physical-chemical properties of adsorbents (i.e. porosity, density, surface area, pore size and volume, functional groups, etc.).

Among all agro-waste materials studied herein, agave bagasse has a sorption capacity of Cr (III) as high as polymeric resins, even at low metal concentrations. In addition agave bagasse is cheaper than other adsorbents (i.e. activated carbons, polymeric resins, etc.). Therefore, this agro-waste material is a promising biosorbent for the removal of metals from water.

Finally, biosorption of heavy metals by using agro-waste materials is a promising way of treating the wastewater of several industries such as leather tannery, finishing, metal plating, mining, textile, organic chemicals, among others. In addition, these biosorbents are affordable throughout the world and have a comparable or even higher sorption capacity than commercial adsorbents.

Chapter 6

6.1 GENERAL CONCLUSIONS

Agro-waste materials are able to sequester metal ions such as Chromium (III) from aqueous solution. Furthermore these biosorbents can also be used to remove other metal cations such as lead (II), cadmium (II), zinc (II), nickel (II), copper (II), etc. from water.

The sorption mechanism of Cr (III) is coupled with the release of calcium or hydrogen ions. Nevertheless complexation of metals also takes place on oxygen-containing groups (i.e. carboxyl and hydroxyl). Carboxyl groups on agro-waste materials are the main binding-sites on chromium (III) removal. However, hydroxyl groups are capable of complexing metal cations as well.

Low desorption percentages of chromium-loaded biosorbents are obtained by using various eluting agents at 25°C. However, quelating agents (such as EDTA) seem to be a promising alternative to regenerate chromium-loaded agro-waste materials without apparent weight loss of biosorbents in contrast to either acid or alkaline eluting-agents which hydrolyze the biopolymer components to a greater extent.

Among all the structural components of agro-waste materials involved in metal adsorption, but taking into account that sequential extraction methods are not totally selective and may affect the composition of biopolymers on agro-waste biosorbents, in general hemicelluloses and lignin are the major contributors to the Cr (III) removal from aqueous solutions. In addition, cellulose apparently does not participate in the removal of metal cations. These findings also support the idea of adsorption of metal cations on carboxyl groups. However, metal cations can also be adsorbed by electrostatic interaction with ionized sulfate groups attached to the lignin fraction. Likewise, metal cations can also form coordinated bonds with hydroxyl groups of lignin.

On the other hand, although empirical models have been extensively used in predicting the adsorption kinetics of metals, diffusion models can adequately predict the concentration decay data of Cr (III) on agro-waste materials and also help to explain the mass transfer process occurring in the adsorption phenomena. The film diffusion model (a single-resistance model) predicts very well the adsorption kinetics of Cr (III) on agro-waste adsorbents for some experiments even better or similar to the pseudo second order reaction model. These results clearly demonstrate that adsorption of metal cations on agro-waste biosorbents is limited by an external mass transfer resistance since the agro-waste materials have a low porosity, low surface area and low pore volume and hence the intraparticle diffusion may be neglected.

Finally, biosorption of heavy metals by using agro-waste materials is a promising way of treating the wastewater of several industries such as leather tannery and finishing, metal plating, mining, textile, organic chemicals, among others. In addition, these biosorbents are affordable throughout the world and have a comparable or even higher sorption capacity than commercial adsorbents.

6.2 FUTURE WORK

Biosorption is an emerging technology that has been explored in the last decades. The findings reported in this thesis intended to clarify and explain more in detail the fundamentals of the biosorption of chromium (III) on agro-waste materials. Nonetheless, there are future works that can be conducted for a better understanding of the biosorption processes. Many of these studies are listed and briefly discussed below.

First, it has been reported that the sorption mechanism of Cr (III) on agro-waste materials is associated in part to an ion exchange process with calcium (see Chapter 2), but it is required to determine the cation exchange capacity and the density of carboxyl groups of these biosorbents. These experiments will help to elucidate accurately the contribution of carboxyl groups to the metal cation adsorption capacity. Moreover, since calcium ions neutralize carboxyl groups on agro-waste adsorbents, results reported on Chapter 2 in this thesis may be underestimated (Table 2.1). The acid-base titrations conducted to estimate the functional groups on agro-waste materials is based on pH variations; however the release (if any) of calcium ions does not modify the solution pH contrary to the release of protons associated to carboxyl groups. For the aforementioned reasons, density of carboxyl groups of agro-waste adsorbents must be more accurately estimated.

Second, desorption of metals previously adsorbed on agro-waste materials was significantly improved by using eluting agents such as EDTA at 55°C without apparent damage of functional groups (see Chapter 2). Adsorption and desorption cycles can be conducted to determine the adsorption capacity loss due to the regeneration step with several eluting agents such as mineral acids (i.e. HCl, HNO_3, etc.) and chelating agents (e.g. EDTA and citric acid). Acid-base titrations, FTIR analyses as well as the reducing sugars in solution may help to identify the functional groups damaged by the sorption/desorption cycles. Desorption kinetics of Cr (III) can also be performed to determine the optimal conditions (time,

solid/liquid proportion, concentration of eluting agent, temperature, etc.) in the desorption process.

Third, hemicelluloses and lignin are the main contributors to Cr (III) removal from aqueous solutions (see Chapter 3). Another opportunity to complement this research is to determine the density and equilibrium constants of the functional groups on each fraction to verify the contribution of carboxyl and sulfate groups to the metal adsorption on the fractions of agro-waste materials. Similarly, the neutral detergent fiber procedure seems to be a promising treatment to improve the metal adsorption capacity of oats straw and sorghum straw; therefore more equilibrium and kinetic adsorption experiments can be carried out to assess the applicability of this treated fraction to the removal of metal cations from aqueous solutions. In addition, because lignin fraction is more recalcitrant than the other structural components of agro-waste adsorbents, more adsorption studies are required by using lignin to determine its feasibility of use in adsorption processes.

Fourth, adsorption kinetics of Cr (III) on agro-waste adsorbents (see Chapter 4) can be predicted adequately with the film diffusion model. This model can also be applied to describe the desorption kinetics of calcium due to the adsorption of Cr (III) ions on agro-waste adsorbents. In addition, it is necessary to conduct once again adsorption kinetic experiments of Cr (III) on water-washed oats straw at 400 min^{-1} and initial Cr (III) concentration of 50 mg L^{-1} because of the contradictory results found under these conditions. These results will help to corroborate that the gradient concentration affects the external mass transfer coefficient as reported with the other agro-waste materials (WSS and WAB).

Finally, a fixed-bed column is the most preferred configuration in a real adsorption process. Therefore the next step in developing a biosorption continuous operation is to granulate the biosorbents materials. Such particles should be as small as practical to minimize the pressure drop across the column and should be mechanically and chemically resistant to be used in a packed column. Moreover, reinforcement of biosorbents should allow the metal ions diffusion towards the binding sites of the adsorbent particles.

In summary, because of the complexity of these biosorbents, there are many challenges to fully understanding and developing a biosorption process in a real application. The results presented as well as the future work listed herein may contribute to meet the main challenge: to make biosorption a cost-effective technology for treating metal containing wastewaters.

6.3 LIST OF PUBLICATIONS

- Garcia-Reyes Refugio Bernardo, Rangel-Mendez Jose Rene, and Alfaro-De la Torre Ma. Catalina (2009), **Chromium (III) uptake by agro-waste biosorbents: chemical characterization, sorption-desorption studies, and mechanism,** Journal of Hazardous Materials, 170(2-3) 845-854.

- Garcia-Reyes Refugio Bernardo and Rangel-Mendez Jose Rene (2009), **Contribution of agro-waste materials main components (hemicelluloses, cellulose, and lignin) to the removal of chromium (III) from aqueous solution**, Journal of Chemical Technology and Biotechnology, 84(10) 1533-1538.

- Garcia-Reyes Refugio Bernardo and Rangel-Mendez Jose Rene (2009), **Adsorption kinetics of chromium (III) ions on agro-waste materials,** to be submitted to the Journal of Colloid and Interfaces.

6.4 EXTENDED ABSTRACTS

- García-Reyes Refugio Bernardo y Rangel-Méndez José René (2009), **Adsorción de Cromo (III) en Fracciones de Residuos Agrícolas**, XXX Encuentro Nacional de la AMIDIQ, Mazatlán, Sinaloa, México, 19-22 de mayo de 2009, 1044-1049.

- Garcia-Reyes Refugio Bernardo and Rangel-Mendez Jose Rene (2008), **Sorption and Desorption of Chromium (III) from Aqueous Solution by Agro-Waste Materials**, AIChE Annual Meeting 2008, ISBN 978-0-816910-1050-2, Philadelphia, PA, EUA, November 17-21, 2008.

- Garcia-Reyes Refugio Bernardo and Rangel-Mendez Jose Rene (2008), **Chromium (III) Sequestration by Oats Straw and Agave Bagasse: Sorption Mechanism**, AIChE Annual Meeting, ISBN 978-0-816910-1050-2, Philadelphia, PA, EUA, November 17-21, 2008.

- Garcia-Reyes Refugio Bernardo and Rangel-Mendez Jose Rene (2008) **Agricultural residues characterization and their application to remove Chromium (III) from water**, 1st IWA Mexico National Young Water Professionals Conference, Instituto de Ingeniería, UNAM, ISBN 978-970-32-5515-3, Mexico, D.F., Octubre de 2008, 311-317. This work has been awarded with an "**Honorable Mention"** by International Water Association (IWA), Instituto de Ingeniería de la Universidad Autónoma de México (I de I-UNAM), Universidad Autónoma de México (UNAM), FEMISCA and AIDIS.

6.5 ATTENDANCE AT CONFERENCES

- **Adsorción de Cromo (III) en Fracciones de Residuos Agrícolas**, XXX Encuentro Nacional de la AMIDIQ, Mazatlán, Sinaloa, México, 19-22 de mayo de 2009.

- **Sorption and Desorption of Chromium (III) from Aqueous Solution by Agro-Waste Materials**, AIChE Annual Meeting, Philadelphia, PA, EUA, November 20, 2008.

- **Chromium (III) Sequestration by Oats Straw and Agave Bagasse: Sorption Mechanism**, AIChE Annual Meeting, Philadelphia, PA, EUA, November 17, 2008.

- **Agricultural residues characterization and their application to remove Chromium (III) from water**, 1st IWA Mexico National Young Water Professionals Conference, Instituto de Ingeniería, UNAM, Mexico, D.F., 9-11 de Abril de 2008.

6.6 POSTER PRESENTATION

- Garcia-Reyes Refugio Bernardo and Rangel-Mendez Jose Rene, **Biosorbentes para la Remoción de Compuestos Tóxicos Presentes en Solución Acuosa**, Ion Exchange and Arsenic Remediation from Drinking Water, IPICyT, San Luís Potosí, S.L.P., 20-24 de Agosto de 2007

Appendix A

To estimate the quantity of functional groups (b_j) and their equilibrium constants (pK_a) of agro-waste adsorbents, the experimental data obtained from potentiometric titrations were processed according to the physical-chemical method proposed by Yun *et al.* (2001). Briefly, this method considers the functional group dissociation reaction and the equilibrium constant as:

$$b_jH \leftrightarrow b_j^- + H^+ \qquad k_a = \frac{[b_j^-][H^+]}{[b_jH]} \tag{1}$$

Then, the number of total groups is equal to the sum of the protonated and dissociated functional groups as follows:

$$[b_j]_T = [b_jH] + [b_j^-] \tag{2}$$

In potentiometric titrations experiments, the electro-neutrality condition must be satisfied:

$$[Na^+]_{added} + [H^+] = \sum_{j=1}^{n} [b_j^-] + [OH^-] \tag{3}$$

Finally, combining all equations (1–3), the model to estimate the functional groups quantity and their equilibrium constant is obtained:

$$[OH^-]_{added} = \sum_{j=1}^{n} \left(\frac{b_j * X}{1 + \frac{[H^+]}{k_a}} \right) + \frac{k_w}{[H^+]} - [H^+] \tag{4}$$

Results of the acid-base titrations experiments by using AAB (Table A1 second and fourth column) were fitted with a nonlinear regression to determine b and pK_a by using equation (4).

Table A2 shows the functional groups (b) of agro-waste materials and their equilibrium constants (pK_a) obtained by using equation (4) with 1, 2 or 3 parameters.

Figure A1 shows the experimental and the predicted values of the potentiometric titration experiments. The titrations curve was described adequately with a model with 3 parameters (black line in Figure A1).

Readers are referred to section 2.2.3 in Chapter 2 for detail of the acid-base titration procedures.

Table A1. Results of the acid-base titration experiments by using AAB.

Added volume of 0.1 N NaOH/HCl solution (mL)	Added OH^- concentration (mol/L)	Equilibrium pH	$[H^+]$ (mol/L)	*$[OH^-]$ (mol/L)*			
				Experimental	*Model with 1 parameter*	*Model with 2 parameters*	*Model with 3 parameters*
-2.50	-9.99E-03	2.14	7.24E-03	-9.99E-03	-7.24E-03	-7.23E-03	-7.23E-03
-2.00	-7.99E-03	2.19	6.46E-03	-7.99E-03	-6.46E-03	-6.44E-03	-6.44E-03
-1.00	-4.00E-03	2.56	2.75E-03	-4.00E-03	-2.75E-03	-2.71E-03	-2.71E-03
-0.50	-2.00E-03	2.84	1.45E-03	-2.00E-03	-1.44E-03	-1.37E-03	-1.37E-03
-0.25	-9.99E-04	3.14	7.24E-04	-9.99E-04	-7.23E-04	-5.83E-04	-5.78E-04
-0.10	-4.00E-04	3.31	4.90E-04	-4.00E-04	-4.88E-04	-2.88E-04	-2.83E-04
-0.05	-2.00E-04	3.44	3.63E-04	-2.00E-04	-3.61E-04	-1.02E-04	-9.64E-05
0.00	0.00E+00	3.47	3.39E-04	0.00E+00	-3.37E-04	-6.20E-05	-5.65E-05
0.05	1.99E-04	3.56	2.75E-04	1.99E-04	-2.73E-04	5.30E-05	5.78E-05
0.10	3.99E-04	3.71	1.95E-04	3.99E-04	-1.91E-04	2.35E-04	2.37E-04
0.15	5.98E-04	3.89	1.29E-04	5.98E-04	-1.23E-04	4.48E-04	4.43E-04
0.20	7.98E-04	4.02	9.55E-05	7.98E-04	-8.81E-05	6.01E-04	5.88E-04
0.30	1.20E-03	4.53	2.95E-05	1.20E-03	-5.62E-06	1.16E-03	1.08E-03
0.45	1.79E-03	6.18	6.61E-07	1.79E-03	8.87E-04	1.91E-03	1.86E-03
0.50	1.99E-03	6.39	4.07E-07	1.99E-03	1.30E-03	2.04E-03	2.04E-03
0.60	2.39E-03	6.81	1.55E-07	2.39E-03	2.43E-03	2.48E-03	2.58E-03
0.70	2.79E-03	6.98	1.05E-07	2.79E-03	2.93E-03	2.75E-03	2.85E-03
0.80	3.19E-03	7.14	7.24E-08	3.19E-03	3.38E-03	3.04E-03	3.12E-03
0.85	3.39E-03	7.21	6.17E-08	3.39E-03	3.56E-03	3.18E-03	3.23E-03
0.90	3.59E-03	7.51	3.09E-08	3.59E-03	4.21E-03	3.81E-03	3.67E-03
1.00	3.99E-03	7.61	2.45E-08	3.99E-03	4.38E-03	4.01E-03	3.79E-03
1.10	4.39E-03	9.34	4.57E-10	4.39E-03	5.17E-03	5.36E-03	4.50E-03
1.30	5.18E-03	10.54	2.88E-11	5.18E-03	5.51E-03	5.72E-03	5.55E-03
1.50	5.98E-03	10.57	2.69E-11	5.98E-03	5.53E-03	5.75E-03	5.61E-03
2.50	9.97E-03	11.52	3.02E-12	9.97E-03	8.47E-03	8.69E-03	9.98E-03

For each experiment, 125 mg of agro-waste material were added to 25 mL of solutions. Ionic strength was fixed with 0.1 N NaCl.

Table A2. Functional groups (b, mmol/g) of AAB and their equilibrium constants (pK_a).

	Model with 1 parameter	Model with 2 parameters	Model with 3 parameters
b1	1.03	0.73	0.57
pKa_1	6.86	7.38	10.97
b2	–	0.34	0.58
pKa_2	–	4.19	7.05
b3	–	–	0.31
pKa_3	–	–	4.12

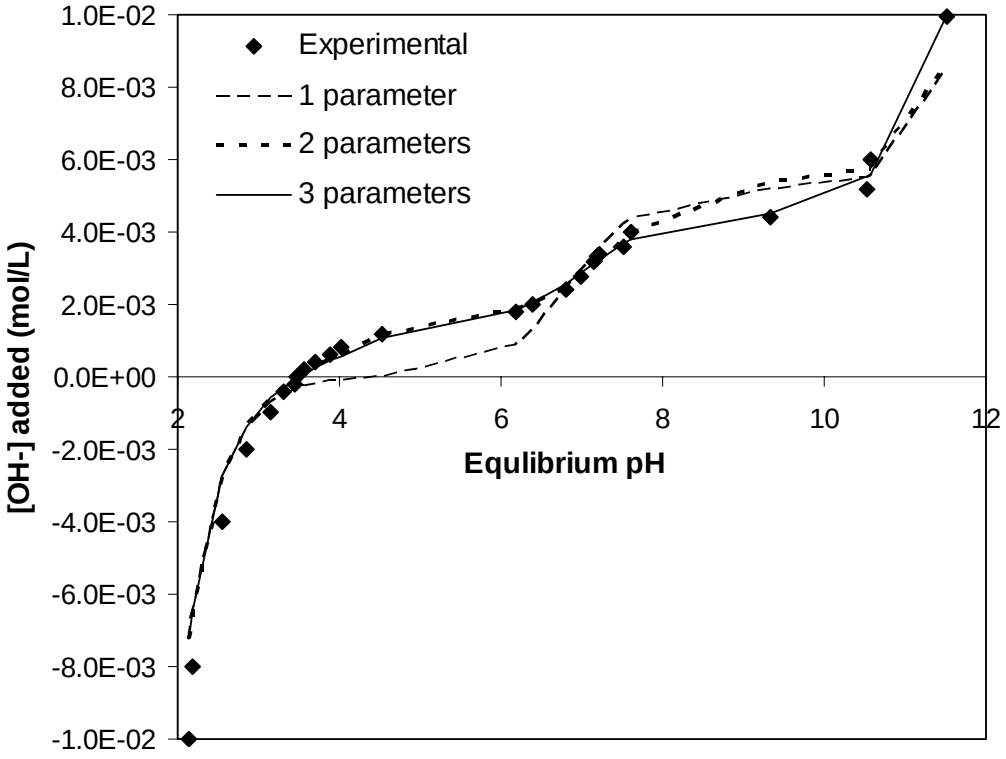

Figure A1. Potentiometric titrations data by using AAB. Symbols represent the experimental measurements and the lines represent the predicted values with the titration model shown in equation 4.

Appendix B

To identify functional groups of agro-waste materials, ATR-FTIR analyses were conducted and the main characteristic bands are shown in Table B1 and Figure 2.1 (A) in Chapter 2.

Table B1. Wavenumber (cm^{-1}) of the major characteristic peaks of the infrared spectra of agro-waste biosorbents.

Biosorbent	Functional group			
	O-H	***C=O***	***N-H***	**C-O**
WSS	3357	1739, 1657	1609	1243, 1163, 1037
ASS	3350	1740, 1670	1615	1246, 1163,1038
WOS	3357	1749, 1650	1612	1242, 1163,1041
AOS	3354	1741, 1657	1612	1240, 1061, 1034
WAB	3346	1738, 1635	1608	1246, 1159, 1038
AAB	3343	1739, 1630	1602	1245, 1162, 1031

Appendix C

Both Langmuir and Freundlich isotherm models fitted reasonable well the experimental data based on the correlation coefficient ($0.85<r^2<0.99$). The estimated isotherms parameters are given on Table C1.

Table C1. Isotherm parameters estimated by using the experimental data of the chromium (III) adsorption on agro-waste biosorbents.

Biosorbent	Conditions	Langmuir			Freundlich		
		Q_{max}	b	r^2	k	n	r^2
WSS	pH 4 25°C	5.329	0.233	*0.95*	2.047	4.604	*0.97*
WOS		10.551	0.091	*0.92*	2.157	2.860	*0.99*
WAB		10.837	0.271	*0.99*	4.006	3.997	*0.95*
ASS		6.958	0.112	*0.90*	1.656	3.173	*0.98*
AOS		12.974	0.136	*0.94*	3.297	3.163	*0.98*
AAB		11.437	0.772	*0.95*	5.727	5.843	*0.93*
ASS	pH 3 25°C	1.553	0.069	*0.91*	0.273	2.764	*0.85*
AOS		8.316	0.051	*0.99*	0.993	2.254	*0.96*
AAB		9.064	0.150	*0.98*	2.800	3.895	*0.92*
ASS	pH 4 35°C	11.728	0.092	*0.97*	2.457	2.968	*0.98*
AOS		18.951	0.046	*0.95*	2.120	2.158	*0.98*
AAB		18.807	0.891	*0.99*	7.959	4.609	*0.97*

Q_{max} (mg/g); b (L/mg); k ($L^{1/n}/mg^{1-1/n}\ g^{-1}$); n, r^2 (dimensionless).

Appendix D

The pseudo-first order reaction model (Eq. 1 in Chapter 4) was used to predict the adsorption kinetics of Cr (III) on agro-waste materials. Table D1 shows the parameters of the pseudo-first order model estimated from the experimental data of the adsorption kinetics of Cr (III) on agro-waste materials.

The pseudo-first order reaction model did not adequately predict the experimental results based on the percentage average deviation (0.6<%D<6.6). In contrast, the pseudo-second order reaction model did predict well (0.8<%D<2.3) the adsorption kinetics of Cr (III) at different stirring speeds and concentrations (see Table 4.3 in Chapter 4).

The predicted and the concentration decay results for WSS and WOS are shown in Figures D1, D2, D3 and D4. The film diffusion model predicted adequately the adsorption rate of Cr (III) on WSS and WOS based on the low deviation (0.8<%D<2.0) between the experimental data and the predicted values. In addition the physical properties of the agro-waste materials (low surface area, low pore volume, and pore size of mesopores and macropores (see Figure D5 and Table 4.1 in Chapter 4)) support the idea that intraparticle diffusion may be neglected and that the adsorption of Cr (III) is limited mainly by the film resistance surrounding the adsorbent particle.

Table D1. Pseudo-first order model parameters estimated by using the experimental data of the adsorption kinetics of Cr (III) on agro-waste materials at pH 4 and 25°C.

Biosorbent	C_o (mg L^{-1})	Stirring speed (min^{-1})	Pseudo-first order		
			k_1 (min^{-1})	X (mg g^{-1})	%D
WSS	22.05	200	0.0009	2.011	4.04
	21.69	300	0.0009	1.509	5.38
	20.52	400	0.0223	4.932	2.63
	53.00	**400**	**0.0166**	**2.613**	**1.83**
WOS	21.77	200	0.0155	3.490	3.68
	22.74	300	0.0056	2.471	6.60
	22.86	400	0.0047	3.606	4.78
	52.26	**400**	**0.0196**	**7.922**	**0.62**
WAB	19.75	200	0.0005	9.823	5.93
	19.57	300	0.0075	9.591	6.30
	20.02	400	0.0103	9.136	5.19
	55.25	**400**	**0.0130**	**6.899**	**5.80**

C_o: Initial metal concentration; k_1: Adsorption rate constant; X: Adsorption capacity at equilibrium; %D: Percentage average deviation (dimensionless).

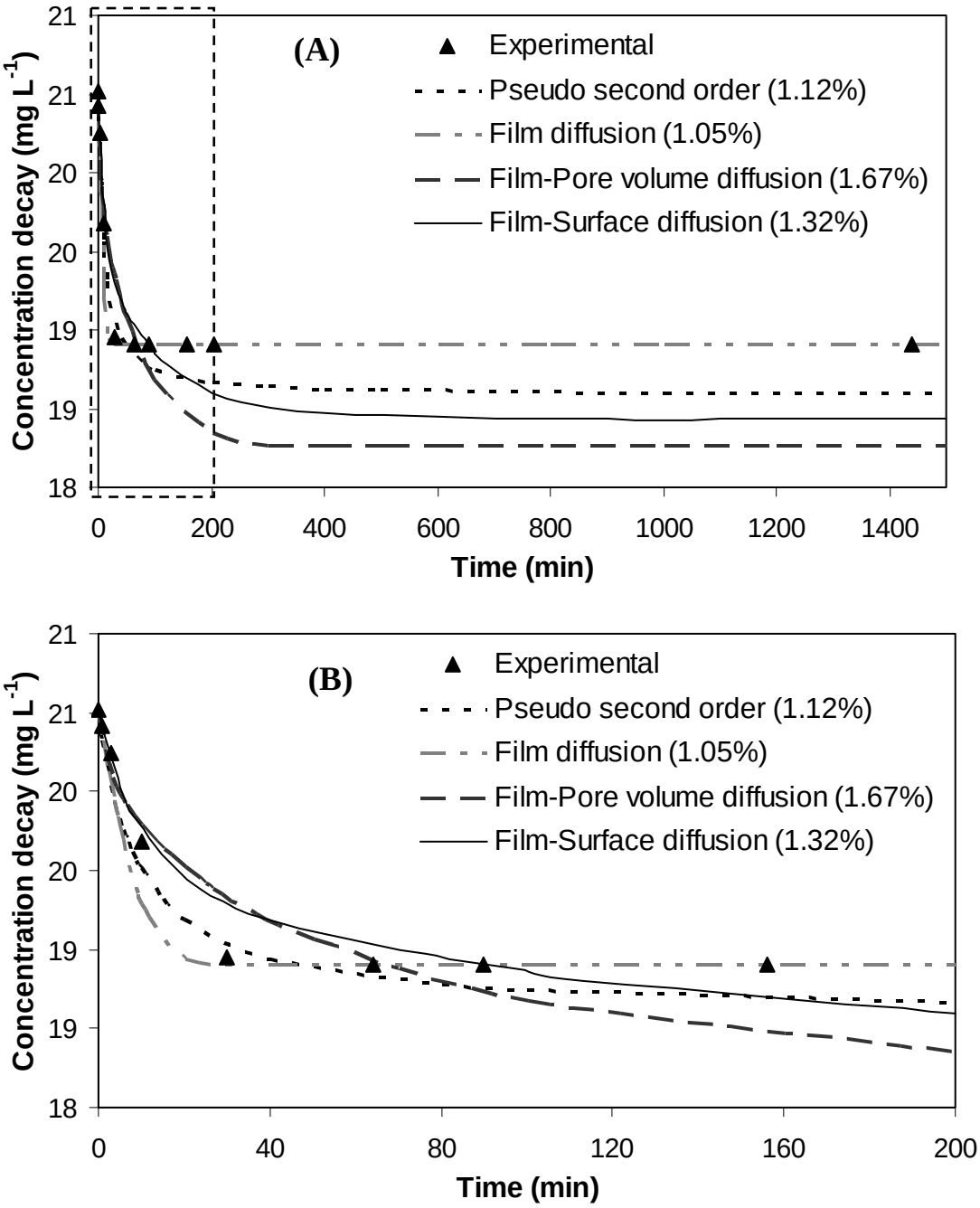

Figure D1. Adsorption kinetics of Cr (III) ions on WSS at pH 4, 25°C, using 250 mg of biosorbent in 1 L, 400 min^{-1}, C_o=20.52 mg L^{-1}. Dashed square in (A) is enlarged in (B) for better clarity. Symbols represent the experimental results and the lines the predicted values by the models. Percentage deviations are given in parentheses.

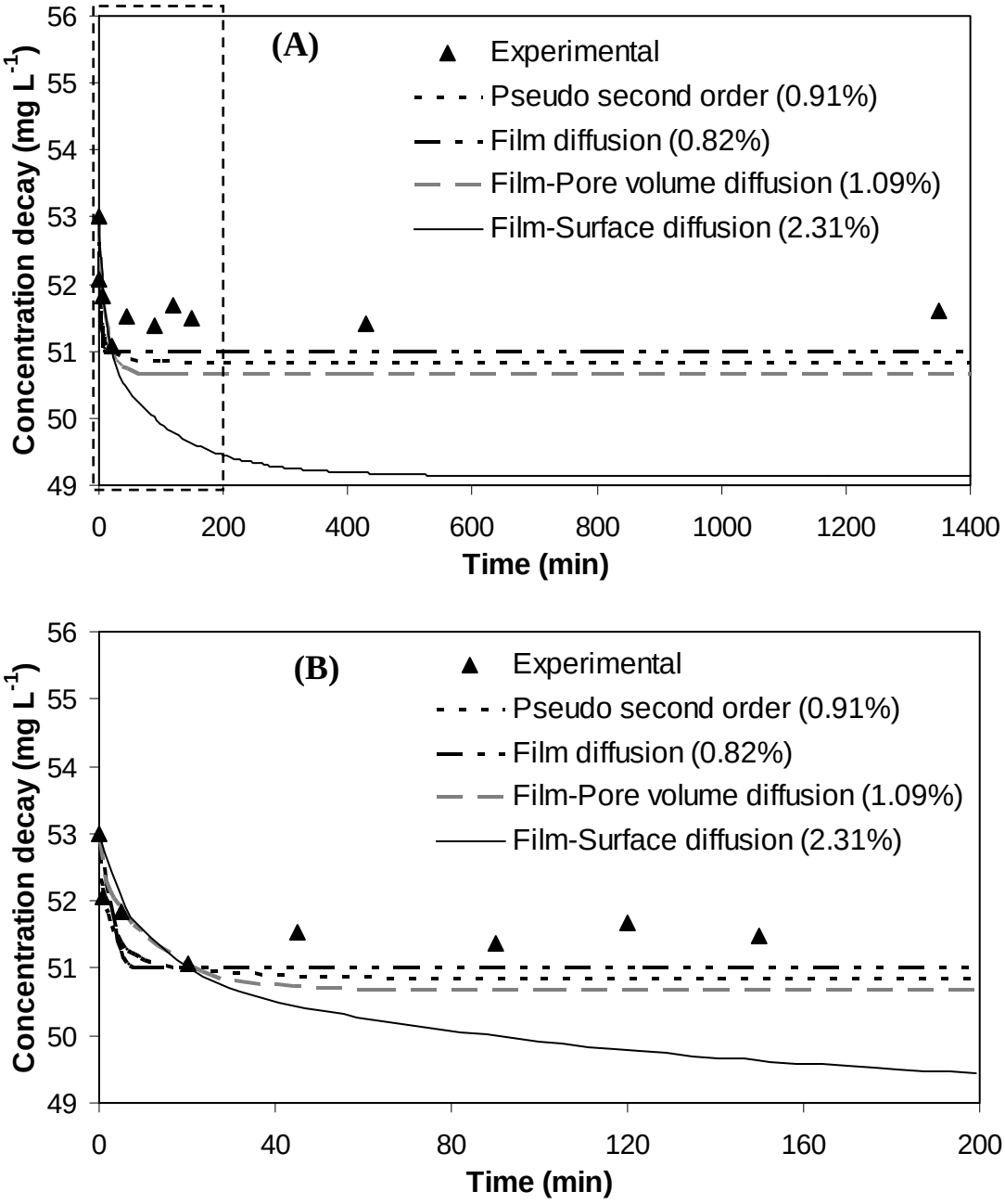

Figure D2. Adsorption kinetics of Cr (III) ions on WSS at pH 4, 25°C, using 250 mg of biosorbent in 1 L, 400 min^{-1}, C_o=53.00 mg L^{-1}. Dashed square in (A) is enlarged in (B) for better clarity. Symbols represent the experimental results and the lines the predicted values by the models. Percentage deviations are given in parentheses.

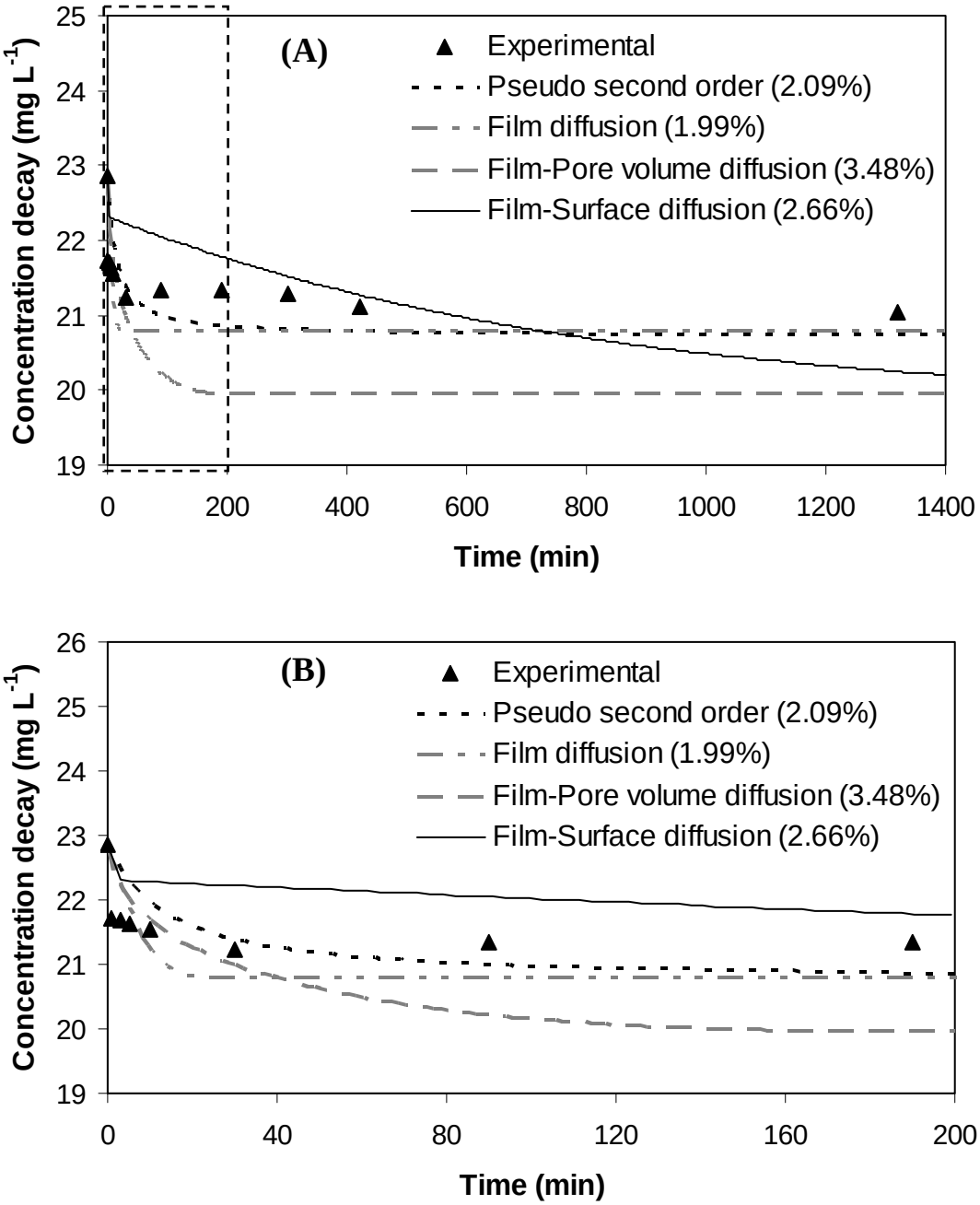

Figure D3. Adsorption kinetics of Cr (III) ions on WOS at pH 4, 25°C, using 250 mg of biosorbent in 1 L, 400 min^{-1}, C_o=22.86 mg L^{-1}. Dashed square in (A) is enlarged in (B) for better clarity. Symbols represent the experimental results and the lines the predicted values by the models. Percentage deviations are given in parentheses.

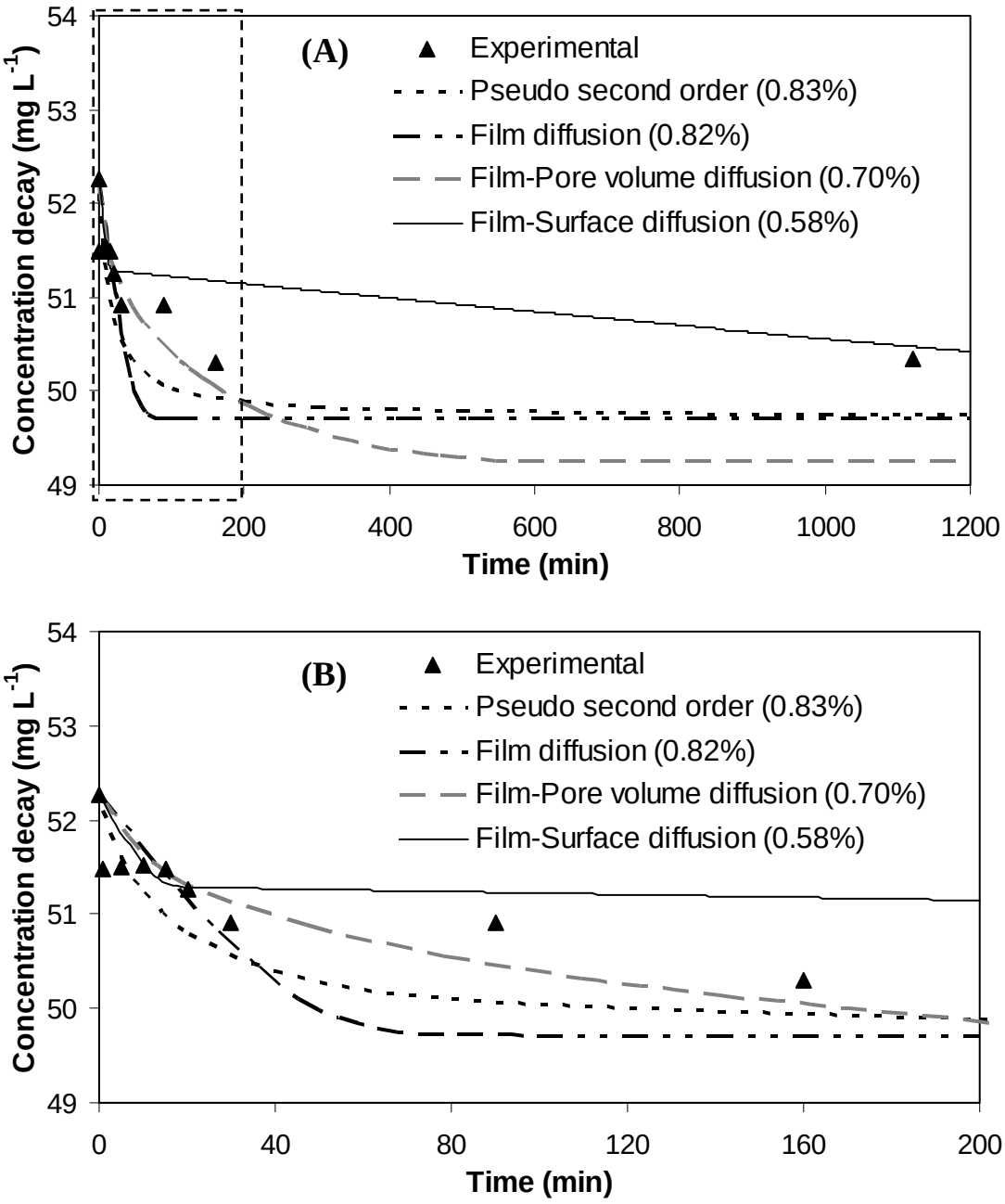

Figure D4. Adsorption kinetics of Cr (III) ions on WOS at pH 4, 25°C, using 250 mg of biosorbent in 1 L, 400 min^{-1}, C_o=52.26 mg L^{-1}. Dashed square in (A) is enlarged in (B) for better clarity. Symbols represent the experimental results and the lines the predicted values by the models. Percentage deviations are given in parentheses.

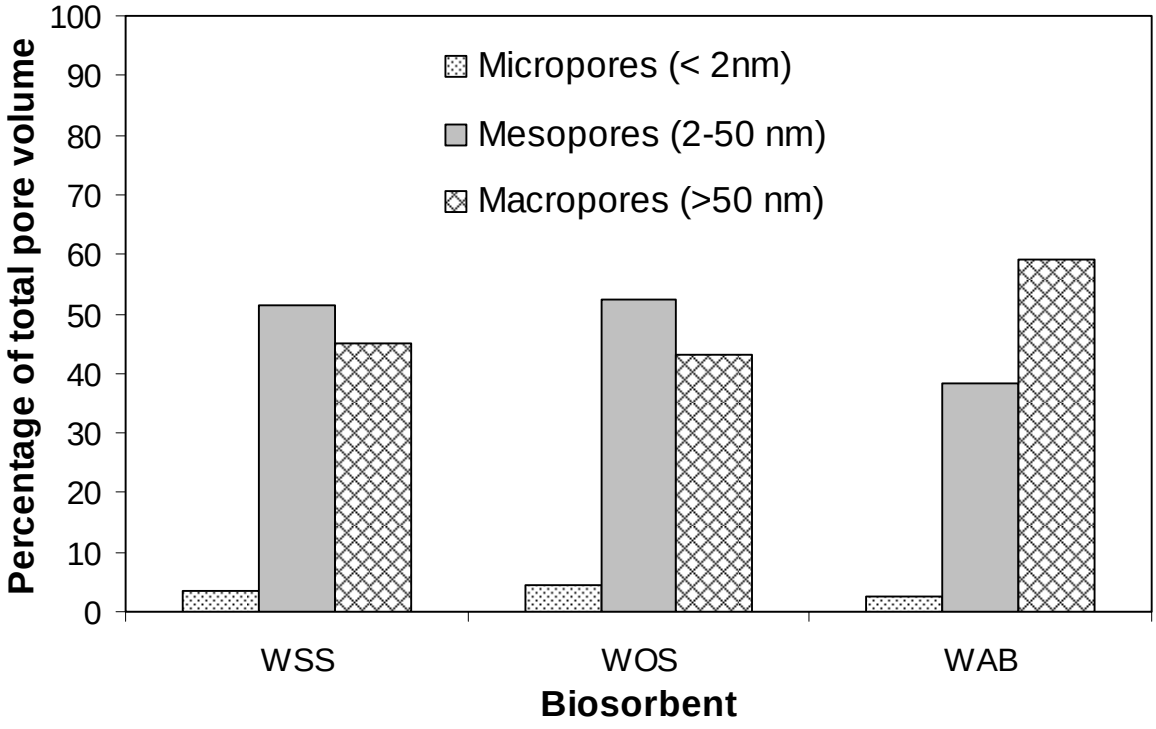

Figure D5. Pore-size distribution of agro-waste materials estimated with the N_2 BJH method.

Appendix E

To obtain the diffusion model parameters, the model equations (see section 4.2.1.2 and 4.2.1.3) must be simultaneously solved by numerical methods. It is important to mention that model equations were programmed in PDESOL 2.0 to be solved. The programs required the experimental conditions, physical properties of the adsorbents (Table 4.1 in Chapter 4), and the isotherm parameters (Table 4.2) to predict the concentration decay curves.

As an example, the programs used to estimate the diffusion models parameters that predict adequately the adsorption kinetics of Cr (III) on WAB at pH 4 and 25°C are shown in the following sections.

E1. Film diffusion model

'Experimental conditions

'Initial concentration (g/cm^3)

Co=0.00005525

'Mass of adsorbent (g)

m=0.251

'Volume of the solution (cm^3)

V=1000

'Physical properties of the adsorbents

'Average radius of adsorbent particle (cm)

R=0.0375

'Average pore-volume (cm^3/g)

Vp=0.003133

'Density of the adsorbent particle (g/cm^3)

rho=1.5216

'Porosity (dimensionless)

E=Vp/(Vp+1/rho)

'Outer surface area of particle (cm^2)

Area=3*m/(rho*R*(1-E))

'Dimesionless variable

Alpha=rho*V/m

'Isotherm parameters

'Maximum adsorption capacity (g/g) estimated with the Langmuir isotherm

qm=0.02238

'Langmuir isotherm constant (cm^3/g)

b=320000

'Adsorption capacity (g/g) calculated by using the Langmuir isotherm

qo=qm*b*Co/(1+b*Co)

‘Dimesionless variable
w=rho*qo/Co

‘Parameter of the film diffusion model
‘External mass transfer coefficient (cm/s)
k=0.005

‘Initial conditions
phi@t0=1
Qave@t0=0

‘Differential model equations to be simultaneously solved by numerical methods
eta=Qave/((qm/qo-Qave)*b*Co)
Qave_t=Alpha/w*(phi-eta)
phi_t=-w/Alpha*Qave_t

‘Real time (s)
Realtime=V*t/(Area*k)

‘Concentration of solute in solution (mg/L)
C=phi*Co*1E6

‘For each value of k, a concentration decay curve is obtained. The deviation between the experimental and the predicted data is used to select the k that represents the adsorption kinetics of adsorbate on the adsorbent for a particular experiment.

E2. Pore-volume diffusion model with external mass transfer resistance

'Experimental conditions

'Initial concentration (g/cm^3)

Co=0.00005525

'Mass of adsorbent (g)

m=0.251

'Volume of the solution (cm^3)

V=1000

'Physical properties of the adsorbents

'Average radius of adsorbent particle (cm)'

R=0.0375

'Average pore-volume (cm^3/g)

Vp=0.003133

'Density of the adsorbent particle (g/cm^3)

rho=1.5216

'Porosity (dimensionless)

E=Vp/(Vp+1/rho)

'Dimesionless variable

Alpha=rho*V/m

'Isotherm parameters

'Maximum adsorption capacity (g/g) estimated with the Langmuir isotherm

qm=0.02238

'Langmuir isotherm constant (cm^3/g)

b=320000

'Part of the Langmuir isotherm

AL=1+b*Co

'Dimesionless variable

w=rho*qm/Co

'Parameters of the pore-volume diffusion model with external mass transfer resistance

'External mass transfer coefficient (cm/s)

k=5E-2

'Effective pore volume diffusivity (cm^2/s)

Dep=1.5E-5

'Smith number

Nsh=2*k*R/Dep

'Initial conditions

phi@t0=1

Qave@t0=0

'Boundary conditions

Qave_x=dx(Qave)

Qave_x@xL=0

Qave_x@xU=(Nsh/2)*(phi-Qave@xU)

'Differential model equations to be simultaneously solved by numerical methods

''Dimensionless mass balance

FPQave=AL/(1+(AL-1)*Qave)^2

phi_t=-((3*Nsh)/(2*Alpha))*(phi-Qave@xU)

'Diffusion equation

Qave_t=1/(E+w*FPQave)*(1/(x>1e-2)^2)*dx(x^2*Qave_x)

'Real time (s)

Realtime=(t*R^2)/Dep

‘Concentration of solute in solution (mg/L)

C=phi*Co*1E6

‘For each value of k and Dep, a concentration decay curve is obtained. The deviation between the experimental and the predicted data is used to select the k and Dep values that represent the adsorption kinetics of adsorbate on the adsorbent for a particular experiment.

E3. Homogeneous solid diffusion model (HSDM) with external mass transfer resistance

'Experimental conditions

'Initial concentration (g/cm^3)

Co=0.00005525

'Mass of adsorbent (g)

m=0.251

'Volume of the solution (cm^3)

V=1000

'Physical properties of the adsorbents

'Average radius of adsorbent particle (cm)

R=0.0375

'Average pore-volume (cm^3/g)

Vp=0.003133

'Density of the adsorbent particle (g/cm^3)

rho=1.5216

'Porosity (dimensionless)

E=Vp/(Vp+1/rho)

'Dimesionless variable

Alpha=rho*V/m

'Isotherm parameters

'Maximum adsorption capacity (g/g) estimated with the Langmuir isotherm

qm=0.02238

'Langmuir isotherm constant (cm^3/g)

b=320000

'Adsorption capacity (g/g) calculated by using the Langmuir isotherm

qo=qm*b*Co/(1+b*Co)

‘Dimesionless variables

beta=qm*qo

w=rho*qo/Co

‘Parameters of the HSDM with external mass transfer resistance

‘External mass transfer coefficient (cm/s)

k=5E-3

‘Surface diffusivity (cm^2/s)

Ds=2E-7

‘Initial conditions

phi@t0=1

Qave@t0=0

‘Boundary conditions

Qave_x=dx(Qave)

Qave_x@xL=0

eta=Qave@xU/((beta-Qave@xU)*b*Co)

Qave_x@xU=k*Co*R*(phi-eta)/(rho*Ds*qo)

‘Differential model equations to be simultaneously solved by numerical methods

'Diffusion equation

Qave_t=(1/(x>1e2)^2)*dx(x^2*Qave_x)

'Dimensionless mass balance

phi_t=-3*w/Alpha*Qave_x@xU

‘Real time (s)

Realtime=(t*R^2)/Ds

‘Concentration of solute in solution (mg/L)

C=phi*Co*1E6

‘For each value of k and Ds, a concentration decay curve is obtained. The deviation between the experimental and the predicted data is used to select the k and Ds values that represent the adsorption kinetics of adsorbate on the adsorbent for a particular experiment.